ON PRESENT STATUS OF R-PARITY VIOLATING SUPERSYMMETRY

VADIM BEDNYAKOV[1], AMAND FAESSLER[2] and SERGEY KOVALENKO[1]

1. Joint Institute for Nuclear Research, 141980 Dubna, Russia
2. Institute für Theoretische Physik der Universität Tübingen, Auf der Morgenstelle 14, D-72076 Tübingen, Germany

ABSTRACT

We review the phenomenological status of the minimal supersymmetric standard model without R-parity conservation. We focus on the issues of the lepton and baryon number/flavor violation possible in this framework for various low energy processes. Special emphasis is made to the constraints on the R-parity violating parameters derived from the experimental data on these processes.

KEYWORDS

Supersymmetry, R-parity violation, rare decays.

1 Introduction

During the last decade the minimal supersymmetric (SUSY) standard model (MSSM) was getting a new paradigm of the particle physics instead of the traditional Standard Model (SM). The MSSM is the minimal extension of the SM to include SUSY (for review see [1, 2]). The need of the SUSY for the low-energy realm steams mainly from the SM itself if one tries to understand a co-existence of the two fundamental energy scales separated by a huge distance on the energy axis. They are the Fermi scale M_F 250 GeV and the Planck scale M_{Pl} 10^{19} GeV. Quantum effects make this difference unstable and push the scalar masses to the M_{Pl} making the SM meaningless. This is a manifestation of the so-called "hierarchy" problem. The most elegant known solution of this problem is offered by the SUSY which leads to cancellation of dangerous quadratic quantum loop corrections and stabilizes the mass scales.

The MSSM includes many new fields and couplings compared to the SM. The well known feature of the SM is the presence of the two accidental global symmetries U_{1B} and U_{1L} corresponding to the baryon B and lepton L number conservation. These symmetries are consequence of the SM gauge symmetry and of the minimal field content. Changing to the MSSM we find U_{1B} and U_{1L} broken and, therefore, the lepton and baryon number violating processes are possible. This fact may have a dangerous impact on the low-energy phenomenology. In particular, it means that matter is unstable due to the proton decay.

The standard lore to cope with this problem is to introduce an ad hoc discrete symmetry such as the R-parity [3]. This is a multiplicative Z_2 symmetry defined as

$$R_p = (-1)^{3B+L+2S}; \tag{1}$$

where S, B and L are the spin, the baryon and the lepton quantum numbers. It implies that all the SM particles have the conserving multiplicative quantum number $R_p = +1$ while their superpartners $R_p = -1$.

R-parity conservation prevents lepton (L-) and baryon (B-) number violating processes, the superpartners are produced in associated production and the lightest SUSY particle is stable. The latter leads to the celebrated missing E_T signature of the SUSY event in high energy detectors and renders a cold dark matter particle candidate. Although desirable for many reasons the R-parity conservation has no well motivated theoretical grounds.

On the other hand relaxing the R-parity conservation in a special way we may get a new insight into the long standing problems of particle physics, in particular, to the neutrino mass problem. Remarkable, that in this framework neutrinos can acquire the tree-level supersymmetric mass via the mixing with the gauginos and higgsinos at the weak scale [4]–[9]. This mechanism does not involve the physics at the large energy scales M_{int} $O(10^{12}$ GeV) in contrast to the see-saw mechanism but relates the neutrino mass to the weak-scale physics accessible for experimental searches.

The R-parity can be broken ($R\!\!\!/_p$) either explicitly [4] or spontaneously [10]–[12]. The first option allows one to establish the most general phenomenological consequences of R-parity violation while a predictive power in this case is rather weak due to the large number of free parameters. Spontaneous realization of $R\!\!\!/_p$ SUSY is a much more predictive scheme leading to many interesting phenomenological consequences [12]. However, it represents a particular model of the R-parity violation and in certain cases it might be not satisfactory. At present it is an open question which underlying high-energy scale physics stands behind R-parity, protecting or violating it at the weak scale.

Many aspects of the $R\!\!\!/_p$ SUSY models in high and low energy processes have been investigated in the literature (for review see [13]–[16]). Recently, growing interest to the supersymmetric models without R-parity conservation was stimulated in particular by the HERA experiments, which reported an anomaly in deep inelastic e^+p-scattering [17] which can be elegantly explained within this theoretical framework in terms of the lepton number violating interactions.

In a model without R_p, the supersymmetric particles can decay alone into ordinary particles. Therefore the R-parity odd interactions can be probed by any usual particle detector. In order to estimate a possibility of detecting the R_p violating SUSY in future experiments one needs to know the current

constraints on the R-parity violating couplings from the existing data. Especially stringent constraints can be naturally extracted from data on the processes forbidden or highly suppressed in the SM.

In this paper we give a review of the present status of the MSSM without R-parity conservation ($\not{R}_p$MSSM). We consider the most general case of R-parity violation in the superpotential and in the soft SUSY breaking sector. We start with the theoretical introduction into the $\not{R}_p$MSSM, specifying and discussing main attributes of this model. Then we discuss the currently known constraints on R-parity violating SUSY. It is important to note right from the beginning that all known constraints on the R-parity violating ($\not{R}_p$) parameters in particular those we present in this paper are model-dependent. Since we always deal with several contributions to a considered observable quantity there is no other way to evaluate the size of individual terms and the corresponding $\not{R}_p$ parameters but to employ the assumptions of the dominance of one/several couplings or the assumption of the absence of an unnatural fine-tuning between different contributions. The latter in many cases is equivalent to the former. To extract the physical parameters based on these assumptions is widely used in the literature. Nevertheless one has to keep these notes in mind considering various constraints in this paper and also in the original papers.

2 Minimal supersymmetric standard model

In this section we introduce and discuss the main ingredients of the minimal supersymmetric standard model (MSSM). We consider some theoretical motivations for R-parity (R_p) conservation or non conservation ($\not{R}_p$). The two options with and without R_p conservation are commonly denoted as MSSM and $\not{R}_p$MSSM. This section is mainly intended to give a basis for the subsequent sections where phenomenological status of the $\not{R}_p$MSSM is addressed.

2.1 Superpotential and soft supersymmetry breaking

The minimal supersymmetric standard model is a minimal extension of the SM to incorporate supersymmetry. The model is based on the SM gauge group $G_{SM} = SU(3)_c \quad SU(2)_L \quad U(1)_Y$ and involves the fields listed in Table 1.

Note that the list of superfields in Table 1 includes two Higgs doublets $\hat{H}_1$ and $\hat{H}_2$ with weak hypercharges $Y = \quad 1; +1$ respectively, instead of one Higgs doublet in the SM. The second Higgs superfield $\hat{H}_2$ is necessary for constructing the SUSY Yukawa couplings $\hat{H}_2\hat{Q}\hat{U}^c$ which provide after the electroweak symmetry breaking masses to up-quarks. In the SM one could use for this purpose the complex conjugate field $i_2 H_1^y$ without introducing an independent H_2. In the SUSY framework the use of $\hat{H}_1^y$ is forbidden by the symmetry argument. The superpotential terms $i_2\hat{H}_1^y\hat{Q}\hat{U}^c$ allowed by gauge symmetry are forbidden by SUSY since $\hat{H}_1^y$ transforms under the SUSY algebra as a right-handed chiral superfield while $\hat{Q}_i$ and $\hat{U}^c$ transforms as left-handed ones. Furthermore, it can be shown that the existence of the second Higgs field is required to avoid gauge anomaly which would otherwise result from unpaired chiral fermion existing in the Higgs supermultiplet and known as higgsino [18].

The most general gauge invariant form of the renormalizable superpotential reads

$$W = W_{R_p} + W_{\not{R}_p}: \tag{2}$$

The R_p conserving part has the standard MSSM form

$$W_{R_p} = \varepsilon_{ab}\Big[h^E_{ij}\hat{H}_1^a\hat{L}_i^b\hat{E}_j^c + h^D_{ij}\hat{H}_1^a\hat{Q}_i^b\hat{D}_j^c \quad h^U_{ij}\hat{H}_2^a\hat{Q}_i^b\hat{U}_j^c \quad \hat{H}_1^a\hat{H}_2^b\Big]; \tag{3}$$

where $i,j = 1,2,3$ are generation indices and $a,b = 1,2$ are $SU(2)_L$ ones. A completely antisymmetric tensor ε is defined as $\varepsilon_{12} = \quad \varepsilon_{21} = 1$. Hat denotes a superfield. Further we will drop the superfield hats unless it is misleading.

The R_p violating part of the superpotential (2) can be written as [4, 19],

$$W_{\not{R}_p} = \varepsilon_{ab}\Big[\frac{1}{2}\lambda_{ijk}\hat{L}_i^a\hat{L}_j^b\hat{E}_k^c + \lambda'_{ijk}\hat{L}_i^a\hat{Q}_j^b\hat{D}_k^c \quad \kappa_j\hat{L}_j^a\hat{H}_2^b + \frac{1}{2}\lambda''_{ijk}\hat{U}_i^c\hat{D}_j^c\hat{D}_k^c\Big]: \tag{4}$$

Table 1. The MSSM field content.

Super fields	Bosons	Fermions	$SU(3)_c \quad SU(2)_L \quad U(1)_Y$, $Y = 2(Q \quad T_3)$
$\hat{g}^{(a)}$	$g^{(a)}$	$\tilde{g}^{(a)}$	$(8;1;0)$
$\hat{W}^{(k)}$	$W^{(k)}$	$\tilde{W}^{(k)}$	$(1;3;0)$
$\hat{B}$	B	$\tilde{B}$	$(1;1;0)$
$\hat{L}$	$L = \begin{pmatrix} e_L \\ e_L \end{pmatrix}$	$L = \begin{pmatrix} \nu_L \\ e_L \end{pmatrix}$	$(1;2; \quad 1)$
$\hat{E}^C$	$E^C = (e_R)^C$	$E^C = e_R{}^C = i_2 \, e_R{}^y$	$(1;1;2)$
$\hat{Q}$	$Q = \begin{pmatrix} u_L \\ d_L \end{pmatrix}$	$Q = \begin{pmatrix} u_L \\ d_L \end{pmatrix}$	$(3;2;\frac{1}{3})$
$\hat{U}^C$	$U^C = (u_R)^C$	$U^C = (u_R)^C = i_2 \, u_R{}^y$	$(3;1; \quad \frac{4}{3})$
$\hat{D}^C$	$D^C = (d_R)^C$	$D^C = (d_R)^C = i_2 \, d_R{}^y$	$(3;1;\frac{2}{3})$
$\hat{H}_1$	$H_1 = \begin{pmatrix} H_1^0 \\ H_1^- \end{pmatrix}$	$\tilde{H}_1 = \begin{pmatrix} \tilde{H}_1^0 \\ \tilde{H}_1^- \end{pmatrix}$	$(1;2; \quad 1)$
$\hat{H}_2$	$H_2 = \begin{pmatrix} H_2^+ \\ H_2^0 \end{pmatrix}$	$\tilde{H}_2 = \begin{pmatrix} \tilde{H}_2^+ \\ \tilde{H}_2^0 \end{pmatrix}$	$(1;2;1)$

The coupling constants (^{00}) are antisymmetric in the first (last) two indices as required by the SU(2) and SU(3) invariance.

The SUSY can offer a realistic phenomenology only if it is explicitly broken at low energies so that superpartners split in masses. Otherwise it would contradict the observed particle mass spectrum. SUSY can be broken in the so called "soft" way saving the generic ultraviolet property of the SUSY: absence of quadratic divergences. Recall that this property of SUSY allows a solution of the notorious hierarchy problem which was a main reason for invoking the SUSY to low-energy particle physics.

The soft SUSY breaking terms of the R_pMSSM Lagrangian are:

$$L_{soft} = \quad V_{R_p}^{soft} \quad V_{R_p}^{soft} + L_{GM}^{soft}; \tag{5}$$

where the R-parity violating $V_{R_p}^{soft}$ and the R-parity conserving $V_{R_p}^{soft}$ parts of the scalar potential have the form:

$$V_{R_p}^{soft} = (M_Q^2)_{ij} \tilde{Q}_i^a \tilde{Q}_j^a + (M_U^2)_{ij} \tilde{u}_{Ri} \tilde{u}_{Rj} + (M_D^2)_{ij} \tilde{d}_{Ri} \tilde{d}_{Rj} + (M_L^2)_{ij} \tilde{L}_i^a \tilde{L}_j^a + (M_E^2)_{ij} \tilde{e}_{Ri} \tilde{e}_{Rj} + m_{H_1}^2 H_1^a H_1^a$$
$$+ m_{H_2}^2 H_2^a H_2^a + \varepsilon_{ab} \left[A_U^{ij} h_{ij}^U \tilde{Q}_i^a \tilde{u}_{Rj} H_2^b + A_D^{ij} h_{ij}^D \tilde{Q}_i^b \tilde{d}_{Rj} H_1^a + A_E^{ij} h_{ij}^E \tilde{L}_i^b \tilde{e}_{Rj} H_1^a \quad B \; H_1^a H_2^b + H.c. \right]; \tag{6}$$

$$V_{R_p}^{soft} = \varepsilon_{ab} \left[{}^{0}_{ijk} \tilde{L}_i^a \tilde{L}_j^b \tilde{e}_{Rk} + {}^{0}_{ijk} \tilde{L}_i^a \tilde{Q}_j^b \tilde{d}_{Rk} + e_{2j}^2 \tilde{L}_j^a H_2^b + e_{1j}^2 \tilde{L}_j^a H_1^a + {}^{00}_{ijk} \tilde{u}_{Ri} \tilde{d}_{Rj} \tilde{d}_{Rk} + H.c. \right] \tag{7}$$

The "soft" gaugino mass terms are

$$L_{GM}^{soft} = \quad \frac{1}{2} \left[M_1 \tilde{B} \tilde{B} + M_2 \tilde{W}^k \tilde{W}^k + M_3 \tilde{g}^a \tilde{g}^a \right] \quad H.c. \tag{8}$$

In eqs. (6){(8) tilded quantities denote the superpartners of SM fields.

Note that the gluino $\tilde{g}$ soft mass M_3 coincides in this framework with its physical mass denoted hereafter as $m_{\tilde{g}} = M_3$. While the soft masses $M_{1,2}$ are not physical masses of the gauginos $\tilde{W}$ and $\tilde{B}$ since in general they are mixed with each other as well as with higgsinos and neutrinos. Therefore, mass eigenstates are defined by the diagonalization of the $7 \quad 7$ mass matrix as discussed in sect. 2.3.1.

A generic feature of supersymmetric extensions of the SM is the presence of renormalizable operators violating the lepton L and baryon B number conservation laws. These operators violate simultaneously R-parity and are present in (4) and (7). This is in contrast to the SM where L and B violating renormalizable operators are forbidden by the gauge invariance realized for the SM fields. In the supersymmetric extensions of the SM it is not the case because of a wider field content.

A model characterized by the superpotential (2) and the soft SUSY breaking terms (5) does not conserve R-parity and will be denoted as $\not{R}_p$MSSM. It contains 135 independent $\not{R}_p$ parameters. They are: 9 bilinear mass parameters $_j$, $\tilde{}_{1j}$, $\tilde{}_{2j}$, 9 trilinear parameters of the -type, 27 of the ^{0}-type, 9 of the ^{00}-type and 3 27 of the $;\ ^0;\ ^{00}$-types. As will be discussed in sect. 2.5, the simultaneous presence of lepton and baryon number violating terms in eqs. (4) and (7) (unless the couplings are very small) leads to unsuppressed proton decay. Therefore, either only the lepton or the baryon number violating couplings can be present in phenomenologically viable model.

Imposing R-parity conservation one a priori assumes all these terms to vanish. The corresponding model is known as the MSSM. However it is a too restrictive assumption.

Certain discrete symmetries such as the B-parity may originate from an underlying high-energy scale theory and forbid only baryon number violating couplings. This is enough to avoid fast proton decay. This model, usually denoted as B_pMSSM or again as $\not{R}_p$MSSM, is derived from the general version of $\not{R}_p$MSSM by setting $^{00} = \ ^{00} = 0$ in eqs. (4) and (7). This realization of R-parity violation attracts most attention in the literature.

The following note on a specific property of the $\not{R}_p$MSSM is in order. By examining eqs. (3){(7) one finds no difference between the superfields H_1 and L_i. This is because in the $\not{R}_p$MSSM there is no conserving quantum number to distinguish these superfields. Therefore in many cases it is convenient to collect them in a combined superfield $L = (H_1; L_i)$ with $= 0;1;2;3$, implying $L_0 = H_1$. We will use this possibility in the subsequent sections.

2.2 Scalar potential and electro-weak symmetry breaking

Having defined the superpotential (2) and the soft SUSY breaking terms (5) it is straightforward to derive the scalar potential V of the $\not{R}_p$MSSM. It consists of the following four terms:

$$V = V_{R_p}^{soft} + V_{\not{R}_p}^{soft} + \frac{1}{2}\sum_a D^a D^a + \sum_n F_n F_n; \tag{9}$$

where $V_{R_p}^{soft}$ and $V_{\not{R}_p}^{soft}$ are the soft SUSY breaking terms given in eqs. (6) and (7) while the last two terms are SUSY conserving D- and F-terms. The standard definition is (see review [2]):

$$F_n = \frac{@W}{@A_n}; \qquad D^a = gA_n T^a A_n: \tag{10}$$

Here W is the superpotential (2), A_n denotes a scalar component of a superfield, T^a are the gauge group generators and g is the corresponding gauge coupling. We do not reproduce a complete expression for the scalar potential of the $\not{R}_p$MSSM. It can be found in the literature. Analyzing the electroweak symmetry breaking one needs only that part of the scalar potential which contains electrically neutral colourless scalar fields. Let us write down this part of the scalar potential:

$$\begin{aligned} V_{neutral} = & \quad m_{H_2}^2 + j\tilde{}\,j^2 \quad jH_2^0j^2 + \overline{(M_L^2)} \quad + \quad \tilde{}\ \tilde{} \quad b\ \tilde{}\ H_2^0 + b\ \tilde{}\ H_2^0 \\ & + \frac{1}{8}(g_2^2 + g_1^2)\ jH_2^0j^2 \quad j\tilde{}\,j^2{}_2; \end{aligned} \tag{11}$$

where $\ ; \ = 0;1;2;3$ and $\tilde{} = (H_1^0; \tilde{}_i)$ with $\tilde{}_0 = H_1^0$. The $U(1)_Y$, $SU(2)_L$ gauge couplings are denoted as g_1, g_2. We also used the notations:

$$\begin{aligned} & \overline{(M_L^2)}_{ij} = (M_L^2)_{ij}; \qquad \overline{(M_L^2)}_{00} = m_{H_1}^2; \qquad \overline{(M_L^2)}_{0j} = \tilde{}_{1j}^2; \\ & \quad _0 = \quad ; \quad j\tilde{}\,j^2 \quad j\ j^2; \quad b_0 = B \ ; \quad b_j = \quad \tilde{}_{2j}^2: \end{aligned} \tag{12}$$

The electroweak symmetry breaking occurs when the fields involved in the potential (11) acquire non-zero vacuum expectation values (VEV): $\langle H^0_{1,2}\rangle = v_{1,2}$ and $\langle\tilde{\nu}_i\rangle = \omega_i$. The vacuum is defined by minimization conditions for the potential (11) which take the form:

$$(m^2_{H_2} + |\mu|^2)v_2 = b\,\omega - \frac{1}{4}(g_2^2 + g_1^2)(|v_2|^2 - |v_1|^2 - \sum_{k=1}^{3}|\omega_k|^2)v_2, \tag{13}$$

$$\left[(M^2_{\tilde{L}}) + \right]\omega = b\,v_2 + \frac{1}{4}(g_2^2 + g_1^2)(|v_2|^2 - |v_1|^2 - \sum_{k=1}^{3}|\omega_k|^2)\omega : \tag{14}$$

We use the notations $\omega = (v_1, \omega_i)$ with $\omega_0 = v_1$. From eq. (14) it follows that $\omega_i \neq 0$ unless the bilinear R-parity violating parameters do not vanish $\mu_k \neq 0, b_k \neq 0, (M_{\tilde{L}})_{n0} \neq 0$.

The presence of non-zero sneutrino VEVs changes the standard formula for the W-boson mass M_W. This follows from the fact that W-boson mass originates from the kinetic term

$$\sum_i (D\ \ _i)^{\dagger}(D\ \ _i),$$

where D is the gauge covariant derivative and $_i$ are the scalar fields in the theory including the $\tilde{\nu}_i$ fields. Thus, the sneutrino VEVs $\langle\tilde{\nu}_i\rangle = \omega_i$ contribute to the gauge boson masses

$$M_W = \frac{g_2 v}{2}, \qquad v = \sqrt{v_1^2 + v_2^2 + \sum_i^{3}\omega_i^2}. \tag{15}$$

As a consequence, ω_i and the angle defined by

$$\tan = \frac{v_2}{v_1} \tag{16}$$

for real v_i, may be regarded as free parameters of the theory, while v_i are not free any longer, but determined by

$$v_1 = \cos\sqrt{v^2 - \sum_i^{3}\omega_i^2}; \qquad v_2 = \sin\sqrt{v^2 - \sum_i^{3}\omega_i^2}. \tag{17}$$

Evidently, the VEVs of the scalar neutrinos, $\langle\tilde{\nu}_i\rangle = \omega_i$, cannot have arbitrarily large values, but they are bounded from above, as can be readily seen from eqs. (15) and (17).

2.3 R-parity violation and lepton mass matrices

In what follows we present the mass matrices of the neutral and charged fermion sectors of the $\not{R}_p$MSSM. Mixing within these sectors become possible in this model since R-parity is explicitly broken.

2.3.1 Neutral fermion mass matrix

The neutral fermion sector of the $\not{R}_p$MSSM consists of the following electrically neutral Weyl fermion fields: neutrinos ; the third component of the $SU(2)_L$ triplet gaugino $_3$; $U(1)_Y$ gaugino ^{0} and higgsinos $\tilde{H}^0_{1,2}$. Let us introduce the neutral fermion field

$$\Psi^0_{(0)} = (\ _e;\ \ ;\ \ ;\ \ i\,^0;\ \ i\,_3; \tilde{H}^0_1; \tilde{H}^0_2). \tag{18}$$

In this basis the mass term of the neutral fermions is

$$L^{(0)}_{mass} = \frac{1}{2}\ \Psi^0_{(0)} M\ \ ^0_{(0)} \quad H.c.: \tag{19}$$

The 7×7 mass matrix has the distinct see-saw structure

$$M_0 = \begin{pmatrix} 0 & m \\ m^T & M \end{pmatrix} \tag{20}$$

with $M \gg m$. Here the 3×4 matrix

$$m = \begin{pmatrix} M_Z s_W c u_1 & M_Z c_W c u_1 & 0 & {}_1 \\ M_Z s_W c u_2 & M_Z c_W c u_2 & 0 & {}_2 \\ M_Z s_W c u_3 & M_Z c_W c u_3 & 0 & {}_3 \end{pmatrix} \tag{21}$$

originating from the R_p bilinear terms in the superpotential (4) and the soft SUSY breaking sector (6). In eq. (20) M is the usual 4×4 MSSM neutralino mass matrix in the basis $\{ {}_i^0; {}_i, {}_3; \tilde{H}_1^0; \tilde{H}_2^0 \}$

$$M = \begin{pmatrix} M_1 & 0 & M_Z s_W c & M_Z s_W s \\ 0 & M_2 & M_Z c_W c & M_Z c_W s \\ M_Z s_W c & M_Z c_W c & 0 & 0 \\ M_Z s_W s & M_Z c_W s & 0 & 0 \end{pmatrix}. \tag{22}$$

Here $u_i = \langle \tilde{}_i \rangle / \langle H_1^0 \rangle$, $s_W = \cos_W$, $c_W = \cos_W$, $s = \sin$, $c = \cos$. The supersymmetric Higgs mass is defined in eq. (3). In the mass eigenstate basis

$$ {}_{(0)i} = {}_{ij} \, {}^0_{(0)j} \tag{23}$$

the 7×7 neutral fermion mass matrix M_0 (20) becomes diagonal

$$M_0 {}^{\dagger} = \mathrm{diag}\{m_i, m_k\}. \tag{24}$$

The lightest mass eigenstates with masses m_i are identified with the physical neutrinos while the remaining four mass eigenstates with the masses m_k are identified with the physical neutralinos. Remarkable, that as a result of the minimal field content and the gauge invariance the tree-level neutral fermion mass matrix M_0 (20) before diagonalization has such a structure that its first three rows and the last one are linearly dependent and, as a result, two neutrino mass eigenstates are degenerate massless states.

It is natural to identify the massive neutrino state with the tau neutrino $_3 =$ while the two massless states with the $_e$ and . The $_e$– mass degeneracy is lifted by the 1-loop corrections as well as by the non-renormalizable terms in the superpotential giving to $_e$, the small non-equal masses $m_e \neq m \neq 0$ [9]. The 1-loop corrections are discussed in this section below.

By the use of the matrix perturbation theory one may derive simplified formulas for the neutral fermion mass and mixing matrices which allow useful explicit representation for the non-zero neutrino mass m_3. As a small expansion parameter can be taken the matrix

$$= m \quad M^{-1} \tag{25}$$

with the following elements

$$_{i1} = \frac{g_1 M_2}{2 \det M} \; _i; \qquad _{i2} = \frac{g_2 M_1}{2 \det M} \; _i; \tag{26}$$

$$_{i3} = \frac{_i}{} + \frac{g_2 (M_1 + \tan^2 {}_W M_2) \sin \cos_W M_Z}{2 \det M} \; _i; \tag{27}$$

$$_{i4} = \frac{g_2 (M_1 + \tan^2 {}_W M_2) \cos \cos_W M_Z}{2 \det M} \; _i; \tag{28}$$

with $i = 1, 2, 3$. The determinant of the MSSM neutralino mass matrix (22) is

$$\det M = \sin 2 \; M_W^2 \quad (M_1 + \tan^2 {}_W M_2) \quad M_1 M_2 \; ^2. \tag{29}$$

and

$$_i = \ h_i i \quad hH_1^0 i_i : \tag{30}$$

To leading order in the small expansion parameters , an approximate form of the neutral fermion 7 7 mixing matrix introduced in eqs. (23) and (24) is [20]

$$= \begin{pmatrix} V^T & 0 \\ 0 & N \end{pmatrix} \begin{pmatrix} 1 & \frac{1}{2} & ^y \\ \frac{1}{2} & ^y & 1 \quad \frac{1}{2} & ^y \end{pmatrix} = \begin{pmatrix} V^{( )T}(1 \quad \frac{1}{2} & ^y) & V^{( )T} \\ N & ^y & N (1 \quad \frac{1}{2} & ^y) \end{pmatrix} : \tag{31}$$

The second matrix rotates $M_{\ 0}$ to the block-diagonal form $\mathrm{diag}(M \ ; M \ )$, separating the neutralino sector with the mass matrix M from the neutrino sector with the effective mass matrix

$$M \ = \ m \ M^{\ 1} m^T = Z \begin{pmatrix} 0 & & & 1 \\ & ^2 & & \\ & & ^2 & \\ & & & ^2 \end{pmatrix} \begin{matrix} & & \\ e & e & e \\ e & & \end{matrix} : \tag{32}$$

Here

$$Z = g_2^2 \frac{M_1 + \tan^2 \ _W M_2}{4 \det M} : \tag{33}$$

The $4 \quad 4$ matrix N rotates the MSSM neutralino mass matrix M to the diagonal form

$$N \ M \ N^y = \mathrm{diag}\{m \ _i\}; \tag{34}$$

where $m \ _i$ are the physical neutralino masses. Thus, to leading order in the mixing within the neutralino sector is described as in the MSSM by

$$_k = N_{kn} \ ^0_n \tag{35}$$

with $^0_n = (\ i^0; \ i_3; \tilde{H}_1^0; \tilde{H}_2^0)$ being the weak basis.

The $3 \quad 3$ matrix $V^{( )}$ rotates the effective neutrino mass matrix to the diagonal form

$$V^{( )T} M \ \ V^{( )} = \mathrm{diag}\{0; 0; m \ \}: \tag{36}$$

The only non-zero neutrino mass is given by

$$m \ = Z \ \ \tilde{j}^2 : \tag{37}$$

Let us show an explicit form of the neutrino mixing matrix

$$V^{( )} = \begin{pmatrix} & & \\ \cos \ _{13} & 0 & \sin \ _{13} \\ \sin \ _{23} \sin \ _{13} & \cos \ _{23} & \sin \ _{23} \cos \ _{13} \\ \sin \ _{13} & \sin \ _{23} & \cos \ _{13} \cos \ _{23} \end{pmatrix} ; \tag{38}$$

where the mixing angles are expressed through the vector $\tilde{}$ as follows:

$$\tan \ _{13} = \ \frac{1}{\sqrt{\frac{2}{2} + \ \frac{2}{3}}}; \qquad \tan \ _{23} = \frac{2}{3} : \tag{39}$$

The mixing within the neutrino sector to leading order in is described by

$$_k = V^{( )}_{nk} \ ^0_n \tag{40}$$

with $^0_n = (\ _e; \ ; \ )$ being the weak basis.

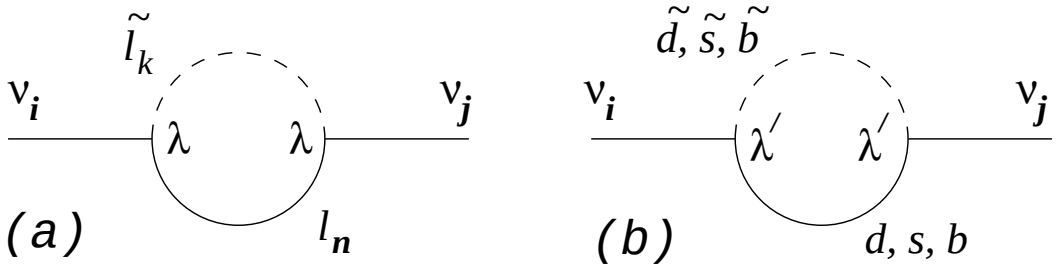

Fig. 1. 1-loop contributions to neutrino masses.

The non-zero neutrino mass in eq. (37) is subject to the experimental constraint m 23 MeV [21]. The m constraints can be evaded assuming an approximate alignment between the two vectors $a_i = (\ _i;\ )$ and $b_i = (h\tilde{\ }_i i; hH_1^0 i)$ which leads to the cancellation in (37) since $j\tilde{\ }j^2 = |a|^2|b|^2$ $(a\ b)^2$. This might be guaranteed by a special global symmetry [5, 7] or by some dynamical reasons [6].

We considered the tree level mass matrix of the neutral fermions of the $R\!\!\!/_p$ MSSM. Presence in the physical neutrino spectrum of the two degenerate massless neutrino states $_{1;2}$ indicates importance of the quantum 1-loop corrections in the neutrino sector.

At one-loop approximation the trilinear $R\!\!\!/_p$ couplings and ^{0} generate contributions to all entries of the neutrino mass matrix via the diagrams in Fig. 1 involving charged lepton-slepton and down-type quark-squark loops [4, 10, 11, 22].

The 1-loop neutrino mass matrix can be written in the form:

$$M_{\ 1\ loop} = M\quad + M\quad + M_{\ 0}; \tag{41}$$

where the first term is the tree level contribution (32) while the second and third ones are the contributions from the 1-loop diagrams in Fig. 1(a) and Fig. 1(b) respectively. Approximately one can write down

$$\begin{aligned} M_{\ (ij)} &\quad \sum_{m,n} \frac{_{inm}\ _{jmn}}{8\ ^2}\, m_{l(n)} m_{l(m)} \frac{A_{E(m)}\qquad \tan}{\tilde{m}_e^2}; \\ M_{\ 0(ij)} &\quad \sum_{k,l,m,n} \frac{3\ ^0_{inm}\ ^0_{jmn}}{8\ ^2}\, m_{d(n)} m_{d(m)} \frac{A_{D(m)}\qquad \tan}{\tilde{m}_d^2}: \end{aligned} \tag{42}$$

Here $\tilde{m}_e$ ($\tilde{m}_d$) is an averaged scalar mass and $A_{L,D}$ are the trilinear soft SUSY breaking parameters defined in (6).

Both contributions are proportional to the fermion mass product $m_{f(n)} m_{f(m)}$ which can be traced back to chiral structure of the $R\!\!\!/_p$ MSSM interactions. Indeed one factor $m_{f(n)}$ originates from the fact that neutrinos have only left-handed component and, therefore, the vertices of diagrams in Fig. 1 contain projection operators $P_L = (1\ _5)/2$ which peak up from the internal fermion propagator the fermion mass $P_L(m_f + k\ )P_L = m_f P_L$. Another factor $m_{f(m)}$ comes from the left-right sfermion mixing $\tilde{f}_L$–$\tilde{f}_R$ which is proportional to the corresponding fermion mass.

Assuming no strong hierarchy among the $A_{L(m)}, A_{D(m)}$ and $_{ijk}$, $^0_{ijk}$ the contributions with $m;n = 3$ dominate. Thus to get an order of magnitude estimate, one can write down

$$\begin{aligned} M_{\ (ij)} &\ , \quad \frac{_{i33}\ _{j33}}{8\ ^2} \frac{m_\tau^2 (A_\tau\qquad \tan)}{\tilde{m}^2} \qquad _{i33}\ _{j33}\ (4\quad 10^{-5}\ \text{eV}) \left(\frac{100\ \text{GeV}}{M_{SUSY}}\right); \\ M_{\ 0(ij)} &\ , \quad \frac{3\ ^0_{i33}\ ^0_{j33}}{8\ ^2} \frac{m_b^2 (A_b\qquad \tan)}{\tilde{m}_b^2} \qquad ^0_{i33}\ ^0_{j33}\ (8\quad 10^{-6}\ \text{eV}) \left(\frac{100\ \text{GeV}}{M_{SUSY}}\right); \end{aligned} \tag{43}$$

where M_{SUSY} is a typical SUSY breaking mass scale. Note that the neutrino mass matrix (41) generically leads to the three different non-zero neutrino mass eigenvalues $m_{\ 1} \neq m_{\ 2} \neq m_{\ 3} \neq 0$.

2.3.2 Charged fermion mass matrix

The mass term of the charged fermion sector has the following form

$$L^{(\ )}_{mass} = \quad ^T_{(\ )} M\quad ^0_{(+)} \quad H.c. \tag{44}$$

in the two component Weyl spinor basis

$$\Psi^{T}_{(-)} = (e_L;\ _L;\ _L;\ \ i\ ;\tilde{H^-_1}); \tag{45}$$

$$\Psi^{T}_{(+)} = (e^+_L;\ ^+_L;\ ^+_L;\ \ i_+;\tilde{H^+_2}): \tag{46}$$

The 5 5 charged fermion mass matrix is

$$M = \begin{pmatrix} M^{(l)} & E \\ E^0 & M \end{pmatrix}; \tag{47}$$

where M is the MSSM chargino mass matrix

$$M = \begin{pmatrix} M_2 & \sqrt{2}M_Z c_W s \\ \sqrt{2}M_Z c_W c & \end{pmatrix}: \tag{48}$$

The sub-matrices E and E^0 lead to the chargino–lepton mixing. They are defined as

$$E = \begin{pmatrix} 0 & \sqrt{2}M_Z c_W c\, u_1 & {}_1 \\ \sqrt{2}M_Z c_W c\, u_2 & {}_2 & \\ \sqrt{2}M_Z c_W c\, u_3 & {}_3 & \end{pmatrix} \quad \text{and} \quad E^0 = \begin{pmatrix} 0 & 0 & 0 \\ M^{(l)}_{1i} u_i & M^{(l)}_{2i} u_i & M^{(l)}_{3i} u_i \end{pmatrix}; \tag{49}$$

where $M^{(l)}$ is the charged lepton mass matrix. In a good approximation it can be treated as a diagonal matrix $M^{(l)} = \mathrm{diag}\{m^{(l)}_i\}$ with $m^{(l)}_i$ being the physical lepton masses. Also, one can safely neglect matrix E^0 compared to the other entries of the full mass matrix (47) taking into account smallness of the lepton masses.

Rotation to the mass eigenstate basis

$$_{(-)i} = \ _{ij}\ ^0_{(-)j}; \tag{50}$$

casts the mass matrix (47) to a diagonal form

$$M\ \ ^{+\ Y} = \mathrm{diag}\{m^{(l)}_i; m_{\ k}\}; \tag{51}$$

where $m^{(l)}_i$ and $m_{\ k}$ are the physical charged lepton and chargino masses.

To leading order in the small expansion parameters ^{L} and ^{R} defined below, an approximate form of the charged fermion 5 5 mixing matrix introduced in eqs. (50) and (51) reads

$$= \begin{pmatrix} V_L(1 - \frac{1}{2}\ ^L\ ^{L^T}) & V_L\ ^L \\ U\ ^{L^T} & U\ (1 - \frac{1}{2}\ ^{L^T}\ ^L) \end{pmatrix}; \tag{52}$$

$$^{+\ Y} = \begin{pmatrix} (1 - \frac{1}{2}\ ^R\ ^{R^T})V^Y_R & {}^R V^Y \\ {}^{R^T} V^Y_R & (1 - \frac{1}{2}\ ^{R^T}\ ^R)V^Y \end{pmatrix}: \tag{53}$$

Here

$$^L_{i1} = \frac{g_2}{\sqrt{2}\ \det M}\ _i; \qquad ^L_{i2} = -\frac{g_2 \sin\ \cos_W M_Z}{\det M}\ _i; \tag{54}$$

with i= 1;2;3 and

$$^R = M^{(l)y}\ ^L\ \ M^{\ 1\ T}: \tag{55}$$

This matrix is much smaller than ^{L} by the factor m_l/M_{SUSY}, where m_l and M_{SUSY} are the lepton masses and the typical SUSY breaking scale M_{SUSY} 100 GeV. Thus the mixing between $(\tilde{e}^+_L;\ ^+_L;\ ^+_L)$

and ($_i$; H_2^+) described by the o diagonal blocks of the $^+$ in (53) is small and, therefore, can be neglected in the phenomenological analysis. In eqs. (52) and (53) the determinant of the MSSM chargino mass matrix is

$$\det M \quad = M_2 \quad \sin 2 \; M_W^2 : \tag{56}$$

The other matrices are defined as follows:

$$\begin{aligned} U \; M \quad V^y &= \text{diag}\{m \; _i\}; \\ V_L M^{(1)} V_R^y &= \text{diag}\{m_{l_i}\}: \end{aligned} \tag{57}$$

To the leading order in $_{L,R}$ the eigenvalues $m \; _i$ and m_{l_i} can be treated as masses of the physical charginos and the charged leptons respectively.

2.4 Some issues of the choice of the field basis

Before going to the phenomenological implications of the $R\!\!\!/_p$ MSSM it is instructive to survey some general properties of the trilinear and bilinear $R\!\!\!/_p$ terms in its Lagrangian. Mixing of the fields in the gauge basis caused by non-diagonality of the mass matrices and by the presence of the bilinear terms brings in specific aspects into phenomenology of the $R\!\!\!/_p$ MSSM and requires special care of the field basis definition. These questions are rather widely discussed in the literature. In the subsequent two subsections we just briefly survey some issues of the choice of the basis for the fields.

2.4.1 Trilinear terms

Let us first write down the Lagrangian corresponding to the trilinear part of the $R\!\!\!/_p$ superpotential $W_{R\!\!\!/_p}$ in gauge (current) eigenstate basis:

$$L_{R\!\!\!/_p} = \tag{58}$$

$$_{fijgk} \Big[\tilde{}_{iL} e_{kR} e_{jL} + \tilde{e}_{jL} e_{kR} \; _{iL} + \tilde{e}^{?}_{kR} \overline{(\; _{iL})^c} e_{jL} - \tilde{}_{jL} e_{kR} e_{iL} - \tilde{e}_{L} e_{kR} \; _{jL} - \tilde{e}^{?}_{kR} \overline{(\; _{jL})^c} e_{iL} \Big]$$

$$+ \; ^{0}_{ijk} \Big[\tilde{}_{iL} d_{kR} d_{jL} + \tilde{d}_{jL} d_{kR} \; _{iL} + \tilde{d}^{?}_{kR} \overline{(\; _{iL})^c} d_{jL} \tag{59}$$

$$- \tilde{e}_{L} d_{kR} u_{jL} - \tilde{u}_{jL} d_{kR} e_{jL} - \tilde{d}^{?}_{kR} \overline{(e_{iL})^c} u_{jL} \Big]$$

$$+ \; ^{00}_{ifjkg} \Big[\tilde{u}^{?}_{iR} \; d_{kR} \; d^{c}_{jR} + \tilde{d}_{jR} \; e_{kR} \; u^{c}_{iR} + \tilde{d}^{?}_{kR} \; \overline{(u_{iR} \;)^c} d_{jR} \Big] + H.c.: \tag{60}$$

The subscripts , , stand for the colour.

Most of the existing experimental bounds on the trilinear coupling constants $_{ijk}$, $^{0}_{ijk}$, $^{00}_{ijk}$ have been derived utilizing the so-called single coupling hypothesis. It assumes that a single coupling constant dominates over all the others, so that essentially only the considered coupling constant contributes [22, 23]. This simplifying approach requires special attention to the choice of the basis for the quark fields. Of course, the physics is basis independent. The point is that the single coupling hypothesis makes the constraints derived on ^{0} basis dependent. An important variant of the single coupling hypothesis is defined at the level of the gauge basis of the quark fields rather than at the level of the mass eigenstate fields. This appears as a more natural assumption in models where the hierarchies in the trilinear couplings originate from physics at higher energy scales. In that case, even if there were only one particular nonzero ^{0}-coupling, quark mixing would generate a plethora of such couplings, related to one another. In what follows we do not confine ourselves to this particular situation, but rather consider the most general lepton number violating $R\!\!\!/_p$ sector.

Note also the following subtlety of the field rotation. Since the Cabibbo-Kobayashi-Maskawa matrix V_{CKM} is different from identity, the $SU(2)_L$ symmetry of the ^{0} terms is no longer manifest itself when expressed in terms of the mass eigenstates.

Let us rewrite the ^{0}-part of the superpotential $W_{\not R_p}$ (4) in the quark mass basis. It can be realized in various ways. The most common representations of $W_{\not R_p}$ in the mass basis are the following two:

$$W(^0) = {}^0_{ijk}(_i d^0_j \quad e_i u^0_j)(d^0_k)^c = {}^{0A}_{ijk}(_i V_{jn} d_n \quad e_i u_j) d^c_k = {}^{0B}_{ijk}(_i d_j \quad e_i V_{jn} u_n) d^c_k; \tag{61}$$

where the superscript in the quark superfields u^0 and d^0 denotes the gauge basis. The rotated couplings take the form

$${}^{0A}_{ijk} = {}^0_{imn}(V_L^{uy})_{mj}(V_R^{dT})_{nk}; \qquad {}^{0B}_{ijk} = {}^0_{imn}(V_L^{dy})_{mj}(V_R^{dT})_{nk}: \tag{62}$$

The matrix rotating the quark fields to the mass basis are defined as:

$$u_{L,R} = V^u_{L,R} \quad {}^0_{L,R}; \qquad d_{L,R} = V^d_{L,R} \quad {}^0_{L,R} \tag{63}$$

and $V \quad V_{CKM} = V_L^u V_L^{dy}$ is the quarks unitary CKM matrix.

The representations with the coupling constants, ${}^{0A}_{ijk}$ or ${}^{0B}_{ijk}$, allow for the presence of flavour changing contributions in the d-quark or u-quark sectors respectively, even when a single $\not R_p$ coupling constant is assumed to dominate [24]. In eqs. (61) we neglected the effects of possible non-alignment of fermion and sfermion mass matrices since such non-alignment is already severely constrained [25, 26].

The ^{0} part of the Lagrangian (59) in the representation B can then be expressed as

$$\begin{aligned} L_{\,0} = {}^{0B}_{ijk}\Big[& \tilde{}_{iL}\overline{d_{kR}}d_{jL} + \tilde{d}_{jL}\overline{d_{kR}}\,{}_{iL} + \tilde{d}^*_{kR}\overline{(\,{}_{iL})^c}d_{jL} \\ & \sum_p V^y_{jp}\big[\tilde{e}_{iL}\overline{d_{kR}}u_{pL} + \tilde{u}_{pL}\overline{d_{kR}}e_{iL} + \tilde{d}^*_{kR}\overline{(e_{iL})^c}u_{pL}\big] + H.c.:\Big] \end{aligned} \tag{64}$$

Having in mind that there is no physical preferences in the field basis, it is instructive to look for basis independent quantities characterizing the strength of R-parity violation. The two sets of mass basis coupling constants, ^{0A,B} and the current basis coupling constants, ^{0}, obey the unitarity sum rule type relations:

$$\sum_{jk} |\,{}^{0A,B}_{ijk}|^2 = \sum_{jk} |\,{}^0_{ijk}|^2: \tag{65}$$

A classification of all possible invariant products of the $\not R_p$ coupling constants has been examined in [27]. Assuming that the linear transformation matrices, $V^{q,l}_{L,R}$, were known, and that one is given a bound on some interaction operator, then by applying the single coupling hypothesis to the current basis coupling constants, one could derive a string of bounds associated to the operators which mix with it by the fields transformations from the gauge to the mass basis. For example, assuming $(V^u_L)_{1i} = (V^u_R)_{1i} = (1; \ ; {}^0)$, starting from the bound on ${}^0_{111}$, one can deduce the following related bounds: ${}^0_{121} < {}^0_{111}= \ ; \ {}^0_{131} < {}^0_{111}= {}^0$ [28].

2.4.2 Bilinear terms

The bilinear terms, ${}_iL_iH_2$ in (4), violate both R-parity and L_i numbers. The physical effects of these interactions are parameterized by 6 parameters, ${}_i$, and the sneutrinos VEVs $!_i$. There are two distinct realization of R-parity violation: spontaneous when ${}_i = 0, !_i \neq 0$ and explicit when ${}_i \neq 0, !_i = 0$ or ${}_i \neq 0, !_i \neq 0$. Viable models of the explicit and spontaneous R-parity violation have been constructed in the literature. A phenomenologically viable version of spontaneous R-parity violation can be realized in models with the gauge singlet right-handed neutrinos. In this case R-parity and lepton numbers are broken by a right-handed sneutrino VEV, $h\tilde{}_R i \neq 0$. A gauge singlet Goldstone boson, the so-called majoron, which originates from the broken global $U(1)_L$ symmetry of the total lepton number, L, decouples from the gauge interactions and, therefore, its presence does not affect existing experimental constraints [11, 12, 22, 29].

The bilinear terms $_iL_iH_2$ are particularly interesting due to the fact that they can cause a mixing between charginos and charged leptons as well as between neutralinos and neutrinos. This gives rise to new observable effects compared to the case when only $R\!\!\!/_p$ Yukawa interactions are taken into account. One of these distinctive effects is that, the lightest neutralino can decay invisibly into three neutrinos, which is not possible if only the $R\!\!\!/_p$ Yukawa terms in $W_{R\!\!\!/_p}$ (4) are present. Implications of the bilinear $R\!\!\!/_p$ terms in the scalar sector of the theory are also rather peculiar and have been investigated recently in the literature [8]. The significance of such bilinear R-violating interactions is supported by the following observations. Although it possible to rotate away the $_iL_iH_2$-terms in the superpotential $W_{R\!\!\!/_p}$ by the redefinition of the lepton and Higgs superfields, as discussed below, they creep into the phenomenology via the scalar potential $V^{soft}_{R\!\!\!/_p}$ (6). Another point is that even if one may rotate away these terms at one energy scale, they reappear at another scale due to the renormalization effects [30]. Moreover, the $$- and ^{0}-terms themselves generate the bilinear terms at the one-loop level [31]. It has been also argued that if R-parity violation is derived from the GUTs then the trilinear interactions in $W_{R\!\!\!/_p}$ are naturally rather small like $O(10^{-3})$ [4]. Whereas, the superrenormalizable bilinear terms $_iL_iH_2$ are not suppressed.

Now, let us survey some general features of the bilinear $R\!\!\!/_p$ terms.

In the limit of vanishing superpotential, the minimal supersymmetric standard model possesses an SU(4) global symmetry which transforms the column vector of Higgs boson and leptons chiral supermultiplet fields,

$$\begin{pmatrix} H_1 \\ L_i \end{pmatrix} \;\to\; U \begin{pmatrix} H_1 \\ L_i \end{pmatrix}, \tag{66}$$

where U is an unitary matrix in SU(4). The symmetry group SU(4) reduces to SU(3) by switching on the bilinear R-parity odd superpotential term $_iL_iH_2$ and is completely broken down by switching on matter–Higgs-bosons trilinear interactions. For vanishing $!_i$, one can apply the superfield transformation,

$$U = \frac{1}{\sqrt{2}} \begin{pmatrix} 1 & {}_i \\ {}_i & 1 \end{pmatrix}, \quad \text{with} \quad {}_i = \frac{!_i}{}, \quad = \sqrt{\sum_i !_i^2}, \tag{67}$$

so as to rotate away the lepton–Higgs-boson mixing terms, leaving behind the Higgs boson mixing superpotential term, H_2H_1, along with trilinear R-parity odd interactions of specific structure,

$$_{ijk} = \frac{1}{2}\left(h^E_{ji\,k} - h^E_{jk\,i}\right), \qquad ^0_{ijk} = \frac{{}_i h^D_{jk}}{\sqrt{2}}. \tag{68}$$

For non-vanishing three-vector of VEVs, $!_i$, the remnant SU(3) symmetry is spontaneously broken down to SU(2). This induces bilinear mass terms which mix neutrinos with neutralinos and charged leptons with charginos. Combining these terms with the lepton–higgsino $_iL_i\tilde{H}^-_1$ mixing from the superpotential (4) we end up with 7×7 neutral fermion and 5×5 charged fermion mass matrices as explained in sect. 2.3. Rotating the MSSM Lagrangian to the mass eigenstate basis one obtains the new lepton number and lepton flavor violating interactions. These interactions bring many interesting implications for the low and high energy phenomenology. In sect. 5 we consider the effect of these $R\!\!\!/_p$-operators in the neutrinoless double beta decay and muon–electron conversion.

2.5 R-parity and other discrete symmetries

Lepton and baryon number violating terms in the superpotential $W_{R\!\!\!/_p}$ (4) and in the soft SUSY breaking scalar potential $V_{R\!\!\!/_p}$ (6) may lead to unacceptably fast proton decay. It may happen via products of the lepton and baryon number violating couplings like ^{00}, ^{00} and $^{00}_i$ as illustrated in Fig. 2(a) and Fig. 5. In order to obey the experimental limits on the proton lifetime these coupling combinations must be so small that it is more natural to assume that they are forbidden at all. This can be assured

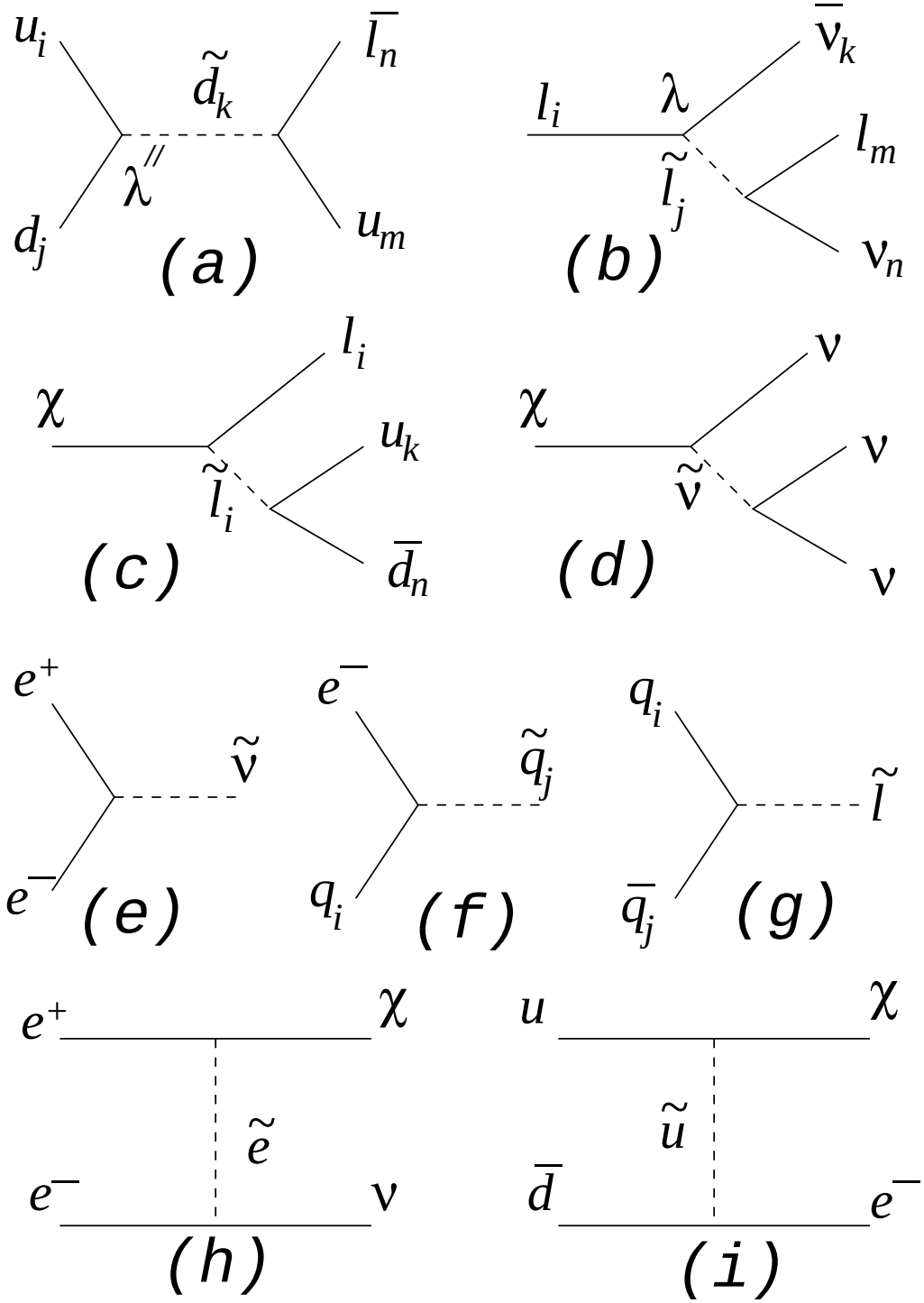

Fig. 2. Various R-parity violating processes.

by imposing a certain symmetry. Farrar and Fayet [3] proposed in 1978 a discrete Z_2 symmetry, known as R-parity, acting on the superpotential and soft SUSY breaking terms as

$$\begin{aligned} \hat{R}\ W_{R_p} &= W_{R_p}; \qquad \hat{R}\ W_{\not R_p} = -W_{\not R_p}; \\ \hat{R}\ V_{R_p} &= V_{R_p}; \qquad \hat{R}\ V_{\not R_p} = -V_{\not R_p}: \end{aligned} \tag{69}$$

The multiplicative quantum number

$$R_p = (-1)^{3B+L+2S} \tag{70}$$

is assigned to each MSSM field with the spin S, baryon B and lepton L numbers. According to this definition, the R_p of the ordinary SM field is +1 and R_p of the superpartners is −1.

Being imposed on the MSSM as an ad hoc symmetry it forbids R-parity violating interactions and automatically guarantees the B and L conservation at the level of renormalizable operators. Late on we will see that it is not the case for the non-renormalizable operators.

The R-parity is not a unique solution of the proton stability problem in the MSSM. An alternative discrete symmetry with an equivalent physical effect is the matter parity transforming the superfields as

$$(L_i; E_i; Q_i; U_i^C; D_i^C) \to (L_i; E_i^C; Q_i; U_i^C; D_i^C), \qquad (H_2; H_1) \to (H_2; H_1). \tag{71}$$

R-parity and matter parity conservation forbid all the terms $W_{\not R_p}; V_{\not R_p}$ and thus protect the proton from decay. Recall that the proton decay happens if both lepton and baryon violating couplings are present. Thus, in place of R_p one may choose a less restrictive discrete symmetry which forbids either B- or L-violating couplings. A known example is the B-parity symmetry acting differently on the quarks and leptons:

$$(Q_i; U_i^C; D_i^C) \to (Q_i; U_i^C; D_i^C), \qquad (L_i; E_i^C; H_2; H_1) \to (L_i; E_i^C; H_2; H_1). \tag{72}$$

This symmetry protects the proton but allows the $\not R_p$ operators $L_iL_jE_k^C$ and $L_iQ_jD_k^C$ of the $\not L$- type. On the contrary, if only the $\not R_p$ interactions $U_i^C D_j^C D_k^C$ of the $\not B$- type are allowed, the proton is also stable provided that it is lighter than the lightest supersymmetric particle (LSP). This possibility can be realized by introducing L-parity defined as

$$(L_i; E_i^C) \to (L_i; E_i^C), \quad (Q_i; U_i^C; D_i^C; H_1; H_2) \to (Q_i; U_i^C; D_i^C; H_1; H_2). \tag{73}$$

This symmetry does not prevent the proton decay, if the proton mass is $m_p > m_{\pi^+} + m_{\pi^0}$ where m_{π^+} and m_{π^0} are the lightest neutralino and the pion masses. In this case the decay $p \to \pi^+ + \pi^0$ becomes possible.

In the literature one can find other examples of discrete symmetries which stabilize the proton (see, for instance, [32]).

2.6 Theoretical reasons for R-parity (non-)conservation

We start our discussion of motivations for the R-parity (non-)conservation with the following note. The ad hoc R-parity symmetry imposed on a theory is not sufficient for suppressing all the dangerous B and L violating interactions. It successfully excludes these interactions only at the level of renormalizable operators. Treating the MSSM as an effective theory, which represents the low-energy limit of a more fundamental theory acting at the high-energy scale M_X, one must take care of all possible gauge invariant non-renormalizable operators. In this logic one may write down, for instance, the following superpotential terms:

$$\begin{aligned} W_3 = {} & \frac{(z_1)_{ijkl}}{M_X}(Q_iQ_j)(Q_kL_l) + \frac{(z_2)_{ijkl}}{M_X}(U_i^C U_j^C D_k^C)E_l^C + \frac{(z_3)_{ij}}{M_X}(L_iL_j)(H_2H_2) \\ & + \frac{(z_4)_{ijk}}{M_X}(Q_iQ_j)(Q_kH_1) + \frac{(z_5)_{ijk}}{M_X}(Q_iH_1)(U_j^C E_k^C) + \frac{(z_6)_i}{M_X}(L_iH_1)(H_2H_2). \end{aligned} \tag{74}$$

It is readily seen that the first three operators respect R-parity but violate B and L.

As was already mentioned, the discrete symmetries discussed in the previous section have no deep theoretical motivation other than to ensure stability of the proton. All those symmetries have no a priori preference from this stand point. The question of which of these symmetries, if any, are realized in the Nature should be addressed to a more fundamental theory at the high-energy scale M_X. Let us shortly discuss several concrete examples.

2.6.1 Grand Unified Theories (GUT)

In the GUT framework quarks and leptons typically belong to the same multiplets and, therefore, have the same quantum numbers. On the contrary, the discrete symmetries of $\not R_p$-type like L- or B-parities

typically distinguish quarks and leptons. This fact causes certain problems for reconciling the GUT structure with the discrete symmetries of the discussed class. The GUT models leading at low energies to $\not{R}_p$ have been constructed in the literature [4], [33]–[38].

The R-parity violation is typically derived in this framework from the non-renormalizable operators involving Higgs fields at the GUT scale M_X. These operators become renormalizable $\not{R}_p$–operators after the GUT symmetry breaking. The models of this type have been constructed for the gauge groups SU(5) [4, 34], SO(10) [34] and SU(5) $\times$ U(1) [33, 34]. These models by construction create at low energies $\not{R}_p$ operators either of L-type LLE^c, LQD^c, or of B-type $U^cD^cD^c$. Therefore, the proton is stable since the lepton and baryon number violating couplings are not simultaneously present.

However, in this approach one must introduce certain additional symmetry beyond the GUT gauge group in order to ensure that only the required set of non-renormalizable operators are allowed. This is equally true for both R_p-conservation and $\not{R}_p$. Thus in grand unified models we do not find a preference for either R_p-conservation or $\not{R}_p$.

2.6.2 String theory

The unification can be achieved in string models not only on the basis of a simple gauge group unlike in the GUT models. This fact allows one to arrange distinct quantum numbers for quark and lepton superfields. Therefore, the discrete symmetries like B – or L–parities can be naturally realized in this approach. R-parity can be also accommodated in this framework. In the literature both R_p-conserving and $\not{R}_p$ string theories have been constructed [39]. At present, string theories do not make reasonable preference for either of these two possibilities.

2.6.3 Discrete gauge symmetries

In case a discrete symmetry is a remnant of a broken gauge symmetry it is called a discrete gauge symmetry. It has been argued that quantum gravity effects maximally violate all discrete symmetries unless they are discrete gauge symmetries [40]. The condition that the underlying gauge symmetry is anomaly-free can be translated into conditions on the discrete symmetry. A systematic analysis of all Z_N symmetries [41] has been performed. It was found that only two symmetries were discrete gauge anomaly-free: R_p and B–parity (72). B–parity was slightly favoured since in addition it prohibits dimension-5 proton-decay operators. It has since been shown [42] that the non-linear constraints in [41] are model dependent and thus possibly allowing a larger set of discrete symmetries. Several examples of the gauged models with $\not{R}_p$ have been constructed in the literature [5, 43]

Summarizing the discussion of possible theoretical motivations for the R-parity we conclude that at present there is no convincing preference between the SUSY models with or without R-parity conservation. Thus, searching for the SUSY we have to pay equal attention to both options of SUSY models which have rather different phenomenology. In the next sections we are addressing the question of what window for the $\not{R}_p$ is allowed by the existing experimental data.

2.7 R-parity violation: main changes in SUSY phenomenology

Changes introduced by the R-parity violation to the SUSY phenomenology are caused by the presence of lepton and baryon number violating operators in the $\not{R}_p$ SUSY Lagrangian. They lead to the following generic features the $\not{R}_p$ SUSY phenomenology:

Baryon– and/or lepton–number violating processes become possible. The proton decay triggered by the subprocess in Fig. 2(a) as well as some exotic processes such as $\quad ! \; e^+ \; + \; + \; _e$ in Fig. 2(b) are a priori not forbidden.

Neutrinos acquire Majprana type masses from mixing with gauginos and higgsinos as well as from the 1–loop corrections (Fig. 1).

The LSP is not stable and can decay in a detector or outside according to the diagrams in Fig. 2(c,d). The invisible decay mode in Fig. 2(d) involves $\tilde{\nu}$-vertex generated by the bilinear term .

Being unstable the LSP is no longer a good dark matter candidate.

The neutralino is not necessarily the LSP. The latter can be any of the following

$$\text{LSP} \quad 2 \quad \{ {}^{0}_{1};\ {}_{1};\tilde{g};\tilde{q};\tilde{t};\tilde{\nu};\tilde{g} \}: \tag{75}$$

In each case the collider phenomenology can be quite distinct.

The single production of supersymmetric particles is possible. Examples of the corresponding subprocesses are given in Fig. 2(e–i).

In the rest of the paper we will focus on the phenomenological implications of the R-parity violation for the low-energy processes mainly those which are observed or might be observed in non-accelerator experiments. We do not exclude from our consideration accelerator searches but touch this subject only superficially referring readers for more comprehensive discussion to recently appeared reviews, for instance [16, 44].

3 Lepton properties and decays

In this section we turn to the leptonic sector of the $\not{R}_p$MSSM where we find distinct effects which allow one to derive from their non-observation very stringent constraints on the R-parity violation. One of the most prominent consequence of the R-parity violation is an appearance of small non-zero Majorana neutrino mass. Various lepton number violating processes represent an inherent feature of R-parity non-conservation as well. The most precise low-energy measurements in leptonic physics are the lepton flavor-violating decays such as $\to e\gamma$, $\to eee$, the anomalous magnetic moment of the muon a, and the EDM of the electron. They are very sensitive probes of physics beyond the SM in general and the R-parity violating SUSY extensions of the SM in particular.

3.1 Neutrino masses and mixings in presence of R-parity violation

The problem of neutrino masses and mixings has been in focus of particle physics since 60's when the idea of neutrino oscillations was formulated [45]. Despite heavy experimental efforts the neutrino masses have not yet been unambiguously detected. Only recently the atmospheric neutrino experiment Super-Kamiokande [46] derived the first indication of neutrino oscillations. If true, it would mean presence of non-zero neutrino masses and non-trivial mixing. We will return to this question in the next subsection.

What is firmly established at present is the following set of upper limits [21]:

$$m_{e} \quad 4.5\ \text{eV}; \qquad m \quad 160\ \text{keV}; \qquad m \quad 23\ \text{MeV} \tag{76}$$

derived from the direct experimental searches. These limits can place certain constraints on the $\not{R}_p$SUSY parameters.

As discussed in sect. 2.3.1 in the $\not{R}_p$ SUSY framework the neutrino Majorana mass matrix M receives the contribution from the bilinear $\not{R}_p$ terms at tree level via the neutrino–gaugino–higgsino mixing and from the trilinear $\not{R}_p$ couplings at 1-loop level via the lepton–slepton and quark–squark neutrino self-energy loops. Thus, one obtains for neutrino masses

$$m \quad m^{\text{tree}}; \qquad m_{e} \quad {}^{1\ \text{loop}}_{e}; \qquad m \quad {}^{1\ \text{loop}}. \tag{77}$$

Here m^{tree} is the tree-level contribution given by (37). The 1-loop contributions ${}^{1\ \text{loop}}_{e;}$ can be derived from eqs. (41)–(43). Assuming no cancellation between different terms in r.h.s. of (77) one obtains from

the experimental bounds

$$\begin{aligned} {}_i &< 15 \quad \tilde{R}^{1=2}\,\mathrm{GeV}; \quad h\tilde{\nu}_i i < 7 \quad \tilde{R}^{1=2}\,\mathrm{GeV}; \\ {}_{133} &< 3 \quad 10^{3} \quad \tilde{R}^{1=2}; \quad {}^{0}_{133} < 7 \quad 10^{4} \quad \tilde{R}^{1=2}; \quad {}^{0}_{122} < 2 \quad 10^{2} \quad \tilde{R}^{1=2}; \end{aligned} \tag{78}$$

where $R = M_{SUSY}=(100\,\mathrm{GeV})$ with M_{SUSY} being the typical SUSY breaking scale. Of course, these bounds are only indicative and may essentially vary from point to point in the MSSM parameter space.

3.2 Solar and atmospheric neutrinos constraints on $\tilde{R}_p$ SUSY

Now, let us turn to neutrino oscillations in vacuum. The survival probability for a given neutrino flavor is described by the formula [47]

$$P(\quad !\quad) = 1 \quad 4\sum_{i<j} P_{\ j}P_{\ i}\sin^2\frac{m^2_{ji}\quad L}{4E}; \tag{79}$$

where E and L are the energy of a neutrino beam and the distance between a detector and a neutrino source. We also use the notations: $m^2_{ji} = m^2_{\ j} \quad m^2_{\ i}$ and $P_{\ j} = V^{(\ )^2}_{j}$. The neutrino mixing matrix $V^{(\ )}_{j}$ in the $\tilde{R}_p$ MSSM is defined according to eq. (38).

From the combined fit to the Super-Kamiokande [46] and the CHOOZ [48] data the following constraints at 95% C.L. were recently found in [49]:

$$0{:}5 \qquad m^2_{atm}=(10^{\ 3}\,\mathrm{eV}^2) \quad 10{:}0; \tag{80}$$

$$0{:}00 \qquad P_{e3} \quad 0{:}08; \tag{81}$$

$$0{:}25 \qquad P_{\ 3} \quad 0{:}75; \tag{82}$$

$$0{:}25 \qquad P_{\ 3} \quad 0{:}75{:} \tag{83}$$

The analysis of [49] was made under the assumption $|\,m^2_{atm}\,| >> |\,m^2_{sol}|$, with $m^2_{atm} = \quad m^2_{32} \qquad m^2_{31}$ and $m^2_{sol} = \quad m^2_{21}$. This covers a particular case of the $\tilde{R}_p$ MSSM neutrino mass spectrum in eq. (36) which leads to the relations

$$m^2_{atm} = \quad m^2_{32} = \quad m^2_{31} = m^{\ 2}_{\ 3} = F^2_{M\,SSM}\left(\sum_{\quad}^{\quad} \quad j\ \tilde{j}^{\ 2}\right)^2: \tag{84}$$

and $m^2_{atm} >> \quad m^2_{sol} = m^{\ 2}_{\ 2} \quad m^2_{\ 1}$ since $m_{\ 1;2}$ are zero at the tree level.

The mixing parameters in (81){(83) are determined by the tree level mixing matrix (38) as

$$P_{\ 3} = \frac{\left(\sum_{\quad}^{\quad} \quad j\ \tilde{j}^{\ 2}\right)^2}{\sum_{\quad}^{\quad} \quad j\ \tilde{j}^{\ 2}}: \tag{85}$$

It is useful to introduce the effective SUSY parameters [50]

$$A \qquad ^2 \quad F_{M\,SSM} = P_{\ 3} \quad \sqrt{m^2_{atm}}: \tag{86}$$

An advantage of these parameters for the analysis follows from the fact that they depend on the $\tilde{R}_p$ parameters $h\tilde{\nu}\ i$, from only one generation unlike parameters $P_{\ 3}$, m^2_{atm}, depending on the $\tilde{R}_p$ parameters from different generations.

Equations (80){(83) cast the constraints on the effective parameters A [50]:

$$0 \quad A_e \quad 8 \quad 10^{\ 3}\,\mathrm{eV}; \quad 5{:}6 \quad 10^{\ 3}\,\mathrm{eV} \quad A_{\ ,} \quad 7{:}5 \quad 10^{\ 3}\,\mathrm{eV}: \tag{87}$$

This constraint represents a complex exclusion condition imposed by the neutrino oscillation data on the $\tilde{R}_p$ MSSM parameter space.

It is instructive to obtain typical individual constraints on the superpotential parameters and on the sneutrino vacuum expectation values $h\tilde{\nu}_i$. These constraints can be derived from (87) at typical weak scale values of the MSSM parameters $M_{1,2}$ M_{SUSY}. Here M_{SUSY} is a characteristic SUSY breaking mass scale varying most likely in the interval $100\ GeV < M_{SUSY} < 1\ TeV$ motivated by non-observation of the SUSY particles and by the "naturalness" arguments. Following common practice, one can also assume absence of a significant cancellation between the two terms in definition of given in eq. (30). Thus, one comes up with the following constraints [50]:

$$f\begin{pmatrix}0\\ 66\ KeV\end{pmatrix}\frac{|\langle\tilde{\nu}_i\rangle|}{\bar{p}\,\bar{x}}\ f\begin{pmatrix}78\ KeV\\ 240\ KeV\end{pmatrix};\qquad = e,\ = ; \tag{88}$$

$$f\begin{pmatrix}0\\ 27\ KeV\end{pmatrix}\frac{|\ |}{x^{3=2}\sqrt{1+t^2}}\ f\begin{pmatrix}32\ KeV\\ 96\ KeV\end{pmatrix};\qquad = e,\ = ; \tag{89}$$

where $f = \sqrt{|0.8\ x^{\ 2}\sin 2\ \ 1|}$ and $x = (M_{SUSY}/100\ GeV)$, $t = \tan\ $. At $x\ \ 2$ the function f very weakly depends on x and $\sin 2\ $ and with acceptable precision can be replaced with the constant $f\ \ 1$. Equations (88) and (89) allow one to determine the typical limits on $h\tilde{\nu}_i;\ $ at various values of the $\tan\ $ and the SUSY breaking mass scale M_{SUSY}.

It is interesting to note that in the $R\!\!\!/_p$ MSSM the generation average Majorana neutrino mass is given at tree level by the formula:

$$hm\ i = \sum_i m_{\ i}\ V_{ei}^{(\ )\ 2} = P_{e3}\ \sqrt{m^2_{atm}}\ : \tag{90}$$

Thus, it is expressed in terms of the neutrino oscillation parameters.

As is known the parameter $hm\ i$ plays a clue role in the phenomenology of the $0\ \ $-decay. It determines the classical Majorana neutrino exchange contribution to the $0\ \ $-decay half-life as [51]

$$[T^0_{1=2}\ \ (0^+\ !\ \ 0^+)]^{\ 1} = G_{01}|M\ \ |^2\ \frac{hm\ i}{m_e}^2\ : \tag{91}$$

Here G_{01} and $M\ \ $ are the phase space factor and the nuclear matrix element. For $0\ \ $-decay of ^{73}Ge one has $G_{01} = 7.93\ \ 10^{15}\ years^{\ 1}$ [52] and $M\ \ = \ \ 3.4$ [53]. The contribution (91) represents a dominant effect of the bilinear R-parity violation in $0\ \ $-decay [53]. From the best experimental limit on $0\ \ $-decay half-life of ^{76}Ge [54] $T^0_{1=2}\ \ (0^+\ !\ \ 0^+)\ \ \ 1.1\ \ 10^{25}$ years (90% C.L.) one obtains $hm\ i\ \ \ 0.50\ eV$. The corresponding limit from the Super-Kamiokande and CHOOZ constraints (80){(83) is significantly more stringent [50]

$$hm\ i\ \ \ 0.80\ \ 10^{0}\ eV : \tag{92}$$

Thus we conclude that at present the neutrino oscillation experiments are more sensitive to the bilinear R-parity violation than the $0\ \ $-decay experiments. This conclusion holds for the whole parameter space of the MSSM since both type of the experiments place constraints on the same effective parameter A_e which absorbs the dependence on the MSSM parameters. To be comparable in sensitivity to this parameter with the present neutrino oscillation experiments the $0\ \ $-experiments have to reach the half-life lower limit $T^0_{1=2}\ \ > \ \ 10^{29}$ years. This is unrealistic for the running experiments and might only be possible for recently proposed large scale germanium detector [55].

We will return back to R-parity violation in the neutrinoless double beta decay latter in sect. 4.

3.3 Electric dipole moment

The electric dipole moment (EDM) of the leptons and the neutron are stringently restricted experimentally [21]

$$d_e = (3\ \ 8)\ \ 10^{27}\ e\ cm;\quad d\ = (3.7\ \ 3.4)\ \ 10^{19}\ e\ cm;\quad d\ < (3.7\ \ 3.4)\ \ 10^{17}\ e\ cm; \tag{93}$$

for the leptons, and for the neutron

$$d_n < 1.1 \quad 10^{25} e\,cm: \tag{94}$$

The electric dipole moment of an elementary fermion with mass m is defined through its electromagnetic form factor $F_3(q^2)$ ($q = p^0 - p$) found from the matrix element

$$\langle f(p^0)|J^{\mu}(0)|f(p)\rangle = \bar{u}(p^0)\Gamma^{\mu}(q)u(p); \tag{95}$$

$$\Gamma^{\mu}(q) = F_1(q^2)\gamma^{\mu} + F_2(q^2)i\sigma^{\mu\nu}q_{\nu}/2m + F_A(q^2)(\gamma^{\mu}\gamma_5 q^2 - 2m\gamma_5 q^{\mu}) + F_3(q^2)\sigma^{\mu\nu}\gamma_5 q_{\nu}/2m: \tag{96}$$

The EDM of the fermion field f is then given by

$$d_f = F_3(0)/2m; \tag{97}$$

corresponding to the effective dipole interaction in the static limit

$$L_e = \frac{i}{2}d_f\bar{f}\sigma^{\mu\nu}\gamma_5 fF_{\mu\nu}: \tag{98}$$

Since a non-vanishing d_f in the SM results in fermion chirality flip, it requires both CP violation and $SU(2)_L$ symmetry breaking. Even if one allows for CP violation in the leptonic sector of the SM, the lepton EDM's vanish to one-loop level due to the cancellation of all the CP-violating phases. Two-loop calculations for the electron [56] and for quarks [57] also yield a zero EDM. In the MSSM, however, there are more sources of CP violation than in the SM. In addition to the usual Kobayashi-Maskawa phase from the quark mixing matrix, there are phases arising from complex parameters in the superpotential and in the soft supersymmetry breaking terms. The phases of particular interest are those coming from the so-called A-terms, $A_{u,d} = |A_{u,d}|\exp(i\ _{A_{u,d}})$ [58]. The CP-violating effects arise from the squark mass matrix which has the following form:

$$L_{\tilde{q}} = (\tilde{u}_L^{y}\ \tilde{u}_R^{y}) \begin{pmatrix} {}^2_L + m_u^2 & A_u m_u \\ A_u m_u & {}^2_R + m_u^2; \end{pmatrix} \begin{pmatrix} \tilde{u}_L \\ \tilde{u}_R \end{pmatrix}; \tag{99}$$

and similarly for $L_{\tilde{d}}$, where the mass parameters $|A_u|$, $_L$ and $_R$ are expected to be of the order of the W-boson mass M_W. The fields $\tilde{u}_L$, $\tilde{u}_R$ can be transformed into mass eigenstates $\tilde{u}_1$, $\tilde{u}_2$,

$$\begin{aligned} \tilde{u}_L &= \exp(-\frac{1}{2}i\ _{A_u})(\cos\ \tilde{u}_1 + \sin\ \tilde{u}_2); \\ \tilde{u}_R &= \exp(\frac{1}{2}i\ _{A_u})(\cos\ \tilde{u}_2 - \sin\ \tilde{u}_1); \end{aligned} \tag{100}$$

where the mixing angle is given by $\tan 2 = 2|A_u|m_u/(\ ^2_L - \ ^2_R)$; and the physical masses, $M_{1,2}$, corresponding to the eigenvalues of the mass matrix in (99) are

$$M^2_{1,2} = \frac{1}{2}[\ ^2_L + \ ^2_R + 2m_u^2 \mp [(\ ^2_L - \ ^2_R)^2 + 4m_u^2|A_u|^2]^{1/2}]: \tag{101}$$

The lepton EDM's at one-loop order are generated by the interactions in Fig. 3 (with similar Feynman diagrams for the muon and the tau) and resemble those in the MSSM with charginos or neutralinos in the loop.

The contributions to the lepton EDM's are then given by [59]

$$\begin{aligned} d_{e_i} = & \quad |\lambda'_{ijk}|^2\frac{4e}{3}\frac{m_{d_k}}{m^3_{\tilde{f}}}|A_{u_j}|\sin\ \cos\ \sin(\ _{A_u})f_3(x_{d_k}) \\ & - |\lambda'_{ijk}|^2\frac{2e}{3}\frac{m_{d_k}}{m^3_{\tilde{f}}}|A_{u_j}|\sin\ \cos\ \sin(\ _{A_u})f_4(x_{d_k}) \\ & - |\lambda'_{ijk}|^2\frac{2e}{3}\frac{m_{u_j}}{m^3_{\tilde{f}}}|A_{d_k}|\sin\ \cos\ \sin(\ _{A_d})f_3(x_{u_j}) \\ & - |\lambda'_{ijk}|^2\frac{4e}{3}\frac{m_{u_j}}{m^3_{\tilde{f}}}|A_{d_k}|\sin\ \cos\ \sin(\ _{A_d})f_4(x_{u_j}); \end{aligned} \tag{102}$$

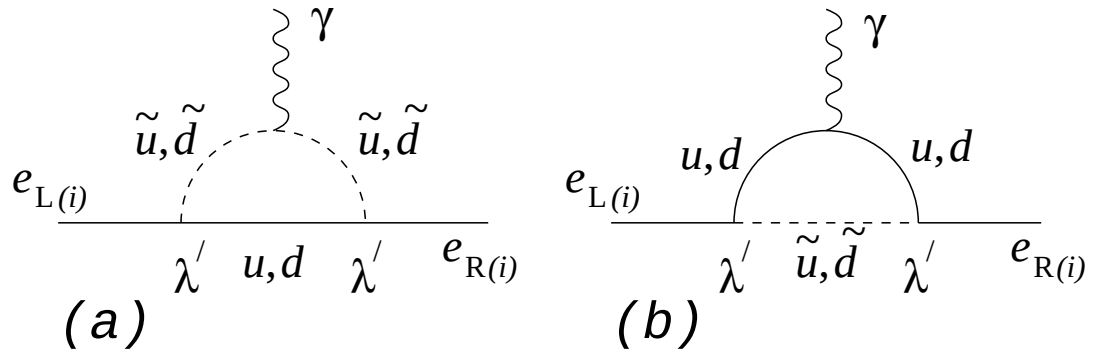

Fig. 3. Graphs contributing to the charged lepton $e_{(i)} = (e; ;)$ electric dipole moment.

where $x_{u;d} = (m_{u;d}=m_{f})^2$, with f being scalar quark in the loop, and the loop integrals are expressed in a familiar form in terms of the functions

$$f_3(x) = \frac{1}{2(1-x)^2}\left[1 + x + \frac{2x\ln x}{1-x}\right]; \qquad f_4(x) = \frac{1}{2(1-x)^2}\left[3 - x + \frac{2\ln x}{1-x}\right]:$$

Unfortunately estimating d_e, d , and d numerically is not completely straightforward since no model-independent experimental information is available on squark masses and mixing angles. However order of magnitude estimates are possible under certain assumptions.

One can assume, without great loss of generality, that $\cos = \sin = 1=\sqrt{2}$ and $_{A_u} = _{A_d}$ and $|A_{u_j;d_k}| \quad m_{\tilde{f}} = O(M_W)$. Then one gets the formula:

$$d_{e_i} = \sum_{n} |\tilde{}^{0}_{ijk}| \frac{1}{3}\left[\frac{m_{\tilde{f}}}{100\ \mathrm{GeV}}\right]^2 \left\{ m_{d_k}\left[4f_3(x_{u_j}) + 2f_4(x_{u_j})\right] + m_{u_j}\left[2f_3(x_{d_k}) + 4f_4(x_{d_k})\right]\right\} \quad 10^{18}\ e\ cm; \tag{103}$$

where the e ective coupling is introduced $\tilde{}^{0}_{ijk} = {}^{0}_{ijk}\sqrt{\sin(_A)}$. Using this simplied formula, the limits on the individual $\tilde{}^{0}_{ijk}$ parameters from the electron ($\tilde{}^{0}_{1jk}$), muon ($\tilde{}^{0}_{2jk}$) EDM's were derived in [59] and are given in Table 2. Unfortunately it is not possible to extract limits directly on the ${}^{0}_{ijk}$ parameters since the phase factor $\sin(_A)$ is unknown.

Table 2. Upper bounds on the R-parity violating parameters from the electron ($\tilde{}^{0}_{1jk}$) and muon ($\tilde{}^{0}_{2jk}$) electric dipole moments.

	$m_{\tilde{f}} = 100$ GeV	$m_{\tilde{f}} = 1$ TeV		$m_{\tilde{f}} = 100$ GeV	$m_{\tilde{f}} = 1$ TeV
$\lvert\tilde{}^{0}_{111}\rvert$	$3 \quad 10^{9}$	$2{:}4 \quad 10^{7}$	$\lvert\tilde{}^{0}_{211}\rvert$	$3 \quad 10^{1}$	24
$\lvert\tilde{}^{0}_{112}\rvert$	$5 \quad 10^{10}$	$3 \quad 10^{8}$	$\lvert\tilde{}^{0}_{212}\rvert$	$5 \quad 10^{2}$	3
$\lvert\tilde{}^{0}_{113}\rvert$	$9 \quad 10^{11}$	$4 \quad 10^{9}$	$\lvert\tilde{}^{0}_{213}\rvert$	$9 \quad 10^{3}$	$4 \quad 10^{1}$
$\lvert\tilde{}^{0}_{121}\rvert$	$7{:}5 \quad 10^{11}$	$4{:}3 \quad 10^{9}$	$\lvert\tilde{}^{0}_{221}\rvert$	$7{:}5 \quad 10^{3}$	$4{:}3 \quad 10^{1}$
$\lvert\tilde{}^{0}_{122}\rvert$	$6{:}6 \quad 10^{11}$	$4 \quad 10^{9}$	$\lvert\tilde{}^{0}_{222}\rvert$	$6{:}6 \quad 10^{3}$	$4 \quad 10^{1}$
$\lvert\tilde{}^{0}_{123}\rvert$	$4 \quad 10^{11}$	$2 \quad 10^{9}$	$\lvert\tilde{}^{0}_{223}\rvert$	$4 \quad 10^{3}$	$2 \quad 10^{1}$
$\lvert\tilde{}^{0}_{131}\rvert$	$2{:}6 \quad 10^{12}$	$2{:}4 \quad 10^{11}$	$\lvert\tilde{}^{0}_{231}\rvert$	$2{:}6 \quad 10^{4}$	$2{:}4 \quad 10^{3}$
$\lvert\tilde{}^{0}_{132}\rvert$	$2{:}6 \quad 10^{12}$	$2{:}4 \quad 10^{11}$	$\lvert\tilde{}^{0}_{232}\rvert$	$2{:}6 \quad 10^{4}$	$2{:}4 \quad 10^{3}$
$\lvert\tilde{}^{0}_{133}\rvert$	$2{:}5 \quad 10^{12}$	$2{:}3 \quad 10^{11}$	$\lvert\tilde{}^{0}_{233}\rvert$	$2{:}5 \quad 10^{4}$	$2{:}3 \quad 10^{3}$

The strongest limits appear to be the ones on $\tilde{}_{1j3}$ because of e ects of $O(m_t)$.

We shall now briefly comment on possible restrictions coming from the anomalous magnetic moment of the muon, a . Its experimental value is $a^{exp} = 1165922(9) \quad 10^{9}$ and its measured deviation from

the SM prediction lies within a range of $2 \quad 10^{8} \quad a^{exp} \quad 2{:}6 \quad 10^{8}$. The one-loop contributions to the muon magnetic moment also come from Feynman diagrams similar to those in Fig. 3 and are given by $a = F_2(0)=e$, where $F_2(0)$ is the static limit of the electromagnetic form factor defined in (96). Unfortunately, the restrictions that a would place on the R-parity violating couplings and ^{0} are extremely weak compared to those coming from the EDM's. The EDM of the electron is expected to be known to about five orders of magnitude more accurately than its anomalous magnetic moment within a few years. Indeed the precise measurements of the electron $(g \quad 2)$ factor yield $[(g \quad 2)=2] = 1 \quad 10^{11}$, which corresponds to $(F_2(0)=2m_e) = 2 \quad 10^{22}$ e cm. The same is true for the anomalous magnetic moment of the muon [60].

In addition, for the calculation of the form factor $F_2(q^2)$ for the electron (muon) the helicity flip occurs on the external fermion line, giving rise to an amplitude proportional to the electron (muon) mass. These two factors combined, give weaker bounds on the R-parity violating Yukawa couplings than previously found, despite the fact that the anomalous magnetic moment does not require CP violation.

3.4 Charged current and e{ { universality

Universality of the lepton and quark couplings to the W-boson is violated in the presence of the $R\!\!\!/_p$ couplings. Thus one can extract limits on certain $R\!\!\!/_p$ couplings , ^{0} from the present constraints on deviations from the charged current (CC) and the e{ { universality. In fact, the effective 4-fermion Lagrangian derived from the $R\!\!\!/_p$ Lagrangian (58) takes, after Fierz reordering, the form of the SM CC interactions:

$$L_e^{CC} = \frac{j\,^{0}_{i1k}j^2}{2m^2_{\tilde{d}_{Rk}}}(e \quad P_L \quad _e)(u \quad P_L d) + \frac{j\,_{ijk}j^2}{2m^2_{\tilde{e}_{Rk}}}(e_i \quad P_L \quad _i)(\quad _j \quad P_L e_j): \tag{104}$$

These interactions violate the universality of the CC-interactions of quarks and leptons. Here we used the gauge basis for the quark fields in order to contact the results derived in the literature.

From the ratio of the semileptonic quark decay $u \to de^{c}$ to the muon decay $\to e\,_e^{c}$ one can relate the experimental value of V_{ud}^{exp} measured in the CC processes to V_{ud}^{SM} by

$$jV_{ud}^{exp}j^2 \; ' \; jV_{ud}^{SM}j^2\,4 1 + 2\frac{M_W^2}{g_2^2 V_{ud}}\,@\,\frac{j\,^{0}_{11k}j^2}{m^2_{\tilde{d}_{Rk}}}A \quad 2\frac{M_W^2}{g_2^2} \quad \frac{j\,_{12k}j^2}{m^2_{\tilde{e}_{Rk}}}\,!\,3\,5: \tag{105}$$

Assuming the presence of only one $R\!\!\!/_p$ coupling at a time, one obtains [23, 13] for a common $\tilde{m} = 100$ GeV and for each k

$$_{12k} \quad 0{:}05 \quad (1 \ ); \qquad ^{0}_{11k} \quad 0{:}02 \quad (2 \ ): \tag{106}$$

Similarly for the pion leptonic decay ratio one obtains:

$$R \quad \frac{(\quad ! \quad e \quad)}{(\quad ! \quad \quad)} = R^{SM}\,4 1 + 2\frac{M_W^2}{V_{ud}g_2^2}\,@\,\frac{j\,^{0}_{11k}j^2}{m^2_{\tilde{d}_{Rk}}}A \quad 2\frac{M_W^2}{V_{ud}g_2^2}\,@\,\frac{j\,^{0}_{21k}j^2}{m^2_{\tilde{d}_{Rk}}}A\,5\,3:$$

A comparison with experimental result for the ratio $(0{:}991 \quad 0{:}018)$ yields [23], for a common mass $\tilde{m} = 100$ GeV and for each k, assuming only one coupling at a time:

$$^{0}_{11k} \quad 0{:}05; \qquad ^{0}_{21k} \quad 0{:}09; \qquad (1 \ ): \tag{107}$$

The e{ { universality constraint one can obtain from the -lepton decay ratio derived from the Lagrangian (104):

$$R \quad \frac{(\quad ! \quad e \quad)}{(\quad ! \quad \quad)} = R^{SM}\,\Big[\,1 + 2\frac{M_W^2}{g_2^2}\,\frac{j\,_{13k}j^2}{m^2_{\tilde{e}_{Rk}}}\,!\quad 2\frac{M_W^2}{g_2^2}\,\frac{j\,_{23k}j^2}{m^2_{\tilde{e}_{Rk}}}\,!\,\Big]: \tag{108}$$

Using the experimental value $R = R^{SM} = 1.0006 \pm 0.0103$ one obtains the bounds [23, 13]

$$|\lambda_{13k}| < 0.06 \, \frac{m_{\tilde{e}_{Rk}}}{100\,GeV} \; , \quad |\lambda_{23k}| < 0.06 \, \frac{m_{\tilde{e}_{Rk}}}{100\,GeV} \; , \quad k = 1,2,3. \tag{109}$$

Note that in the mass basis for the quark fields the constraints (106) and (107) produce a bulk of constraints on the λ' couplings defined in eq. (62).

3.5 Muon decay

The muon decay and the inverse muon decay at low energy [61] can be parameterized in terms of amplitudes $g_{\epsilon,\gamma}^{\gamma}$ and the Fermi constant G_F, using the matrix element [62]

$$\frac{4G_F}{\sqrt{2}} \sum_{\substack{\gamma = V,S,T \\ \epsilon,\gamma = L,R}} g_{\epsilon,\gamma}^{\gamma} \, \langle \bar{e} | \Gamma^{\gamma} | (\nu_e)_n \rangle \langle \overline{(\nu_\mu)_m} | \Gamma_{\gamma} | \mu \rangle ,$$

where $\gamma = V,S,T$ denotes a vector, scalar, or tensor interaction, ϵ, γ denote the chirality of the electron and muon, respectively, and the chiralities n and m of ν_e and $\bar{\nu}_\mu$ are determined by γ, ϵ, γ. In the standard model, the $(V-A)$ structure requires $g_{LL}^{V} = 1$ and others equal to zero. In the rest frame of the muon, the energy and angular distribution is given by the Michel spectrum:

$$\frac{d^2\Gamma}{dx\,d\cos\theta} \propto 3(1-x) + \frac{2}{3}(4x-3) + \cos\theta \left[1-x + \frac{2}{3}(4x-3) \right] + \rho \left[\frac{4}{3}x(4x-3) + \cos\theta\,(1-x) \right] ,$$

where ρ, η, ξ are functions of $g_{\epsilon,\gamma}^{\gamma}$. The measurements of ρ, η, ξ can constrain various combinations of $g_{\epsilon,\gamma}^{\gamma}$. In order to determine the amplitudes $g_{\epsilon,\gamma}^{\gamma}$ uniquely, it was introduced four probabilities $Q_{\epsilon,\gamma}$ ($\epsilon, \gamma = L,R$) for the decay of a γ-handed muon into a ϵ-handed electron:

$$Q_{\epsilon,\gamma} = \frac{1}{4} \left| g_{\epsilon,\gamma}^{S} \right|^2 + \left| g_{\epsilon,\gamma}^{V} \right|^2 + 3(1-\delta_{\epsilon,\gamma}) \left| g_{\epsilon,\gamma}^{T} \right|^2 .$$

The Q_{LL} is constrained to be very close to unity, while others very close to zero. The relevant current limits on $g_{\epsilon,\gamma}^{\gamma}$ are

$$|g_{RR}^{S}| < 0.066 ; \qquad |g_{LL}^{V}| > 0.96; \qquad (90\%\ C.L.).$$

There are two possible diagrams contributing to the muon decay in R-parity violation SUSY. The first one is via an exchange of $\tilde{\nu}_L$ and the effective Lagrangian term is given by

$$L_1 = - \frac{\lambda'_{131}\lambda'_{232}}{m^2_{\tilde{\nu}_L}} (\bar{e}_R \nu_{eL})(\bar{\nu}_\mu \mu_R).$$

This interaction term contributes to g_{RR}^{S} as follows

$$g_{RR}^{S} = - \frac{\sqrt{2}}{4G_F} \frac{\lambda'_{131}\lambda'_{232}}{m^2_{\tilde{\nu}_L}}.$$

Note that this contribution has a different helicity structure as the SM $(V-A)$ amplitude and, therefore, the experimental limit on the $(V-A)$ structure can effectively constrain the product $|\lambda'_{131}\lambda'_{232}|$. One obtains for $m_{\tilde{\nu}_L} = 100\,GeV$,

$$|\lambda'_{131}\lambda'_{232}| < 0.022 \qquad (90\%\ C.L.). \tag{110}$$

The second diagram is via an exchange of $\tilde{e}_R$, $\tilde{e}_R$, or $\tilde{e}_R$. The corresponding Lagrangian term is given by

$$L_2 = - \sum_{k=1}^{3} \frac{|\lambda'_{12k}|^2}{2m^2_{\tilde{e}_{kR}}} (\bar{e}_L \nu_{eL})(\bar{\nu}_\mu \mu_L).$$

This interaction contributes to g^V_{LL} as

$$g^V_{LL} = \frac{\sqrt{2}}{4G_F} \sum_{k=1}^{3} \frac{|\lambda_{12k}|^2}{2m^2_{\tilde{e}_{kR}}}.$$

The L_2 has the same helicity structure as the SM $(V-A)$ amplitude and, therefore, the $(V-A)$ structure cannot constrain $|\lambda_{12k}|$, but the total rate should be able to do so. This constraint, derived from the CC-universality, we discussed in the previous section.

In the previous section it was also shown [23] that the $e-\mu$ universality is able to constrain λ_{13k} and λ_{23k} to a very small values given in eq. (109). The danger of this limit can be seen from (108). When $|\lambda_{13k}| \simeq |\lambda_{23k}|$ their contributions to R_τ cancel and, therefore, the limits on $|\lambda_{i3k}|$ are no longer valid. Physically, if the partial widths of the tau into muon and electron increased with the same amount, the $e-\mu$ universality in the tau decay could not constrain the λs.

As to the constraints from the muon decay (110) one can see that even in the scenario where $|\lambda_{131}| \simeq |\lambda_{232}|$ relation (110) can constrain them effectively to be

$$|\lambda_{131}| = |\lambda_{232}| < 0.15 \qquad (90\%\ C.L.).$$

Of course, when λ_{131} is very different from λ_{232} the limit from $e-\mu$ universality is more restrictive.

There will be future experiments on measuring the muon decay parameters with better sensitivity. A planned experiment TRIUMF-E614 is scheduled to run and will have a sensitivity of ρ, η, ξ down to 10^{-4}. Such sensitivity on ρ, η, ξ will be able to pin f_{ij}^{kR} down to 10^{-2}, which would then give the limit on $|\lambda_{131}| = |\lambda_{232}|$:

$$|\lambda_{131}| = |\lambda_{232}| < 0.06. \tag{111}$$

Although obtained from muon decay limit on $|\lambda_{131}\ \lambda_{232}| < 0.022$ (or $|\lambda_{131}| = |\lambda_{232}| < 0.15$) is not as good as the previous limits $|\lambda_{13k}| |\lambda_{23k}| < 0.076$ for $m_{\tilde{e}_{kR}} = 100$ GeV at 90% C.L. obtained by the $e-\mu$ universality in τ decay, however, it is useful for the case when $|\lambda_{131}| \simeq |\lambda_{232}|$, in which case the $e-\mu$ universality is satisfied no matter how large the λs are. It should be noted that the scenario of several coexisting R-parity violating couplings is more complicated than the case previously examined in the literature, and one should extract as much information as possible from the existing experiments.

3.6 Decay $\mu \to e\gamma$

The gauge invariant amplitude for the decay $\mu \to e\gamma$ is usually parameterized as

$$T(\mu \to e\gamma) = \bar{u}_e(p')(A + B\gamma_5)i\sigma^{\alpha\beta}\epsilon^*_\alpha q_\beta u_\mu(p), \tag{112}$$

where p, p' and q are the momenta of muon, electron and photon respectively, ϵ is the photon polarization vector and $\sigma^{\alpha\beta} = \frac{i}{2}[\gamma^\alpha, \gamma^\beta]$. The amplitude is nonvanishing only when the muon and the electron are of opposite helicities. The width of the decay can be evaluated using the amplitude and finally the branching ratio from μ lifetime, $\tau_\mu = 192\pi^3/(G_F^2 m_\mu^5)$, with the result

$$B(\mu \to e\gamma) = \frac{24\pi^3}{G_F^2 m_\mu^2}(|A|^2 + |B|^2). \tag{113}$$

Similarly one could study the decay of tau lepton to muon and photon or electron and photon. The experimental limits for the lepton decays are given as [21]:

$$B(\tau \to e\gamma) < 4.9 \times 10^{-11}; \quad B(\tau \to \mu\gamma) < 4.2 \times 10^{-6}; \quad B(\tau \to e\gamma) < 1.2 \times 10^{-6}. \tag{114}$$

In the $R\!\!\!/_p$MSSM one has additional diagrams to those in the ordinary MSSM case. These $R\!\!\!/_p$ diagrams are displayed in Fig. 4.

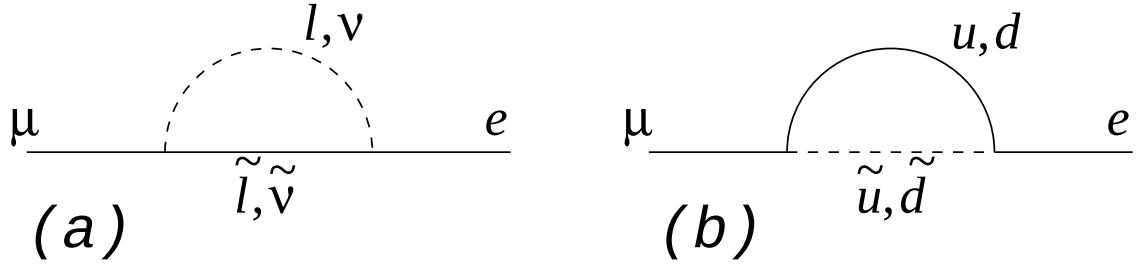

Fig. 4. Graphs contributing to the $\mu \to e$ decay.

Calculation of the corresponding contribution in the form of eq. (112) is straightforward. With Gordon decomposition coefficient A in the amplitude (112) can be written in terms of the following functions

$$A_1 = \frac{{}_{1}{}_{2}Qm}{16\,{}^2 m_{\tilde f}^2}\frac{1}{6(\quad 1)^3}\left[{}^2 + 5\quad + 2\quad \frac{6}{1}\ln\quad\right];$$
$$A_2 = \frac{{}_{1}{}_{2}Qm}{16\,{}^2 m_{\tilde f}^2}\frac{1}{6(\quad 1)^3}\left[2\,{}^2 + 5\quad 1\quad \frac{6\,{}^2}{1}\ln\quad\right]. \qquad (115)$$

There are two lepton number violating vertices in every contribution, characterized by ${}_{1;2} = {}_{ijk}$ or ${}_{1;2} = {}^{0}_{ijk}$ couplings. The functions A_1 and A_2 depend also on the charge of the particle attached to the photon Q, the sfermion mass occurring in the loop $m_{\tilde f}$, and the ratio of the masses of fermion and sfermion in the loop, $= m_f^2/m_{\tilde f}^2$. Proportionality to the mass of the muon, m , reflects the helicity flip on the external muon line. The lack of a term proportional to the electron mass on the other hand indicates that approximation of massless the external electron is used. The A_1 function corresponds to the situation where the photon line is attached to the fermion line and A_2 to the situation where the photon line is attached to the scalar. In all cases $|A| = |B|$.

With eqs. (115) one can extract from the experimental limits in (114) certain constraints on various products of and ^{0} couplings [63]. As always, it is possible only under certain assumptions which we use here and which have already became conventional ones. The assumptions of one or several couplings dominance explained in sect. 2.4.1 were used in deriving constraints shown in Table 3 [63, 64]. One has to keep this point in mind considering this Table.

Table 3. Upper limits on products of ${}_{ijk}$ and ${}^{0}_{ijk}$ couplings from $\mu \to e$ for two different scalar masses in the loop.

	$m_{\tilde f} = 100$ GeV		$m_{\tilde f} = 1$ TeV			$m_{\tilde f} = 100$ GeV		$m_{\tilde f} = 1$ TeV	
$\lvert {}_{121}\ {}_{122}\rvert$	1:0	10^{-4}	1:0	10^{-2}	$\lvert {}^{0}_{211}\ {}^{0}_{111}\rvert$	2:7	10^{-4}	2:7	10^{-2}
$\lvert {}_{131}\ {}_{132}\rvert$	1:0	10^{-4}	1:0	10^{-2}	$\lvert {}^{0}_{212}\ {}^{0}_{112}\rvert$	2:7	10^{-4}	2:7	10^{-2}
$\lvert {}_{231}\ {}_{232}\rvert$	1:0	10^{-4}	1:0	10^{-2}	$\lvert {}^{0}_{213}\ {}^{0}_{113}\rvert$	2:7	10^{-4}	2:7	10^{-2}
$\lvert {}_{231}\ {}_{131}\rvert$	2:0	10^{-4}	2:0	10^{-2}	$\lvert {}^{0}_{221}\ {}^{0}_{121}\rvert$	2:7	10^{-4}	2:7	10^{-2}
$\lvert {}_{232}\ {}_{132}\rvert$	2:0	10^{-4}	2:0	10^{-2}	$\lvert {}^{0}_{222}\ {}^{0}_{122}\rvert$	2:7	10^{-4}	2:7	10^{-2}
$\lvert {}_{233}\ {}_{133}\rvert$	2:0	10^{-4}	2:0	10^{-2}	$\lvert {}^{0}_{223}\ {}^{0}_{123}\rvert$	2:7	10^{-4}	2:7	10^{-2}
					$\lvert {}^{0}_{231}\ {}^{0}_{131}\rvert$	46:7	10^{-4}	3:5	10^{-2}
					$\lvert {}^{0}_{232}\ {}^{0}_{132}\rvert$	46:7	10^{-4}	3:5	10^{-2}
					$\lvert {}^{0}_{233}\ {}^{0}_{133}\rvert$	60:0	10^{-4}	3:5	10^{-2}

For the lighter scalar mass spectrum, one sees from Table 3 that the last three limits are less strict than the others. This is due to the top quark (m_{top} 175 GeV) in the loop, since then the value of is larger than one. Also the effect of the bottom quark is seen in some of the bounds, especially in

the last one, when both top- and bottom-quarks contribute to the result. When the scalar mass in the loop is 1 TeV, one does not anymore see the effect of the bottom quark and also the effect due to the top quark is much less conspicuous.

Certainly one could also study the limits from $\to$ or $\to e$, but as it appears from (114) these limits are rather weak [63].

3.7 Muonium–antimuonium conversion

The muonium is the leptonic hydrogen-like atom with the muon instead of the proton. The lepton flavor violating interactions ($L = L_e = 2$) may convert it into the anti-muonium state:

$$M(^+e) \to \overline{M}(e^+).$$

The diagrams describing the contributions to M–$\overline{M}$ conversion in the R_p MSSM include the s- and t-channel sneutrino exchange between the lepton lines. The relevant low-energy effective Lagrangian is [65]

$$L_e(^+e \to e^+) = \frac{_{321}\,_{312}}{m^2_{e_{L3}}}\,\bar{}_R e_L\,\bar{}_L e_R : \tag{116}$$

Here $m_{e_{L3}}$ is the 3rd generation sneutrino mass. To simplify the sneutrino contributions, it was used the antisymmetry of the couplings, $_{ijk} = -_{jik}$.

The Lagrangian (116) should be compared with the standard parameterization in the form

$$L(M \to \overline{M}) = \frac{G_{M\overline{M}}}{\sqrt{2}}\,(\bar{}e)_{V-A}(\bar{}e)_{V+A} + H.c. \tag{117}$$

with the effective coupling $G_{M\overline{M}}$. Equation (116) is the same as eq. (117) after the Fierz transformation, with the following identification

$$\frac{G_{M\overline{M}}}{\sqrt{2}} = \frac{_{321}\,_{312}}{8m^2_{e_{L3}}}.$$

The muonium conversion probability depends on the external magnetic field B_{ext} in a nontrivial way. This subject was recently addressed in detail by a few groups [66]. Their results are used in the following. From the present upper limit on the transition probability for the external magnetic field $B_{ext} = 1.6$ kG,

$$P_{exp}(M \to \overline{M}) < 2.1 \times 10^{-9} \quad (90\%\ C.L.),$$

one gets the following constraint on $G_{M\overline{M}} < 9.6 \times 10^{-3} G_F$. This in turn implies that [65]

$$|_{231}\,_{132}| < 6.3 \times 10^{-3} \left(\frac{m_{e_{L3}}}{100\ GeV}\right)^2. \tag{118}$$

This constraint on the R-parity violating couplings is in the same order with other constraints derived from lepton-flavor violating decays such as $\to 3l$ or $l \to l' l'' \bar{l}''$ (with $l, l'' = , , $ or e).

3.8 Rare three-body leptonic decays of and

Rare three-body leptonic decays of and can be characterized [67] by the generic transition $e_a \to e_b + e_c + e_d$ where a,b,c,d are generation indices. The reaction proceeds via exchange of a sneutrino e_n in the t-channel as well as in the u-channel. The effective Lagrangian takes the form

$$\begin{aligned}(100\ GeV)^2\, L_e(e_a \to e_b + e_c + e_d) = {} & F_{abcd}\,\bar{e}_{bR} e_{aL}\,\bar{e}_{cL} e_{dR} + F_{dcba}\,\bar{e}_{bL} e_{aR}\,\bar{e}_{cR} e_{dL} \\ & + F_{acbd}\,\bar{e}_{cR} e_{aL}\,\bar{e}_{bL} e_{dR} + F_{dbca}\,\bar{e}_{cL} e_{aR}\,\bar{e}_{bR} e_{dL};\end{aligned} \tag{119}$$

where

$$F_{abcd} \equiv \sum_n n_n \, {}^{n}_{nab} \, {}^{?}_{ncd} \quad \text{and} \quad n_n = \left(\frac{100\ \mathrm{GeV}}{m_{\tilde{e}_n}} \right)^2 : \tag{120}$$

Utilizing the known experimental upper limits on the relevant partial widths (Table 4), one has [67]

$$\begin{aligned}
\mu^- \to e^- e^+ e^- &: \quad |F_{1112}|^2 + |F_{2111}|^2 < 4.3 \quad 10^{-13}; \\
\tau^- \to e^- e^+ e^- &: \quad |F_{1113}|^2 + |F_{3111}|^2 < 3.1 \quad 10^{-5}; \\
\tau^- \to \mu^- e^+ e^- &: \quad |F_{2223}|^2 + |F_{3222}|^2 < 4.1 \quad 10^{-5}; \\
\tau^- \to \mu^+ e^- e^- &: \quad |F_{3112}|^2 + |F_{2113}|^2 < 3.3 \quad 10^{-5}; \\
\tau^- \to e^+ \mu^- e^- &: \quad |F_{3221}|^2 + |F_{1223}|^2 < 3.8 \quad 10^{-5}; \\
\tau^- \to e^+ e^- e^- &: \quad |F_{1123}|^2 + |F_{3211}|^2 + |F_{1213}|^2 + |F_{3121}|^2 < 3.3 \quad 10^{-5}; \\
\tau^- \to e^- \mu^+ e^- &: \quad |F_{3122}|^2 + |F_{2213}|^2 + |F_{3212}|^2 + |F_{2123}|^2 < 4.5 \quad 10^{-5}:
\end{aligned}$$

Assuming that only one product $\lambda\lambda$ is non-zero at a time one derives limits listed in Table 4 [67].

Table 4. Upper bounds on the magnitudes of coupling products derived from flavour changing lepton decays, under the assumption that only one product $\lambda\lambda$ is non-zero. For definition of n_n see eq. (120).

Quantity	Experimental value (bound)	Combinations constrained	Upper bound
$B(\mu^- \to e^- e^- e^+)$	$< 10^{-12}$	$_{121}\ _{122} n_2;\ _{131}\ _{132} n_3;\ _{231}\ _{131} n_3$	$6.6 \quad 10^{-7}$
$B(\mu^- \to e^- e^+ e^-)$	$< 1.3 \quad 10^{-5}$	$_{121}\ _{123} n_2;\ _{131}\ _{133} n_3;\ _{231}\ _{121} n_2$	$5.6 \quad 10^{-3}$
$B(\tau^- \to e^- e^+ e^-)$	$< 1.4 \quad 10^{-5}$	$_{231}\ _{112} n_2;\ _{231}\ _{133} n_3$	$5.7 \quad 10^{-3}$
$B(\tau^- \to e^- e^- e^+)$	$< 1.4 \quad 10^{-5}$	$_{131}\ _{121} n_1;\ _{122}\ _{123} n_2;\ _{132}\ _{133} n_3;$ $_{232}\ _{121} n_2;\ _{131}\ _{233} n_3$	$5.7 \quad 10^{-3}$
$B(\tau^- \to e^- \mu^- e^+)$	$< 1.6 \quad 10^{-5}$	$_{131}\ _{121} n_1;\ _{132}\ _{233} n_3$	$6.2 \quad 10^{-3}$
$B(\tau^- \to \mu^- e^+ e^-)$	$< 1.9 \quad 10^{-5}$	$_{131}\ _{122} n_1;\ _{232}\ _{133} n_3;\ _{232}\ _{122} n_2;$ $_{121}\ _{123} n_1;\ _{231}\ _{233} n_3$	$6.7 \quad 10^{-3}$
$B(\tau^- \to \mu^- e^- e^+)$	$< 1.7 \quad 10^{-5}$	$_{132}\ _{122} n_1;\ _{122}\ _{123} n_1;\ _{232}\ _{233} n_3$	$6.4 \quad 10^{-3}$

3.9 Semileptonic decays

In this section we consider lepton-family number violating tau decays into a vector V or a pseudoscalar P meson and a lepton ($k = 1,2$ corresponds to e and μ),

$$\tau^- \to e_k^- + {}^0; \rho^-, \omega, K^{*-}; \tag{121}$$

$$\tau^- \to e_k^- + {}^0; \pi^-, \eta, K^{0-} \tag{122}$$

The effective Lagrangian describing these processes are derived from the diagrams with the sneutrino $\tilde{\nu}$ as well as up- and down-squarks $\tilde{u}_L, \tilde{d}_R$ internal lines. Integrating out these heavy scalar fields yields [65]

$$L_{\text{eff}} = \sum_n \frac{1}{m^2_{\tilde{\nu}_n}} \left[{}^{0}_{nij} \, {}^{}_{nkl} \bar{e}_{kL} e_{lR} \bar{d}_{jR} d_{iL} + {}^{}_{nlk} \, {}^{0}_{nji} \bar{e}_{kR} e_{lL} \bar{d}_{jL} d_{iR} \right] \tag{123}$$

$$+\sum_{m,n,p}\Big[\frac{V^{y}_{np}V_{pm}}{2m^{2}_{\tilde{u}_{Lp}}}\,{}^{0}_{lnj}\,{}^{0}_{kmi}\,\bar{e}_{kL}\;e_{lL}\,\bar{d}_{jR}\;d_{iR}\;-\;{}^{0}_{lmp}\,{}^{0}_{knp}\frac{V^{y}_{mi}V_{jn}}{m^{2}_{\tilde{d}_{Rp}}}\,\overline{(e_{lL})^{c}}\,u_{iL}\,\bar{u}_{jL}\,(e_{kL})^{c}$$

$$-\;{}^{0}_{lmp}\,{}^{0}_{knp}\frac{V^{y}_{mi}V_{jn}}{2m^{2}_{\tilde{d}_{Rp}}}\,\bar{e}_{kL}\;e_{lL}\,\bar{u}_{jL}\;u_{iL}\Big]+\text{h.c.}\,.$$

The relevant matrix elements can be evaluated using the PCAC conditions,

$$\begin{aligned}
\langle\pi^{0}(p)|\bar{u}\,\gamma_{5}u(0)|0\rangle &= \text{if}\;p = \langle\pi^{0}(p)|\bar{d}\,\gamma_{5}d(0)|0\rangle,\\
\langle\eta(p)|\bar{u}\,\gamma_{5}u(0)|0\rangle &= \frac{\text{if}}{\sqrt{3}}\,p = \langle\eta'(p)|\bar{u}\,\gamma_{5}u(0)|0\rangle,\\
\langle\eta'(p)|\bar{s}\,\gamma_{5}s(0)|0\rangle &= \frac{2\text{if}}{\sqrt{3}}\,p\,,\\
\langle K^{0}(p)|\bar{d}\,\gamma_{5}s(0)|0\rangle &= \text{i}\sqrt{2}f_{K}\,p\,,
\end{aligned}\tag{124}$$

and using CVC conditions,

$$\begin{aligned}
\langle\pi^{0}(p,\lambda)|\bar{u}\,u(0)|0\rangle &= m_{\rho}f_{\rho} = \langle\pi^{0}(p,\lambda)|\bar{d}\,d(0)|0\rangle,\\
\langle\omega(p,\lambda)|\bar{u}\,u(0)|0\rangle &= m_{\omega}f_{\omega} = \langle\omega(p,\lambda)|\bar{d}\,d(0)|0\rangle,\\
\langle\phi(p,\lambda)|\bar{s}\,s(0)|0\rangle &= m_{\phi}f_{\phi}\,,\\
\langle K^{*}(p,\lambda)|\bar{d}\,s(0)|0\rangle &= m_{K^{*}}f_{K^{*}}\,.
\end{aligned}\tag{125}$$

The pseudoscalar meson decay constants are $f_{\pi} = 93$ MeV, $f_{K} = 113$ MeV, $f_{\eta} = 153$ MeV, $f_{\eta'} = 138$ MeV, $f_{\phi} = 237$ MeV, and $f_{K^{*}} = 224$ MeV.

The amplitude of the tau decay into a vector meson and a lepton (121) derived from the Lagrangian (123) is

$$M(\tau^{-}\to e_{k}^{-}+V) = \frac{1}{8}A_{V}f_{V}m_{V}\;\bar{e}_{k}\;(1-\gamma_{5})\,\not{\epsilon}\,,$$

where

$$A_{V} = \sum_{m,n,p}\frac{V^{y}_{mi}V_{jn}}{m^{2}_{\tilde{d}_{Rp}}}\,{}^{0}_{3mp}\,{}^{0}_{knp} + \sum_{m,n,p}\frac{V^{y}_{np}V_{pm}}{m^{2}_{\tilde{u}_{Lp}}}\,{}^{0}_{3nj}\,{}^{0}_{kmi}\,.$$

The rate for the decay is given by

$$\Gamma(\tau^{-}\to e_{k}^{-}+V) = \frac{1}{128\pi}\,|A_{V}|^{2}f_{V}^{2}\,m_{\tau}^{3}\Big(2\frac{k\cdot p'}{m_{\tau}^{2}} - \frac{p\cdot p'}{m_{\tau}^{2}} + \frac{m_{V}^{2}}{m_{\tau}^{2}}\,\frac{k\cdot p}{k\cdot p'}\Big)\Big(1-\frac{m_{V}^{2}}{m_{\tau}^{2}}\Big)^{2}.\tag{126}$$

Table 5. Constraints from tau decay into a vector meson and a lepton $\tau^{-}\to e_{k}^{-}+V$ [65]. Here $u_{p} \equiv (100\,\text{GeV}/m_{\tilde{u}_{Lp}})^{2}$ and $d_{p} \equiv (100\,\text{GeV}/m_{\tilde{d}_{Rp}})^{2}$. Sum over $m,n,p = 1,2,3$ is to be understood.

Quantity	Experimental bound	Combinations constrained	Constraint
$B(\tau^{-}\to e^{-}\pi^{0})$	$< 4.2\times10^{-6}$	$V^{y}_{np}V_{pm}\;{}^{0}_{3n1}\,{}^{0}_{1m1}u_{p}$	$< 3.5\times10^{-3}$
		$V^{y}_{n1}V_{1m}\;{}^{0}_{3np}\,{}^{0}_{1mp}d_{p}$	$< 3.5\times10^{-3}$
$B(\tau^{-}\to eK^{0})$	$< 6.3\times10^{-6}$	$V^{y}_{np}V_{pm}\;{}^{0}_{3n1}\,{}^{0}_{1m2}u_{p}$	$< 3.0\times10^{-3}$
$B(\tau^{-}\to e\eta)$	$< 5.7\times10^{-6}$	$V^{y}_{np}V_{pm}\;{}^{0}_{3n1}\,{}^{0}_{2m1}u_{p}$	$< 4.2\times10^{-3}$
		$V^{y}_{n1}V_{1m}\;{}^{0}_{3np}\,{}^{0}_{2mp}d_{p}$	$< 4.2\times10^{-3}$
$B(\tau^{-}\to eK^{0})$	$< 9.4\times10^{-6}$	$V^{y}_{np}V_{pm}\;{}^{0}_{3n1}\,{}^{0}_{2m2}u_{p}$	$< 3.8\times10^{-3}$

The limits on the $\not{R}_p$ parameters A_V are given in Table 5 [65]. Note that the limits in this Table are comparable to those from $\to 3e; 3\ ; e^+$, and so on in Table 4. However, these two classes of tau decays constrain different combinations of and ^{0} from $\to 3e; e^+$; or 3 . Therefore, it is worthwhile to consider $\to e_k + V$, in addition to $\to e_k +$ and $\to l\bar{l}^0 l^0$, as an independent probe of lepton number violation beyond the SM. These decays are also easier to study experimentally compared with another decays $\to e_k + P$ (122) to be considered below, since one can tag the di-lepton emerging from the decay of a vector meson V (except for K^0 which decays mainly into K).

There are two contributions to tau decays into a pseudoscalar meson and a lepton (122): one from the axial vector current of quarks, and the other from the pseudoscalar density of quarks. Using the equations of motion for the lepton spinors and $p = k \quad k^0$, one can transform the former to the latter:

$$p\ l(k^0; s^0) \quad (1 \quad _5) \quad (k; s) \ \to \ l(\ m_l(1 \quad _5) + m \quad (1 + \ _5)) \quad ' \quad m\ l(1 + \ _5) \ ;$$

ignoring the final lepton mass. The corresponding amplitude derived from the effective Lagrangian (123):

$$M\ (\ \to e_k + P) = \bar{e}_k (A_L^P P_L + A_R^P P_R) \ ;$$

leads to the following decay rate:

$$(\ \to e_k + P) = \frac{m}{64} \ ^h \ |A_L^P + A_R^P|^2 + |A_L^P \quad A_R^P|^2 \ ^i \ ; \tag{127}$$

where $P = (^0; \ ; K)$ denotes the final pseudoscalar meson. The final lepton mass is ignored compared to the tau mass. The relevant amplitudes $A_{L;R}^P$'s are given by the following expressions [65]:

$$A_L^{\ 0} = \sum_n \frac{^{0}_{n11 \ \ n3k}}{2m^2_{\tilde{}_{Ln}}} \frac{f\ m^2}{2m_d};$$

$$A_R^{\ 0} = \sum_n \frac{^{0}_{n11 \ \ nk3}}{2m^2_{\tilde{}_{Ln}}} \frac{f\ m^2}{2m_d} \sum_{m;n;p} \frac{V^y_{np} V_{pm}}{4m^2_{\tilde{d}_{Lp}}}\ m\ f\ ^{0\ \ 0}_{3n1 \ \ km1} + \sum_{m;n;p} \frac{V^y_{m1} V_{1n}}{4m^2_{\tilde{d}_{Rp}}}\ m\ f\ ^{0\ \ 0}_{3mp \ \ knp};$$

$$A_L = \sum_n \frac{^{0}_{n11 \ \ n3k}}{2m^2_{\tilde{}_{Ln}}} \frac{f\ m^2}{2\sqrt{3}\,m_d} + \sum_n \frac{^{0}_{n22 \ \ n3k}}{2m^2_{\tilde{}_{Ln}}} \frac{f\ m^2}{\sqrt{3}\,m_s};$$

$$A_R = \sum_n \frac{^{0}_{n11 \ \ nk3}}{2m^2_{\tilde{}_{Ln}}} \frac{f\ m^2}{2\sqrt{3}\,m_d} \sum_n \frac{^{0}_{n22 \ \ nk3}}{2m^2_{\tilde{}_{Ln}}} \frac{f\ m^2}{\sqrt{3}\,m_s}$$

$$+ \sum_{m;n;p} \frac{V^y_{np} V_{pm}}{4m^2_{\tilde{d}_{Lp}}} \ ^{0\ \ 0}_{3n1 \ \ km1} \quad 2\ ^{0\ \ 0}_{3n2 \ \ km2} \frac{f\ m}{\sqrt{3}} + \sum_{m;n;p} \frac{V^y_{m1} V_{1n}}{4m^2_{\tilde{d}_{Rp}}} \ ^{0\ \ 0}_{3mp \ \ knp} \frac{f\ m}{\sqrt{3}};$$

$$A_L^{K^0} = \sum_n \frac{^{0}_{n3k \ \ n12}}{2m^2_{\tilde{}_{Ln}}} \frac{\sqrt{2} f_K m_K^2}{(m_d + m_s)};$$

$$A_R^{K^0} = \sum_n \frac{^{0}_{nk3 \ \ n21}}{2m^2_{\tilde{}_{Ln}}} \frac{\sqrt{2} f_K m_K^2}{(m_d + m_s)} + \sum_{m;n;p} \frac{V^y_{np} V_{pm}}{4m^2_{\tilde{d}_{Lp}}} \ ^{0\ \ 0}_{3n1 \ \ km2} \sqrt{2} f_K m_K \ :$$

In numerical analysis, the following current quark masses were used: $m_u = 5$ MeV, $m_d = 10$ MeV, $m_s = 200$ MeV. Comparing with the experimental upper limits on these SM-forbidden decays, one gets the constraints shown in Table 6 [65]. For the superparticle masses of 100 GeV, the constraints are all order of $10^{\ 2}$–$10^{\ 3}$, which are in the similar range as the constraints obtained from the decay $\to e_k + V$ (Table 5).

Another important semileptonic tau decay is $\to \quad + \quad$. The contribution to this process is given by the following Lagrangian:

$$L_e \quad = \quad \sum_n \frac{|^{0}_{31n}|^2}{m^2_{\tilde{d}_{Rn}}} \bar{u}^c P_L \quad \bar{} \ d_R P^c : \tag{128}$$

Table 6. Constraints from tau decay into a light pseudoscalar meson and a lepton $\to e_k + P$ [65]. Here $n_n \equiv (100\,GeV/m_{\tilde{\nu}_{Ln}})^2$, $u_p \equiv (100\,GeV/m_{\tilde{u}_{Lp}})^2$, and $d_p \equiv (100\,GeV/m_{\tilde{d}_{Rp}})^2$. Sum over m,n,p is to be understood.

Quantity	Experimental bound	Combinations constrained	Constraint
$B(\to e\,^0)$	$< 1.4 \times 10^{-4}$	$\lambda'_{n31}\lambda'^{*}_{n11} n_n;\ \lambda'_{n13}\lambda'^{*}_{n11} n_n$	$< 6.4 \times 10^{-2}$
		$V^{\dagger}_{np} V_{pm}\,\lambda'_{3n1}\lambda'^{*}_{1m1} u_p;\ V^{\dagger}_{m1} V_{n1}\,\lambda'_{3mp}\lambda'^{*}_{1np} d_p$	$< 6.6 \times 10^{-2}$
$B(\to\ ^0)$	$< 4.4 \times 10^{-5}$	$\lambda'_{n32}\lambda'^{*}_{n11} n_n;\ \lambda'_{n23}\lambda'^{*}_{n11} n_n$	$< 3.6 \times 10^{-2}$
		$V^{\dagger}_{np} V_{pm}\,\lambda'_{3n1}\lambda'^{*}_{2m1} u_p;\ V^{\dagger}_{m1} V_{n1}\,\lambda'_{3mp}\lambda'^{*}_{2np} d_p$	$< 3.7 \times 10^{-2}$
$B(\to eK^0)$	$< 1.3 \times 10^{-3}$	$\lambda'_{n31}\lambda'^{*}_{n12} n_n;\ \lambda'_{n13}\lambda'^{*}_{n21} n_n$	$< 8.5 \times 10^{-2}$
		$V^{\dagger}_{np} V_{pm}\,\lambda'_{3n1}\lambda'^{*}_{1m2} u_p$	$< 4.0 \times 10^{-1}$
$B(\to K^0)$	$< 1.0 \times 10^{-3}$	$\lambda'_{n32}\lambda'^{*}_{n12} n_n;\ \lambda'_{n23}\lambda'^{*}_{n21} n_n$	$< 7.6 \times 10^{-2}$
		$V^{\dagger}_{np} V_{pm}\,\lambda'_{3n1}\lambda'^{*}_{2m2} u_p$	$< 3.6 \times 10^{-1}$
$B(\to e\ )$	$< 6.3 \times 10^{-5}$	$\lambda'_{n31}\lambda'^{*}_{n11} n_n;\ \lambda'_{n13}\lambda'^{*}_{n11} n_n$	$< 4.5 \times 10^{-3}$
		$\lambda'_{n31}\lambda'^{*}_{n22} n_n;\ \lambda'_{n13}\lambda'^{*}_{n22} n_n$	$< 4.5 \times 10^{-2}$
		$V^{\dagger}_{np} V_{pm}\,(\lambda'_{3n1}\lambda'^{*}_{1m1} - 2\,\lambda'_{3n2}\lambda'^{*}_{1m2}) u_p$	$< 7.8 \times 10^{-2}$
		$V^{\dagger}_{m1} V_{1n}\,\lambda'^{*}_{3mp}\lambda'_{1np} d_p$	$< 7.8 \times 10^{-2}$
$B(\to\ )$	$< 7.3 \times 10^{-5}$	$\lambda'_{n32}\lambda'^{*}_{n11} n_n;\ \lambda'_{n23}\lambda'^{*}_{n11} n_n$	$< 4.8 \times 10^{-3}$
		$\lambda'_{n32}\lambda'^{*}_{n22} n_n;\ \lambda'_{n23}\lambda'^{*}_{n22} n_n$	$< 4.8 \times 10^{-2}$
		$V^{\dagger}_{np} V_{pm}\,(\lambda'_{3n1}\lambda'^{*}_{2m1} - 2\,\lambda'_{3n2}\lambda'^{*}_{2m2}) u_p$	$< 8.2 \times 10^{-2}$
		$V^{\dagger}_{m1} V_{1n}\,\lambda'^{*}_{3mp}\lambda'_{2np} d_p$	$< 8.2 \times 10^{-2}$

We use the gauge basis for the quark fields to contact with the constraint derived in the literature [68]. Comparing the theoretical expression for the branching ratio of this process with its experimental value [21]

$$B(\to\ +\ ) = 0.117 \pm 0.004$$

one derives the limit (with squark mass 100 GeV) [68]:

$$\lambda'_{31k} \quad 0.16: \tag{129}$$

4 Hadron properties and interactions

There are a plethora of processes with hadrons which are sensitive to the presence of new physics beyond the SM. Despite hadronic structure in certain cases introduces essential uncertainty in the theoretical predictions the limits on new physics derived from the high statistic experimental data are so stringent that uncertainty within order of magnitude appears to be not crucial. The proton decay represents a very good example of such a situation. Below we consider this and many other processes involved nucleons and mesons which receive non-trivial contributions from the $R\!\!\!/_p$ interactions.

4.1 Proton stability

Non-observation of the proton decay places very strong bounds on the simultaneous presence of both λ' and λ'' couplings [37], [69]–[71]. The effective Lagrangian description of the elementary baryons decays involves dimension-6 operators built with quarks and lepton fields. The $R\!\!\!/_p$ interactions can induce $B-L$ conserving contributions to the two decay processes, $p \to\ ^0 + e^+$ and $\ ^+ +\ $, through tree level $\tilde{d}_{kR}$ squarks s-channel exchange. The corresponding tree-level diagrams are given in Fig. 2(a) and Fig. 5. Also at tree level, there can occur $B+L$ conserving interactions, through the insertion of mass mixing terms in the internal squark line in the diagrams Fig. 5. These terms couple the left and right chirality

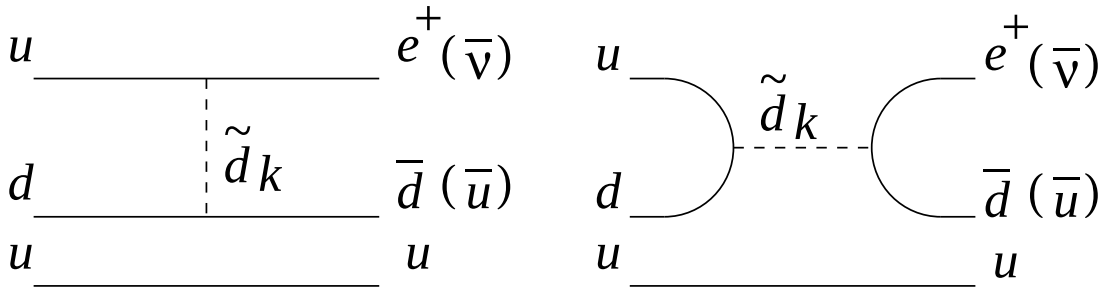

Fig. 5. Contributions to the proton decay.

squarks. The insertion results in the suppression factor $m_q/m_{\tilde{q}}$, where m_q and $m_{\tilde{q}}$ are the quark and its superpartner squark masses. These contribute to the chirality-flip, $B = L = 1$, decay process, $p \to K^+ + \bar{\nu}$. The decay widths can be estimated as

$$\begin{aligned}
(p \to e^+ \pi^0) \quad & \frac{|\lambda'_{11k}|^2 |\lambda''_{11k}|^2}{16\pi^2 m^4_{\tilde{d}_k}} M^5_{proton}; \\
(p \to \mu^+ \pi^0) \quad & \frac{|\lambda'_{i1k}|^2 |\lambda''_{11k}|^2}{16\pi^2 m^4_{\tilde{d}_k}} M^5_{proton}; \\
(p \to \mu^+ K^0) \quad & \frac{|\lambda'_{ik1}|^2 |\lambda''_{11k}|^2}{16\pi^2 m^4_{\tilde{d}_k}} \left(\frac{m_{dk}}{m_{\tilde{d}_k}}\right)^2 M^5_{proton}:
\end{aligned} \tag{130}$$

Given that $\tau(p \to e\pi) > 10^{32}$ years, one obtains [72] for $p \to \pi^0 + e^+$; $K^+ + \bar{\nu}$ and for $p \to K^+ + \bar{\nu}$, respectively,

$$|\lambda'_{i1k}\lambda''_{11k}| < 2 \cdot 10^{-27} \left(\frac{m_{\tilde{d}_{Rk}}}{100\ GeV}\right)^2; \qquad |\lambda'_{ik1}\lambda''_{11k}| < 2 \cdot 10^{-25} \left(\frac{m_{\tilde{d}_{Rk}}}{100\ GeV}\right)^3.$$

There are more complex mechanisms of the proton decay studied in the literature. They provide us with new constraints on the $\not{R}_p$ parameters.

The vertex loop diagrams associated with the Higgs boson dressing of the vertex $\bar{d}\bar{u}d$ and the box diagrams, having the same configurations of external lines as for tree-level diagrams, and propagating charged and neutral Higgs bosons internal lines were considered in [32]. It was found that this mechanism provides competitive bounds on the $\not{R}_p$ coupling constants: $\lambda'\lambda'' < 10^{-7} \cdot 10^{-9}$. Stronger bounds, $\lambda'\lambda'' < 10^{-11}$, hold if ones takes CKM flavour mixing into account. Some representative examples are: $\lambda'_{3j3}\lambda''_{121} < 10^{-7}$; (no matching case) $\lambda'_{2j2}\lambda''_{131} < 10^{-9}$ (matching case), where matching (no matching) refers to the case in which the generation index of d or d^c fields in λ' coincides (differs) from that of the d^c field in λ''. Another mechanism for the proton decay, involving a sequential tree level exchange of $\tilde{b}$, $\tilde{\chi}$, [70] gives bounds for the following three product combinations, $\lambda'_{ijk}\lambda''_{m21} < 10^{-9}$, $\lambda'_{ijk}\lambda''_{m31} < 10^{-9}$, $\lambda'_{ijk}\lambda''_{m32} < 10^{-9}$.

Contributions to the proton decay originating from the L-violating parameters λ_l in the superpotential (4) combined with the λ'''s have been investigated in [73]. Here, the diagram at the tree level produces a constraint, $\lambda''_{112}\lambda_l < 10^{-21}$, for an exchanged scalar mass of 1 TeV. Here $\lambda_l = \lambda_l = \lambda$, with λ assumed to be of the order of 1 TeV. Constraints on the other $\lambda''_{ijk}\lambda_l$-type combinations originate from loop diagrams and hence are weaker. They are typically of the order of 10^{-10}–10^{-14}, always assuming the superparticle masses of the order of 1 TeV. Stringent constraints were also obtained on the basis of the proton decay mechanism which involves the intermediate neutralino [74]. The constraints corresponding to various proton decay channels are presented in Table 7.

4.2 Neutron–antineutron oscillations

The neutron–antineutron oscillations $n \to \bar{n}$ could occur in presence of the baryon number violating interactions such as λ''-ones in the $\not{R}_p$ MSSM superpotential (4). This $B = 2$ transition is described

Table 7. Decay modes for the proton and bounds derived on the couplings for all possible combinations of the baryon violating and the lepton violating vertices. The bounds are on the products $''_{ijk}\ _{i^0j^0k^0}$. All superpartner masses are assumed to be 1 TeV. The ranges in the last column indicate variation due to different CKM projections.

	$''_{112}$		all other $''_{ijk}$	
$i^0j^0k^0$	Decay mode	Bounds	Decay mode	Bounds
$i^0 \neq j^0 \neq k^0, k^0 \neq 3$	$p \to K^+ e$	10^{-16}	$p \to {}^+(K^+)e$	10^{-5}–10^{-7}
$i^0 \neq j^0 \neq k^0, k^0 = 3$	$p \to K^+ + 3$	10^{-14}	$p \to {}^+(K^+) + 3$	10^{-3}–10^{-5}
$j^0 = k^0 = 1$ (or $i^0 = k^0 = 1$)	$p \to K^+$	10^{-17}	$p \to {}^+(K^+)$	10^{-6}–10^{-8}
$j^0 = k^0 = 2$ (or $i^0 = k^0 = 2$)	$p \to K^+$	10^{-20}	$p \to {}^+(K^+)$	10^{-9}–10^{-11}
$j^0 = k^0 = 3$ (or $i^0 = k^0 = 3$)	$p \to K^+$	10^{-21}	$p \to {}^+(K^+)$	10^{-10}–10^{-12}

by the effective Lagrangian

$$L = \quad m \quad {}^c n + H.c. \tag{131}$$

having the form of the neutron Majprana mass term. The oscillation time for free neutrons is estimated to be, $^{1}_{oscill} = \quad = 1= m$. Recall that this is related to the nuclear lifetime against double nucleon decays [75], $NN \to X$, denoted as, $_{NN}$, by the relationship: $_{NN} = a\ m^2=m_N$, where $a \quad 10^{-2}$ is a nuclear wave function factor and m_N is the nucleon mass. The present experimental bound on the oscillation time is, $_{oscill} > 1{:}2\ 10^8$ s. This is to be compared with the bound deduced from, $_{NN} > 10^{32}$ years, which yields: $m < 10^{-28}$, hence $_{oscill} > 10^6$ s.

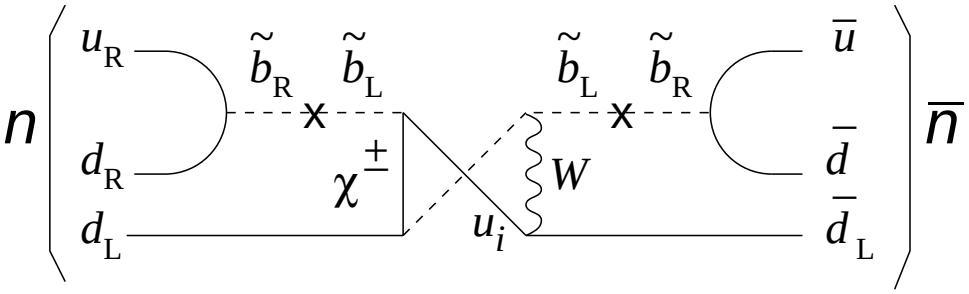

Fig. 6. Quark-level diagram triggering the n–n-oscillation.

The quark-level diagram triggering the n–n-oscillation is given in Fig. 6 [71]. This leads to the effective operator $(u^c d)(d^c d)(u^c d)$. The diagrams of this type with the internal squark $\tilde{q}_i$ have the suppression factor $(m_q=M_W)^2$ with m_q being the mass of the partner quark mass. This factor originates from the $\tilde{q}_L$–$\tilde{q}_R$-mixing involved in the diagram in Fig. 6. Therefore a meaningful bound can be derived from n–n oscillation only for the coupling [71]: $''_{132} < 10^{-3}$.

4.3 Double nucleon decay processes

Strong bounds on $''_{121}$ can be derived from non-observation of double nucleon decay processes which violate the baryon number and the strangeness so that $B = \quad S = \quad 2$. The process of this type [71] $^{16}O \to {}^{14}C + K^+ + K^+ +$ would have been seen in water Cerenkov detectors. The diagram contributing to this process at the quark level is shown in Fig. 7.

This processes is described by the effective dimension-9 six-fermion operators, $O = u_R d_R d_R u_R s_R s_R$. From the experimental bound, $_{NN} > 10^{30}$–^{33} years, one deduces the bounds [71]:

$$''_{121} < 10^{-15} R^{-5=2}; \qquad \text{with} \qquad R = \frac{\tilde{}}{(m_g m_{\tilde{q}}^4)^{1=5}}: \tag{132}$$

Here $\tilde{}$ is the effective nuclear structure parameter. The actual value of R can be in the interval, 10^{-3}–10^{-6}. Therefore one finds: $''_{121} < 10^{-7}$ 10^{0}.

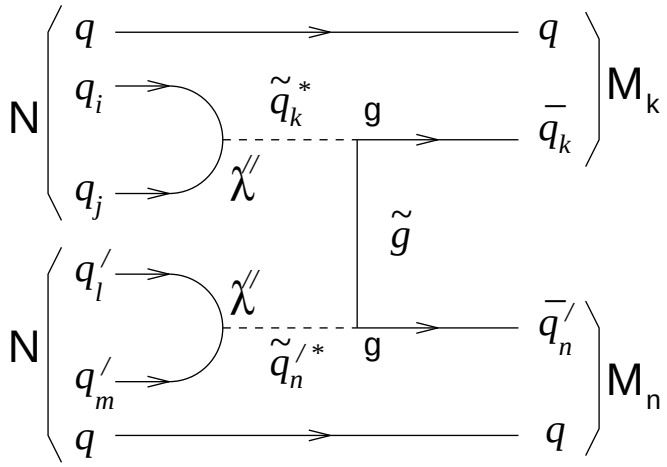

Fig. 7. Quark-level diagram contributing to double nucleon decay process.

4.4 Meson decays into two charged leptons

Let us consider the decays of a neutral meson M into two charged leptons $M \to e_i \bar{e}_j$. We focus on K^0, ^{0} and B_q^0 meson decays with $q = d, s$ for the letter case. In the $R\!\!\!/_p$MSSM these processes are described by the tree-level diagrams in Fig. 8 with t-channel squarks $\tilde{u}_{Li}$, $\tilde{d}_{Ri}$ and s-channel sneutrinos $\tilde{\nu}_i$ [76, 77].

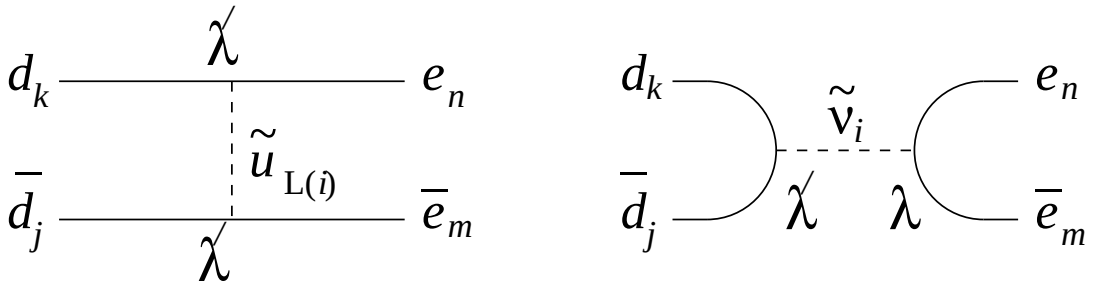

Fig. 8. Tree-level diagrams contributing to neutral meson decay into two charged leptons.

The corresponding low-energy effective Lagrangian in the quark mass basis can be readily derived from the Lagrangian (64). It takes the form

$$\begin{aligned} L_e \;=\; & \frac{2\,{}^{0}_{njk}\,{}^{0}_{nlm}}{m^2_{\tilde{e}_n}}(\bar{e}_j P_R e_k)(\bar{d}_m P_L d_l) \;-\; \frac{V_{nr}V_{ns}\,{}^{0}_{jrk}\,{}^{0}_{lsm}}{2m^2_{\tilde{e}_{Ln}}}(\bar{e}_j \;\; P_L e_l)(\bar{d}_m \;\; P_R d_k) \\ & + \frac{V_{mr}V_{ks}\,{}^{0}_{jrn}\,{}^{0}_{lsn}}{2m^2_{\tilde{e}_{Rn}}}(\bar{e}_j \;\; P_L e_l)(\bar{u}_m \;\; P_R u_k) + H.c.; \end{aligned} \tag{133}$$

where diagonality of the soft mass term matrices is assumed and summation over repeating indexes is implied. With the PCAC (partial conservation of axial-vector current) relations

$$\langle 0|\bar{q}\,\gamma_5 q|M(p)\rangle = i f_M p\,; \qquad \langle 0|\bar{q}\,\gamma_5 q|M(p)\rangle = -\,i f_M \frac{M_M^2}{m_p + m_q}; \tag{134}$$

the decay rate of the processes $M \to e_i e_j^+$ reads

$$\begin{aligned} \Gamma(M[\bar{q}q] \to e_i e_j^+) = {} & \frac{f_M^2 M_M^3 \sqrt{}}{64\pi m^4}\,1 + (\tilde{}^2_{Mi} - \tilde{}^2_{Mj})^2 - 2(\tilde{}^2_{Mi} + \tilde{}^2_{Mj}) \\ & h_M^2\,(|A_{ij}^{pq}|^2 + |B_{ij}^{pq}|^2)(1 - \tilde{}^2_{Mi} - \tilde{}^2_{Mj}) + |C_{ij}^{pq}|^2\,(\tilde{}^2_{Mi} + \tilde{}^2_{Mj}) - (\tilde{}^2_{Mi} - \tilde{}^2_{Mj})^2 \\ & + 4h_M\,\mathrm{Re}(A_{ij}^{pq}B_{ij}^{pq})\,\tilde{}_{Mi}\tilde{}_{Mj} + 2h_M\,\tilde{}_{Mj}\,\mathrm{Re}(A_{ij}^{pq}C_{ij}^{pq})(1 + \tilde{}^2_{Mi} - \tilde{}^2_{Mj}) \\ & + 2h_M\,\tilde{}_{Mi}\,\mathrm{Re}(B_{ij}^{pq}C_{ij}^{pq})(1 + \tilde{}^2_{Mj} - \tilde{}^2_{Mi})\,; \end{aligned} \tag{135}$$

where $_{M\,i}$ $m_{e_i}=M_M$, $h_M = M_M=(m_p + m_q)$. We assume the universal soft mass m. In (135) M_M and f_M are the mass and the usual leptonic decay constant of the M meson. The constants A^{pq}_{ij}, B^{pq}_{ij}, and C^{pq}_{ij} which depend on the generations of leptons and the type of a neutral M meson are given by

$$A^{pq}_{ij} = 2\sum_{n=1}^{3} {}_{nij}\,{}^{0}_{nqp}; \qquad B^{pq}_{ij} = 2\sum_{n=1}^{3} {}_{nji}\,{}^{0}_{npq}; \qquad C^{pq}_{ij} = \frac{1}{2}\sum_{n,p,s=1}^{3} V_{np}V_{ns}\,{}^{0}_{ipq}\,{}^{0}_{jsp} = \frac{1}{2}\sum_{n=1}^{3} {}^{0}_{inq}\,{}^{0}_{jnp}: \quad (136)$$

Note that $A^{pq}_{ij} \neq A^{pq}_{ji}$, etc.

Using the experimental values on the branching ratios of the B^0, K^0-meson decays into two charged leptons [21, 78] from Table 8 and 9 together with eq. (135) one can obtain the limits [76]–[82] on the coefficients A^{pq}_{ij}, B^{pq}_{ij}, and C^{pq}_{ij}.

In the calculations one can safely neglect the SM contributions to the processes under considerations. This is because in the SM, the processes which have different lepton species as decay products are forbidden due to the conservation of each lepton flavor. On the other hand, the processes with the same lepton species are highly suppressed [83] because they can be realized in the SM only at the loop level and contain small CKM factors.

The rare meson decays lead to host of bounds on combinations of R_p couplings like those in (136). Since particular products of ^{0} or $^{0\,0}$ do occur more than once in definitions of various meson decay rates, it is instructive to see what the bounds would be if only one product were non-zero [67, 79]. Under this assumption in Table 8 and 9 the constraints are given for the products relevant to K and B-decays.

The effective Lagrangian (133) also contributes to the decays $^0 \to e^+e$ and $\to l\,l$ as well as the lepton flavor violating decay $^0 \to e$. In these decays, the (pseudo)scalar (pseudo)scalar couplings give the largest contributions because they are enhanced by a factor of $m^2=m_d$ as seen from (134). So we ignore the contributions from last two terms in (133) with the (V–A) quark currents. In this approximation, the decay rate for this process is [65]

$$(\ ^0 \to\ e\ ) = \frac{m}{16}\left[\,|A_L + A_R|^2 + |A_L - A_R|^2\left(1 - \frac{m^2}{m^2}\right)^2\right];$$

$$A_L = \frac{f\,m^2}{8m_d}\sum_n \frac{{}^{0}_{n11}\,{}_{nij}}{m^2_{e_n}}; \qquad A_R = \frac{f\,m^2}{8m_d}\sum_n \frac{{}^{0}_{n11}\,{}_{nji}}{m^2_{e_n}}:$$

For the decays $^0 \to e$, there is a tight upper bound on the branching ratio, $1:72 \quad 10^{8}$. This implies that (for $m_{e_n} = 100$ GeV)

$$\sum_n {}^{0}_{n11}\,{}_{n12}\;\; {}^{0}_{n11}\,{}_{n21} < 0:14:$$

For the lepton number conserving decay $^0 \to e^+e$, the branching ratio is known to be

$$B(\ ^0 \to\ e^+e\ ) = (7:5 \quad 2:0) \quad 10^{8}; \qquad (137)$$

which is dominated by the so-called unitarity bound coming from $^0 \to \quad \to e^+e$. This unitarity bound is calculable, and known to be [84]:

$$\frac{{}_{unit}(\ ^0 \to\ e^+e\ )}{(\ ^0 \to\ \ )} = \frac{^2}{2\ _e}\frac{m^2_e}{m^2}\left[\ln\frac{1+\ _e}{1\ \ _e} \quad !\right]^2 = 4:75 \quad 10^{8}; \qquad (138)$$

with $_e = \sqrt{1 \quad 4m_e^2=m^2_{\ 0}}$. Extracting this unitary bound from the experimental branching ratio and assuming no large contributions from the dispersive part of the two-photon contributions (ReA) or large cancellation between ReA and the R_p contributions, we can put the (90 % C.L.) limit on the contribution from the R_p interactions (with $m_{\tilde{e}} = 100$ GeV) [65]:

$$\sum_n {}^{0}_{n11}\,{}_{n11}\;\; {}^{0}_{n11}\,{}_{n11} < 0:15: \qquad (139)$$

Table 8. Upper bounds on the magnitudes of coupling products derived from rare K decays, under the assumption that only one such product is nonzero [67]. In the entry marked with (?), it was assumed that the CKM matrix elements obey the property $V_{12} = V_{21}$.

Quantity	Experimental value (bound)	Combinations constrained	Upper bound
$B(K_L \to \quad)$	$(7.4 \quad 0.4) \quad 10^{11}$	$122\ {}^{0}_{112};\ 122\ {}^{0}_{121};\ 232\ {}^{0}_{312};\ 232\ {}^{0}_{321}$	$3.8 \quad 10^{7}$
		(?) $\quad {}^{0}_{211}\ {}^{0}_{222};\ {}^{0}_{212}\ {}^{0}_{221}$	$3.3 \quad 10^{5}$
$B(K_L \to \quad ee)$	$< 4.1 \quad 10^{11}$	$121\ {}^{0}_{212};\ 121\ {}^{0}_{221};\ 131\ {}^{0}_{312};\ 131\ {}^{0}_{321}$	$2.5 \quad 10^{8}$
$B(K_L \to \quad e+ \quad e)$	$< 3.3 \quad 10^{11}$	$122\ {}^{0}_{212};\ 122\ {}^{0}_{221};\ 132\ {}^{0}_{312};\ 132\ {}^{0}_{321}$ $121\ {}^{0}_{112};\ 121\ {}^{0}_{121};\ 231\ {}^{0}_{312};\ 231\ {}^{0}_{321}$	$2.3 \quad 10^{8}$
		${}^{0}_{111}\ {}^{0}_{212};\ {}^{0}_{112}\ {}^{0}_{211};\ {}^{0}_{121}\ {}^{0}_{222}$ ${}^{0}_{122}\ {}^{0}_{221};\ {}^{0}_{131}\ {}^{0}_{232};\ {}^{0}_{132}\ {}^{0}_{231}$	$3.5 \quad 10^{7}$

Table 9. Upper bounds on the magnitudes of products of couplings derived from B^0 decays into two charged leptons [80].

Quantity	Experimental value (bound)	Combinations Constrained	Upper bound
$B(B_d \to e^+ e \ )$	$< 5.9 \quad 10^{6}$	${}^{0}_{121}{}_{213},\ {}^{0}_{121}{}_{231},\ {}^{0}_{131}{}_{313},\ {}^{0}_{131}{}_{331}$	$4.6 \quad 10^{5}$
$B(B_d \to e \quad)$	$< 5.9 \quad 10^{6}$	${}^{0}_{121}{}_{113},\ {}^{0}_{121}{}_{131},\ {}^{0}_{121}{}_{231},\ {}^{0}_{122}{}_{213}$	$4.6 \quad 10^{5}$
		${}^{0}_{132}{}_{313},\ {}^{0}_{132}{}_{331},\ {}^{0}_{231}{}_{313},\ {}^{0}_{231}{}_{331}$	$4.6 \quad 10^{5}$
$B(B_d \to e \quad)$	$< 5.3 \quad 10^{4}$	${}^{0}_{123}{}_{213},\ {}^{0}_{123}{}_{231},\ {}^{0}_{131}{}_{113},\ {}^{0}_{131}{}_{131}$	$4.9 \quad 10^{4}$
		${}^{0}_{133}{}_{313},\ {}^{0}_{133}{}_{331},\ {}^{0}_{231}{}_{213},\ {}^{0}_{231}{}_{231}$	$4.9 \quad 10^{4}$
		${}^{0}_{131}\ {}^{0}_{333}$	$5.8 \quad 10^{3}$
$B(B_d \to \quad)$	$< 8.3 \quad 10^{4}$	${}^{0}_{123}{}_{113},\ {}^{0}_{123}{}_{131},\ {}^{0}_{132}{}_{113},\ {}^{0}_{132}{}_{131}$	$6.0 \quad 10^{4}$
		${}^{0}_{232}{}_{213},\ {}^{0}_{232}{}_{231},\ {}^{0}_{233}{}_{313},\ {}^{0}_{233}{}_{331}$	$6.0 \quad 10^{4}$
		${}^{0}_{231}\ {}^{0}_{333},\ {}^{0}_{233}\ {}^{0}_{331}$	$7.4 \quad 10^{3}$
$B(B_d \to \quad ^+ \quad)$	$< 1.6 \quad 10^{6}$	${}^{0}_{122}{}_{113},\ {}^{0}_{122}{}_{131},\ {}^{0}_{232}{}_{313},\ {}^{0}_{232}{}_{331}$	$2.4 \quad 10^{5}$
$B(B_s \to \quad ^+ \quad)$	$< 8.4 \quad 10^{6}$	${}^{0}_{122}{}_{123},\ {}^{0}_{122}{}_{132},\ {}^{0}_{232}{}_{323},\ {}^{0}_{232}{}_{332}$	$5.5 \quad 10^{5}$

4.5 Semileptonic decays of mesons

Let us consider semileptonic decays of K, D and B mesons which provide us with various rather stringent constraints on the R_p parameters.

Recently there was reported [85] an evidence of the decay $K^+ \to \quad ^+ \quad$ with the branching ratio

$$B(K^+ \to \quad ^+ \quad) = 4.2^{+9.7}_{3.5} \quad 10^{10}: \tag{140}$$

In the SM this process can be realized only at the loop level and, therefore, is suppressed. The SM contribution [86] is at least one order of magnitude smaller than the experimental 1 upper limit $(1.4 \quad 10^{9})$.

The R_p MSSM allows the tree-level contributions to this process described by the diagrams shown in Fig. 9 [13, 24], [87]–[90].

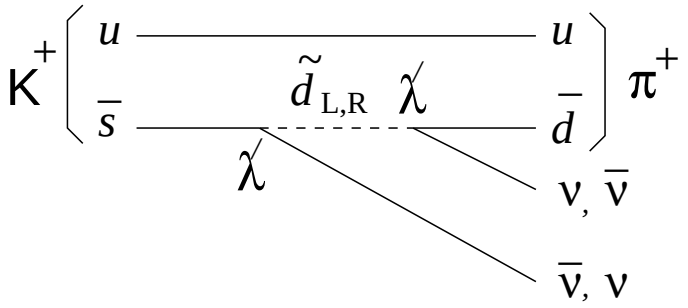

Fig. 9. Tree-level contribution to the semileptonic decay $K^+ \to \pi^+ \nu\bar{\nu}$.

The corresponding low-energy effective Lagrangian governing $K^+ \to \pi^+ \nu\bar{\nu}$ is given by [24, 87]

$$L_{eff} = \frac{1}{2}\left(\frac{\lambda'^{*}_{i2k}\lambda'_{j1k}}{m^2_{\tilde{d}_{Rk}}} + \frac{\lambda'^{*}_{ik1}\lambda'_{jk2}}{m^2_{\tilde{d}_{Lk}}} \right) (\bar{s}\gamma^\mu P_L d)(\bar{\nu}_i \gamma_\mu P_L \nu_j). \tag{141}$$

This Lagrangian has been derived in the qurak mass basis using the definition of the trilinear couplings given in (64). The branching ratio takes the form [79]

$$B(K^+ \to \pi^+ \nu\bar{\nu}) = \frac{1}{(16\pi G_F^2 |V_{us}|)^2} \left[\frac{\lambda'^{*}_{i2k}\lambda'_{j1k}}{m^2_{\tilde{d}_{Rk}}} + \frac{\lambda'^{*}_{ik1}\lambda'_{jk2}}{m^2_{\tilde{d}_{Lk}}} \right]^2 B(K^+ \to \pi^0 e\nu), \tag{142}$$

where $B(K^+ \to \pi^0 e\nu) = 0.0482$. Requiring that the $R\!\!\!/_p$ MSSM contribution (142) saturates the 1σ upper limit deduced from (140) for $m_{\tilde{d}_{Lk}} \simeq m_{\tilde{d}_{Rk}} = 100$ GeV yields [79]

$$\lambda'^{*}_{ik1}\lambda'_{jk2} < 1.6 \times 10^{-5}; \qquad \lambda'^{*}_{i2k}\lambda'_{j1k} < 1.6 \times 10^{-5} \tag{143}$$

In derivation of (143) we assumed that only one product is non-zero at a time.

The semileptonic decays of charged D meson $D^+ \to \bar{K}^0 \mu^+ \nu_\mu$, and $D^+ \to \bar{K}^0 e^+ \nu_e$ are induced at the tree-level by the SM W-boson exchange and by the $R\!\!\!/_p$ MSSM down-squark and selectron exchange as shown in Fig. 10.

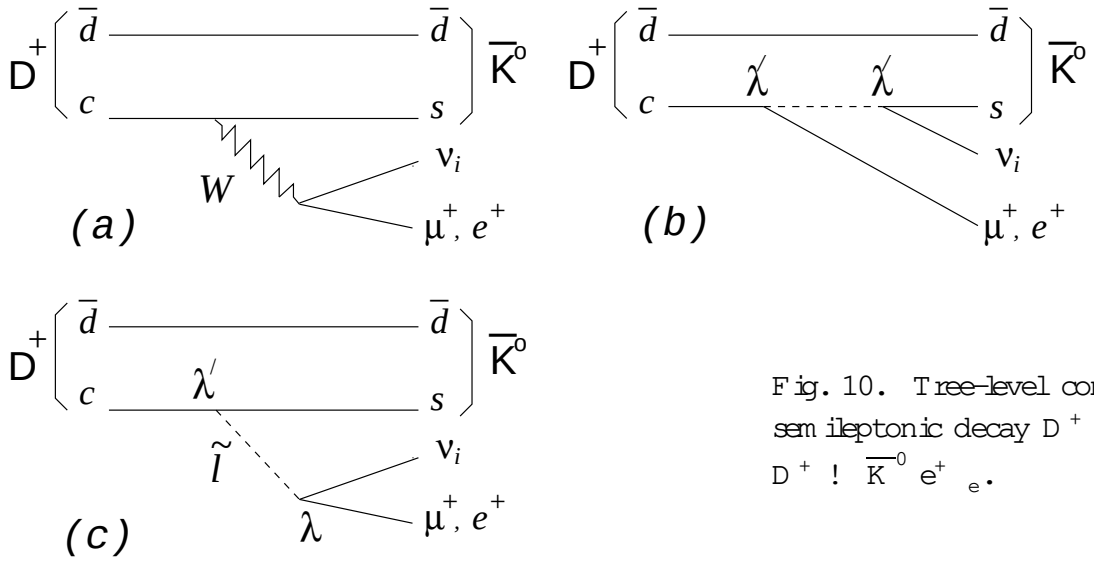

Fig. 10. Tree-level contribution to the semileptonic decay $D^+ \to \bar{K}^0 \mu^+ \nu_\mu$ and $D^+ \to \bar{K}^0 e^+ \nu_e$.

The effective low-energy Lagrangian for this case is given by the formula

$$L_{eff} = V_{cs}\frac{4G_F}{\sqrt{2}}(\bar{s}\gamma^\mu P_L c)(\bar{\tau}_i \gamma_\mu P_L e_i) \tag{144}$$
$$V_{cs}\frac{\lambda'^{*}_{lnk}\lambda'_{i2k}}{2m^2_{\tilde{d}_{Rk}}}(\bar{s}\gamma^\mu P_L c)(\bar{\tau}_i \gamma_\mu P_L e_l) + 2V_{cs}\frac{\lambda'^{*}_{kn2}\lambda'_{ikl}}{m^2_{\tilde{e}_{Lk}}}(\bar{s}P_L c)(\bar{\tau}_i P_L e_l).$$

The first term corresponds to the SM W-exchange contribution. Using the experimental input [21]:

$$\frac{B(D^+ \to \overline{K}^0 \; ^+ \;)}{B(D^+ \to \overline{K}^0 \, e^+ \; _e)} = 0{:}94 \quad 0{:}16; \tag{145}$$

one obtains (at 1) rather weak constraints [15] $^0_{12k}$ 0:3 and $^0_{22k}$ 0:2 (for m = 100 GeV). The form factors related to the hadronic matrix elements cancel in the ratios, thus making the prediction free from the large theoretical uncertainties associated with those matrix elements.

In the MSSM with R-parity conservation a contribution to the semileptonic B decay $b \to q e_l \bar{} _n$ (Fig. 11(a,b)) is described by the effective Lagrangian [76], [91]–[93]

$$L_{eff}(b \to q e_l \bar{} _l) = V_{qb} \frac{4G_F}{\sqrt{2}} \Big[(\bar{q} \; P_L b)(\bar{e}_l \; P_L \; _l) \quad R_l (\bar{q} P_R b)(\bar{e}_l P_L \; _l) \Big]^i ; \tag{146}$$

where $R_l = r^2 m_{e_l} m_b^Y$ and $r = \tan \; / m_H$. An upper index Y denotes the running quark mass, tan is the ratio of the vacuum expectation values of the neutral Higgs fields (16) and m_H is the mass of the charged Higgs fields.

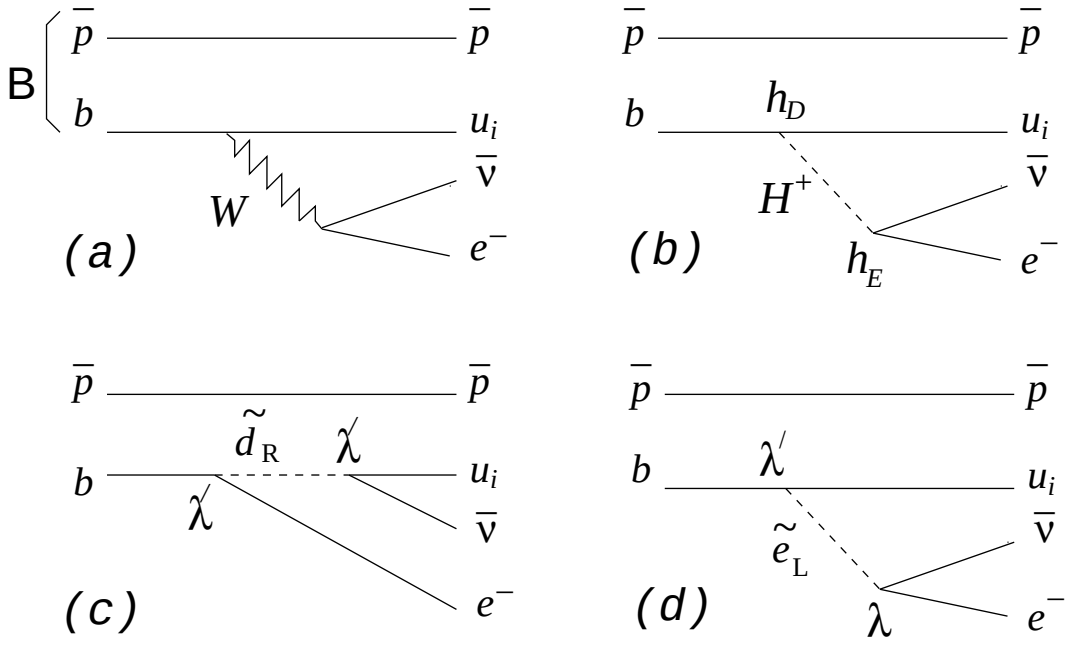

Fig. 11. Contributions to the semileptonic B decay.

The first term gives the SM W-exchange contribution (Fig. 11(a)) and the second one (Fig. 11(b)) gives that of the charged Higgs scalar. Neglecting the masses of the electron (l = 1) and the muon (l = 2), the contribution of the charged Higgs scalars is zero. The contribution of the charged Higgs scalars is not vanishing only when l = 3; $b \to q$. We neglect a term proportional to m_c^Y for $q = c$ since the term is suppressed by the mass ratio m_c^Y / m_b^Y and does not have the possibly large $\tan^2$ factor.

In the $R\!\!\!/_p$ MSSM, the exchanges of the squarks and the sleptons, as shown in Fig. 11(c,d), lead to the additional four-fermion interactions which are relevant for the semileptonic decays of B meson. The effective Lagrangian can be parameterized as

$$L^e_{R\!\!\!/_p}(b \to q e_l \bar{} _n) = V_{qb} \frac{4G_F}{\sqrt{2}} \Big[A^q_{ln} (\bar{q} \; P_L b)(\bar{e}_l \; P_L \; _n) \quad B^q_{ln} (\bar{q} P_R b)(\bar{e}_l P_L \; _n) \Big]^i ; \tag{147}$$

where we assume the matrices of the soft mass terms are diagonal in the fermion mass basis. Note that the operators here take the same form as those of the MSSM with R_p in (146). Comparing with the SM, the above effective Lagrangian includes the interactions even when l and n are different from each

other. The dimensionless coupling constants A and B depend on the species of quark, charged lepton and neutrino and are given by

$$A^{q}_{ln} = \frac{\sqrt{2}}{4G_F V_{qb}} \sum_{i,j=1}^{3} \frac{1}{2m^2_{\tilde{e}_{Ri}}} V_{qj}\, {}^{0}_{n3}\, {}^{0}_{lji}; \qquad B^{q}_{ln} = \frac{\sqrt{2}}{4G_F V_{qb}} \sum_{i,j=1}^{3} \frac{2}{m^2_{\tilde{e}_{Li}}} V_{qj}\, {}^{0}_{inl}\, {}^{0}_{ij3}; \tag{148}$$

where $q = u, c$ and l and n are the generation indices running from 1 to 3. When the species of the charged lepton and the neutrino are the same, the decay rate of the process $b \to q\tilde{e}_{Ll}$ is

$$\Gamma^{q}_{ll} = \frac{|V_{qb}|^2 G_F^2 m_b^5}{192\pi^3} \left(|1 + A^{q}_{ll}|^2 \Gamma_W + \frac{1}{4} |R_l + B^{q}_{ll}|^2 \Gamma_H - 2\mathrm{Re}[(R_l + B^{q}_{ll})(1 + A^{q}_{ll})] \frac{m_{e_l}}{m_b} \Gamma_I \right). \tag{149}$$

And for the different species of the charged lepton and the neutrino, the decay rate of the process $b \to q\tilde{e}_{Ln}$ is

$$\Gamma^{q}_{ln} = \frac{|V_{qb}|^2 G_F^2 m_b^5}{192\pi^3} \left(|A^{q}_{ln}|^2 \Gamma_W + \frac{1}{4} |B^{q}_{ln}|^2 \Gamma_H - 2\mathrm{Re}(B^{q}_{ln} A^{q}_{ln}) \frac{m_{e_l}}{m_b} \Gamma_I \right).$$

The subindices W, H and I of Γ denote the W mediated (SM), charged Higgs mediated and interference contributions respectively. The explicit forms and relations between Γ_W, Γ_H and Γ_I are given in [92]–[94]. For $l = 1$ and 2, R_l and the interference term are vanishing assuming the electron and the muon are massless.

Since the species of the neutrino cannot be distinguished by experiments and the $\not{R}_p$ interactions allow the different kinds of the charged lepton and the neutrino as decay products, we sum the above decay rates over neutrino species to compare with experimental data:

$$\Gamma^{q}_{l} \sum_{n=1}^{3} \Gamma^{q}_{ln}.$$

R-parity non-conservation could results in the lepton non-universality. The semileptonic branching ratios $b \to e X$ and $b \to \mu X$ measured by the L3 Collaborations [95] are

$$B(b \to e X) = (10.89 \pm 0.55)\%; \qquad B(b \to \mu X) = (10.82 \pm 0.61)\%.$$

Considering this lepton universality measurements under the assumption that $\not{R}_p$ does not contribute to these two semileptonic branching ratios simultaneously, we can derive 1σ bounds on single and some products of $\not{R}_p$ couplings slightly stronger than ones from the other processes (see Table 10). All other B meson semileptonic decay modes give the constraints which are weaker than those from the other processes. We do not present these bounds referring readers to [81].

Table 10. Upper bounds on the magnitudes of $\not{R}_p$ couplings from the lepton universality in the semileptonic decays of B meson [81].

Processes	Combinations Constrained	Upper Bound
$b \to e^- X_c$	$\lambda^{0}_{131}\lambda^{0}_{121}$, $\lambda^{0}_{132}\lambda^{0}_{122}$	1.1×10^{-3}
	λ^{0}_{131}, λ^{0}_{132}	1.6×10^{-1}
$b \to \mu^- X_c$	$\lambda^{0}_{231}\lambda^{0}_{221}$, $\lambda^{0}_{232}\lambda^{0}_{222}$, $\lambda^{0}_{233}\lambda^{0}_{223}$	1.1×10^{-3}
	λ^{0}_{231}, λ^{0}_{232}, λ^{0}_{233}	1.6×10^{-1}

The effective Lagrangian which describes the decay $B \to X_s l_i^+ l_j$ is [82]

$$L^{e}_{\not R_p} = \sum_{n=1}^{3} \frac{2}{m^2_{\tilde{e}_n}} \Big[\lambda'_{njk} \lambda'^{*}_{nlm} (\bar{e}_j P_R e_k)(\bar{d}_m P_L d_l) + H.c. \Big] \\ \sum_{n,r,s=1}^{3} \frac{1}{2m^2_{\tilde{e}_{Ln}}} V_{nr} V_{ns} \lambda'_{jrk} \lambda'^{*}_{lsm} (\bar{e}_j \gamma^\mu P_L e_l)(\bar{d}_m \gamma_\mu P_R d_k): \qquad (150)$$

The matrices of the soft mass terms are assumed to be diagonal. Various semileptonic b decays could appear at tree level: $b \to q e^+ e^-$, $q \nu \nu$, $q \nu \tau^+ \tau^-$, $q e^- \tau^+$, $q \nu \tau^+$ with $q = d, s$.

The experimental upper bounds for $b \to s l_i^+ l_j$ (at 90% C.L.) are [21]

$$B(b \to s e^+ e^-) < 5.7 \times 10^{-5}; \qquad (151)$$

$$B(b \to s \tau^+ \mu^-) < 5.8 \times 10^{-5}; \qquad (152)$$

$$B(b \to s e \tau) < 2.2 \times 10^{-5}: \qquad (153)$$

In the SM, the process $b \to s e \tau$ is forbidden due to the conservation of each lepton flavor number. On the other hand, the decay $b \to s \nu \bar{\nu}$ ($b \to s e^+ e^-$) is dominated by the electroweak penguin diagram and receives small contributions from box diagrams and magnetic penguins. A recent analysis gives [96] $B(b \to s e^+ e^-)_{SM} = (8.4 \pm 2.3) \times 10^{-6}$, $B(b \to s \nu \bar{\nu})_{SM} = (5.7 \pm 1.2) \times 10^{-6}$. The experimental bounds are almost one order of magnitude larger than the SM expectations. If we neglect the SM contribution, the decay rate of the processes $b \to s l_i^+ l_j$ reads

$$\Gamma(b \to s l_i^+ l_j) = \frac{m_b^5}{6144\pi^3 m_{\tilde{f}}^4} \Big[4(|A_{ij}|^2 + |B_{ij}|^2) + |C_{ij}|^2 \Big] \qquad (154)$$

The constants A_{ij}, B_{ij} and C_{ij} are given by

$$A_{ij} = 2 \sum_{n=1}^{3} \lambda'_{nji} \lambda'^{*}_{n32}; \qquad B_{ij} = 2 \sum_{n=1}^{3} \lambda'_{nij} \lambda'^{*}_{n23}; \qquad C_{ij} = \frac{1}{2} \sum_{n,p,s=1}^{3} V_{np} V_{ns} \lambda'_{jp3} \lambda'^{*}_{is2} = \sum_{n=1}^{3} \lambda'_{jn3} \lambda'^{*}_{in2}: \qquad (155)$$

These coefficients coincide with those for the pure leptonic decay modes of B meson given in (136) for $p = 2$, $q = 3$. We assume the universal soft mass $m_{\tilde{f}}$ and ignore the lepton mass. To remove the large uncertainty in the total decay rate associated with the m_b^5 factor, it is convenient to normalize $B(b \to s l_i^+ l_j)$ to the semileptonic rate $B(b \to c e^- \bar{\nu})$. We then obtain

$$4(|A_{ij}|^2 + |B_{ij}|^2) + |C_{ij}|^2 = \frac{6144\pi^4 m_{\tilde{f}}^4 G_F^2 |V_{cb}|^2 f_{ps}(m_c^2/m_b^2)}{192} \frac{B(b \to s l_i^+ l_j)}{B(b \to c e^- \bar{\nu})}, \qquad (156)$$

where $f_{ps}(x) = 1 - 8x + 8x^3 - x^4 - 12x^2 \ln x$ is the usual phase-space factor. Using $B(b \to c e^- \bar{\nu}) \simeq 10.5\%$, $f_{ps}(m_c^2/m_b^2) \simeq 0.5$, $|V_{cb}| \simeq 0.04$, we obtain

$$4(|A_{ij}|^2 + |B_{ij}|^2) + |C_{ij}|^2 = 3.3 \times 10^{-3} \left(\frac{m_{\tilde{f}}}{100\ GeV} \right)^4 B(b \to s l_i^+ l_j): \qquad (157)$$

Substituting to the right hand side of this formula the experimental values given in (151)–(153) one obtains the upper bounds given in Table 11.

The $B_s \to l_i^+ l_j$ process is described with the same parameters A, B, C and in some cases gives slightly more stringent bounds [80]. But, two things make the decay $b \to s l_i^+ l_j$ more useful than the $B_s \to l_i^+ l_j$ process. One thing is that the contribution of the product combinations of $\lambda' \lambda'^{*}$ type is vanishing in the limit of zero lepton mass and so these parameters cannot be constrained in the case of the decays $B_s \to l_i^+ l_j$. The other thing is that the experimental upper limit on the branching ratios exist only in the $B_s \to \tau^+ \mu^-$ process at present.

Table 11. Upper bounds on the magnitudes of products of couplings derived from $b \to s l_i^+ l_j^-$ [82].

Decay Mode	Combinations Constrained	Upper bound
$b \to s e^+ e^-$	$\lambda'_{121}\lambda'_{232}, \lambda'_{131}\lambda'_{332}, \lambda'_{121}\lambda'_{223}, \lambda'_{131}\lambda'_{323}$	2.2×10^{-4}
	$\lambda'_{113}\lambda'_{112}, \lambda'_{123}\lambda'_{122}, \lambda'_{133}\lambda'_{132}$	4.3×10^{-4}
$b \to s \mu^+ \mu^-$	$\lambda'_{122}\lambda'_{132}, \lambda'_{232}\lambda'_{332}, \lambda'_{122}\lambda'_{123}, \lambda'_{232}\lambda'_{323}$	2.2×10^{-4}
	$\lambda'_{213}\lambda'_{212}, \lambda'_{223}\lambda'_{222}, \lambda'_{233}\lambda'_{232}$	4.4×10^{-4}
$b \to s e^\pm \mu^\mp$	$\lambda'_{122}\lambda'_{232}, \lambda'_{132}\lambda'_{332}, \lambda'_{121}\lambda'_{132}, \lambda'_{231}\lambda'_{332}$	1.4×10^{-4}
	$\lambda'_{122}\lambda'_{223}, \lambda'_{132}\lambda'_{323}, \lambda'_{121}\lambda'_{123}, \lambda'_{231}\lambda'_{323}$	1.4×10^{-4}
	$\lambda'_{113}\lambda'_{212}, \lambda'_{123}\lambda'_{222}, \lambda'_{133}\lambda'_{232}, \lambda'_{213}\lambda'_{112}, \lambda'_{223}\lambda'_{122}, \lambda'_{233}\lambda'_{132}$	2.7×10^{-4}

4.6 Nonleptonic B decay

Many interesting bounds on the $''$ couplings can be obtained from the two-body nonleptonic decays of heavy-quark mesons. Following [70] we consider in this subsection B decays only via the product of the baryon number violating couplings $''\,''$. Bounds on $'\,''$ derived in this case are not competitive with those obtained from the proton decay. Since any B decay will change the number of "b- avor" by one unit, bounds from there will apply to products of the form $_{u_i b s}\ _{u_j s d}$ or $_{u_i b d}\ _{u_j s d}$.

In nonleptonic decays the hadronic structure becomes much more involved than in the previously considered cases of (semi-)leptonic decays. However the presence of heavy b-quark in the initial meson facilitates treatment of hadronic matrix elements. These matrix elements were calculated in [70] using the computational method developed in [97] and based upon the formalism of Brodsky and Lepage [98].

The decay $B^+ \to \overline{K}^0 K^+$ (or equivalently, $B \to K^0 K$) has an extremely small rate in the SM, being penguin-suppressed and also reduced by the small CKM element V_{ub} in the amplitude.

The dominant diagrams contributing to this process for non-zero $''$ couplings are shown in Fig. 12.

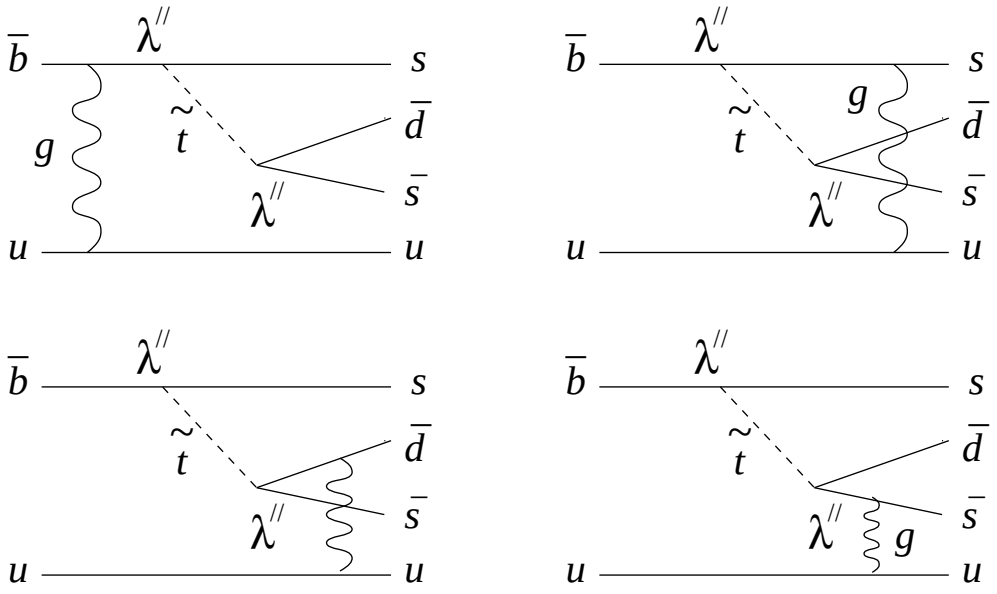

Fig. 12. Dominant diagrams contributing to the decay $B^+ \to \overline{K}^0 K^+$.

In each of these diagrams, the gluon is spacelike and the squark (of charge 2/3) is timelike. This generates from the gluon propagator an overall enhancement factor of $m_B/(m_B - m_b) \simeq 10$ in the amplitude, m_B and m_b being the B meson and b quark masses respectively. (This factor is just the inverse of the fraction of the B-momentum assigned to the light quark.) One can draw similar diagrams interchanging the squark and gluon internal lines and appropriately relabeling the quark lines. Each of

these latter diagrams would have a timelike gluon and a spacelike squark (now of charge 1=3). For these, however, the overall factor of $m_B=(m_B - m_b)$ does not materialize so that contributions from these diagrams are significantly subdominant and can be neglected. It is of interest to point out that the decay $B^0 \to K^+K^-$ can proceed only through these latter diagrams, with the squark having charge 2=3, and therefore yields a significantly weaker bound on the same product of $''$ couplings than does $B^+ \to \overline{K}^0 K^+$, in spite of stronger experimental limits on the branching ratio.

It is convenient to analyze a ratio of $(B^+ \to \overline{K}^0 K^+)$ to the partial width of another B^+ decay channel (specifically $B^+ \to K^+ J/\psi$) that proceeds unsuppressed in the SM. This allows one to eliminate many of the uncertainties in the coefficient factors depending, in particular, on the hadronic matrix elements. Following [70] one finds

$$\frac{(B^+ \to \overline{K}^0 K^+)}{(B^+ \to K^+ J/\psi)} = \left(1 - \frac{m_{J/\psi}^2}{m_B^2}\right)^2 \left(\frac{f_K}{f_{J/\psi}}\right)^2 \frac{|''_{i32}\,''_{i21}|^2 (m_W/m_{\tilde{e}_i})^4}{(G_F m_W^2)^2 |V_{cb}|^2 |V_{cs}|^2} \qquad (9.8 \quad 10^2): \qquad (158)$$

Here, $m_{\tilde{e}_i}$ are the masses of the scalar up-squarks, $m_{J/\psi}$ is the mass of the J/ψ meson, f_K and $f_{J/\psi}$ are the decay constants of the K and J/ψ mesons, which are related to their wave functions at the origin, and V_{cb} and V_{cs} are CKM elements. One can use $f_{J/\psi}/f_K \simeq 2.55$. With the experimental branching ratio for $B^+ \to K^+ J/\psi$ [21] being equal to $10.2 \quad 10^4$, one gets

$$B(B^+ \to \overline{K}^0 K^+) \simeq 1.97 |''_{i32}\,''_{i21}|^2 (m_W/m_{\tilde{e}_i})^4. \qquad (159)$$

Recent experimental upper bound on this quantity $B(B^+ \to \overline{K}^0 K^+) = 2.1 \quad 10^5$ [21] leads with the universal squark mass $m_{\tilde{e}}$ to the constraint [70]

$$\frac{|''_{i32}\,''_{i21}| m_W^2}{m_{\tilde{e}}^2} < 3.2 \quad 10^3. \qquad (160)$$

One can repeat the calculations for the decay $B^+ \to K^0 \pi^+$ (or equivalently $B^- \to \overline{K}^0 \pi^-$) in much the same way as in the previous case. The final result is [70]

$$B(B^+ \to K^0 \pi^+) = 1.32 |''_{i31}\,''_{i21}|^2 \left(\frac{m_W}{m_{\tilde{e}_i}}\right)^4. \qquad (161)$$

Recent experimental value [21] for this branching ratio is $B(B^+ \to K^0 \pi^+) = 2.3 \quad 1.1 \quad 10^5$. Assuming that the $R\!\!\!/_p$ contribution in (161) saturates 1 experimental upper limit one gets

$$\frac{|''_{i31}\,''_{i21}| m_W^2}{m_{\tilde{e}}^2} < 3.4 \quad 10^3. \qquad (162)$$

The above limits depend on an approach to estimation of the hadronic matrix elements. In particular, the perturbative QCD corrections may essentially affect these limits [99]. However, the theoretical uncertainty are not expected to exceed 20{15% [70, 99].

4.7 K–$\overline{K}$ and B–$\overline{B}$ systems

The mass differences m_{B_1} between B_1 and B_2 as well as m_K between K_1 and K_2 arise due to mixing in the meson systems B_d^0–$\overline{B_d^0}$ as well as K^0–$\overline{K^0}$. The mass differences can be expressed in terms of the following matrix elements of the low-energy effective Lagrangians

$$m_K = 2\,\mathrm{Re}\langle K^0 | L_e^{S=2} | \overline{K}^0 \rangle, \qquad m_B = 2\,\mathrm{Re}\langle B_d^0 | L_e^{B=2} | \overline{B}_d^0 \rangle. \qquad (163)$$

The ^{0}-couplings of the Lagrangian in (64) generate the $S = 2$ and $B = 2$ low-energy effective Lagrangians at the tree level. One finds they explicitly

$$L_{eff}^{S=2} = \sum_{n} \frac{\lambda'_{n21}\lambda'_{n12}}{m^2_{\tilde{e}_n}} \bar{d}_R s_L \bar{d}_L s_R ; \qquad L_{eff}^{B=2} = \sum_{n} \frac{\lambda'_{n31}\lambda'_{n13}}{m^2_{\tilde{e}_n}} \bar{d}_R b_L \bar{d}_L b_R : \tag{164}$$

It is useful to define the following "normalized" quantities:

$$\eta_n \equiv \left(\frac{100\,GeV}{m_{\tilde{e}_{nL}}}\right)^2 ; \quad \upsilon_n \equiv \left(\frac{100\,GeV}{m_{\tilde{e}_{nL}}}\right)^2 ; \quad \delta^L_n \equiv \left(\frac{100\,GeV}{m_{\tilde{d}_{nL}}}\right)^2 ; \quad \delta^R_n \equiv \left(\frac{100\,GeV}{m_{\tilde{d}_{nR}}}\right)^2 : \tag{165}$$

We calculate the contributions of (164) to m_B, m_K and require them not to exceed the corresponding experimental numbers [21] $m_K < 3.5 \times 10^{-12}$ MeV and $m_B < 3.4 \times 10^{-10}$ MeV.

Finally, from m_B and m_K respectively one have

$$\sum_i \lambda'_{i31}\lambda'_{i13}\left(\frac{100\,GeV}{m_{\tilde{e}_i}}\right)^2 < 3.3 \times 10^{-8}; \qquad \sum_i \lambda'_{i21}\lambda'_{i12}\left(\frac{100\,GeV}{m_{\tilde{e}_i}}\right)^2 < 4.5 \times 10^{-9}: \tag{166}$$

First upper bound is comparable with that (6.2×10^{-8}) obtained in [100, 101] from the lack of observation of neutrinoless double beta decay. In contrast, the second bound is three orders of magnitude stronger than the 10^{-6} obtained by those authors.

In [79] there were found a lot of additional constraints from the $\not{R}_p$ contributions to the effective $S = 2$, $B = 2$ effective Lagrangians at the one-loop level. These contributions include set of $S = 2$ and $B = 2$ box graphs in each of which there is one $\tilde{f}_i$ propagator between two ^{0}-type vertices and one of W (transverse W boson), G (longitudinal W boson in the 't Hooft–Feynman gauge) and H (charged Higgs) as the other non-fermionic propagator. The nature of the internal fermion lines are decided by the flavour indices associated with the two ^{0}-vertices. These diagrams are present in any $\not{R}_p$ supersymmetric theory [79], they serve to constrain other flavour combinations of product couplings in addition to those considered above. With H (or G) as one scalar propagator and, as always, $\tilde{f}_i$ as another between the ^{0}-vertices, box graphs with t-quarks in internal lines contribute more than those with c- or u-quarks, despite the relatively larger CKM-suppressions associated with the former. For light quarks (c or u) as internal fermions, box graphs with internal W dominate over those with internal H or G, for the same choice of ^{0}-couplings. These loop level constraints are listed in Table 12.

4.8 Infrared fixed points

In direct analogy with the familiar estimate for the top-quark mass

$$m_t(pole) \quad (200\,GeV)\sin\ ; \tag{167}$$

which is derived by assuming the existence of an infrared fixed point in the Yukawa coupling constant, h^U_{33}, one can deduce similar fixed point bounds for the third generation $\not{R}_p$ coupling constants. The argument is again based on the vanishing of the beta function in the renormalization group flow, via the competition between Yukawa and gauge interactions, as displayed schematically by the equation,

$$(4\ )^2\frac{@\ln\ _{ijk}}{@t} = \frac{8}{5}g_1^2 + 3g_2^2 \quad (\ _{j3} + 2\ _{k3})\ ^{u2}_{33}; \qquad \text{with} \qquad t = \ln m_X^2/Q^2; \tag{168}$$

where the c-number coefficients in front of the coupling constants represent the fields anomalous dimensions. Equivalently, this reflects on the assumption of perturbative unitarity (absence of Landau poles) for the $\not{R}_p$ coupling constants at high energies scales. The predicted fixed point bounds [71, 102, 103] are:

$$_{233} \quad 0.90; \qquad ^{0}_{333} \quad 1.01; \qquad ^{00}_{323} \quad 1.02; \qquad ^{00}_{2ik} \quad 1.25; \qquad ^{00}_{123} \quad 1.25:$$

Table 12. The loop level constraints from $K-\overline{K}$ and $B-\overline{B}$ systems [79].

Quantity	$^{0}_{ijk}$: $^{0}_{lmn}$		Upper limits		$^{0}_{ijk}$: $^{0}_{lmn}$		Upper limits	
	(131)	(132)	7.7	10^{-4}	(231)	(232)	7.7	10^{-4}
	(331)	(332)	7.7	10^{-4}	(131)	(122)	1.0	10^{-4}
	(231)	(222)	1.0	10^{-4}	(331)	(322)	1.0	10^{-4}
	(121)	(122)	1.4	10^{-6}	(221)	(222)	1.4	10^{-6}
	(321)	(322)	1.4	10^{-6}	(111)	(112)	1.4	10^{-6}
m_{K}	(211)	(212)	1.4	10^{-6}	(311)	(312)	1.4	10^{-6}
	(122)	(111)	6.1	10^{-6}	(222)	(211)	6.1	10^{-6}
	(322)	(311)	6.1	10^{-6}	(132)	(121)	1.1	10^{-4}
	(232)	(221)	1.1	10^{-4}	(332)	(321)	1.1	10^{-4}
	(132)	(111)	4.7	10^{-4}	(232)	(211)	4.7	10^{-4}
	(332)	(311)	4.7	10^{-4}	(131)	(112)	2.4	10^{-5}
	(231)	(212)	2.4	10^{-5}	(331)	(312)	2.4	10^{-5}
	(131)	(133)	1.3	10^{-3}	(231)	(233)	1.3	10^{-3}
	(331)	(333)	1.3	10^{-3}	(131)	(123)	1.8	10^{-4}
	(231)	(223)	1.8	10^{-4}	(331)	(323)	1.8	10^{-4}
	(111)	(113)	3.6	10^{-3}	(211)	(213)	3.6	10^{-3}
m_{B_d}	(311)	(313)	3.6	10^{-3}	(121)	(113)	3.1	10^{-4}
	(221)	(213)	3.1	10^{-4}	(321)	(313)	3.1	10^{-4}
	(111)	(123)	1.6	10^{-3}	(211)	(223)	1.6	10^{-3}
	(311)	(323)	1.6	10^{-3}	(121)	(123)	1.4	10^{-3}
	(221)	(223)	1.4	10^{-3}	(321)	(323)	1.4	10^{-3}
	(132)	(133)	2.5	10^{-3}	(232)	(233)	2.5	10^{-3}
	(332)	(333)	2.5	10^{-3}	(132)	(113)	1.5	10^{-3}
	(232)	(213)	1.5	10^{-3}	(332)	(313)	1.5	10^{-3}
	(112)	(113)	1.4	10^{-3}	(212)	(213)	1.4	10^{-3}
m_{B_s}	(312)	(313)	1.4	10^{-3}	(122)	(113)	1.2	10^{-3}
	(222)	(213)	1.2	10^{-3}	(322)	(313)	1.2	10^{-3}
	(112)	(123)	3.2	10^{-3}	(212)	(223)	3.2	10^{-3}
	(312)	(323)	3.2	10^{-3}	(122)	(123)	2.7	10^{-3}
	(222)	(223)	2.7	10^{-3}	(322)	(323)	2.7	10^{-3}

5 Nuclear processes

Some of the nuclear processes which are forbidden or suppressed in the SM may offer unique opportunities for probing the physics beyond the SM [104, 105]. The neuterinoless double beta decay ($0\nu\beta\beta$)

$$(A;Z) \;\to\; (A;Z+2) + 2e \tag{169}$$

and muon-electron conversion in nuclei

$$\mu + (A;Z) \;\to\; e + (A;Z) \tag{170}$$

are the nuclear processes of this type. Both these processes are forbidden in the SM (with massless neutrinos $m_\nu = 0$) due to the fact that the $0\nu\beta\beta$ decay and μ–e conversion violate the conservation laws of the total lepton number and the lepton flavor respectively. Recall that in the SM with $m_\nu = 0$ the total lepton number is a conserving quantity what is guaranteed by an accidental global U_1 symmetry. The lepton flavor violation $L_i \neq 0$ can be rotated away by redefinition of the massless neutrino fields producing no physical effect.

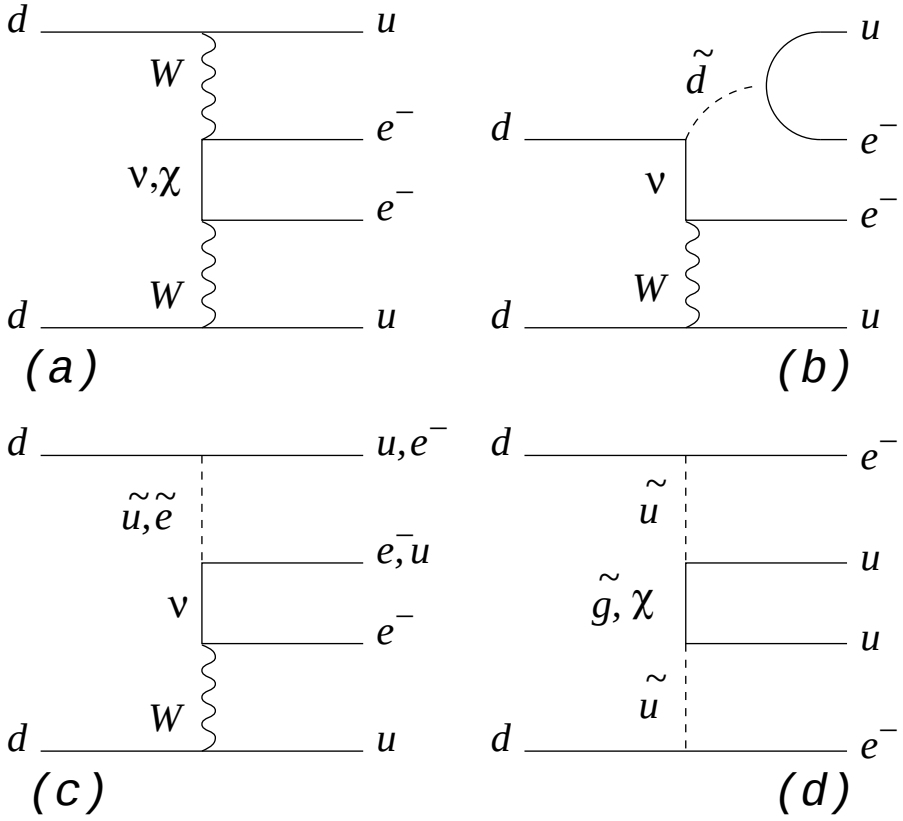

Fig. 13. Leading $\not{R}_p$ MSSM diagrams contributing to neutrinoless double beta decay.

In the $\not{R}_p$ SUSY there are both $\Delta L \neq 0$ and $\Delta L_i \neq 0$ interactions. As yet there is no any experimental evidence for either $0\nu\beta\beta$ decay or μ–e conversion. Thus one can derive from non-observation of these exotic processes the limits on the $\not{R}_p$ parameters. These limits derived in [53, 64, 65, 100, 101], [106]–[109] proved to be very stringent. In the subsequent subsections we will shortly discuss the derivation of these nuclear physics limits on the $\not{R}_p$ SUSY.

5.1 Neutrinoless double beta decay

The simplest mechanism of $0\nu\beta\beta$ decay with a Majorana neutrino in the intermediate state is given in Fig. 13(a). This is a well known classical mechanism. The lepton number violation necessary for $0\nu\beta\beta$ decay to proceed is introduced in this case via the Majorana neutrino mass.

An example of the $\not{R}_p$ SUSY contribution to $0\nu\beta\beta$ decay was first found by Mohapatra [104] and later studied in more details by Vergados [110]. All the possible tree-level $\not{R}_p$ MSSM contributions to the $0\nu\beta\beta$ decay were specified and comprehensively analyzed in [53, 100, 101], [106]–[108].

Let us consider the underlying $\Delta L = 2$ quark-level $0\nu\beta\beta$ transition

$$dd \to uu + 2e : \tag{171}$$

It can be realized in the $\not{R}_p$ MSSM via the tree level diagrams shown in Fig. 13. Here we presented only those diagrams which according to [53, 101] give rise to phenomenologically most valuable effect. Notice that in this list we included the classical Majorana exchange diagram Fig. 13(a) as well. This is because in the $\not{R}_p$ MSSM with the bilinear R-parity violation the neutrino masses and mixing angles are non-trivial. They are determined at the tree-level by $\langle \tilde{\nu}_i \rangle, \langle e_i \rangle$ as well as by the MSSM parameters with respect to eqs. (36)–(39). Therefore, the Majorana exchange contribution is a generic one for the $\not{R}_p$ MSSM.

All the $\not{R}_p$ contributions to $0\nu\beta\beta$ decay can be straightforwardly derived starting from the lepton number violating Lagrangian of the $\not{R}_p$ MSSM

$$L(\Delta L = 1) = L_{\not{R}_p} + L_{mix} : \tag{172}$$

The first term in this formula contains all the $^0\nu\beta\beta^c$ operators given in the component fields in (59). The second term is generated by the rotation to the mass basis in the sector of the neutral fermions ($_i; e; \tilde{Z}; \tilde{H}^0_{1,2}$) and the charged fermions ($e_L; _L; _L; \tilde{W}^-; \tilde{H}^-_1$) of the R_p MSSM as explained in sect. 2.4.1. It takes the form [53]:

$$\begin{aligned} L_{mix} &= -\frac{g_2}{\sqrt{2}} {}_n W^- e P_L {}_n \\ &+ \sqrt{2} g_2 \left({}^{d}_{k} {}_k P_R d \tilde{d}^c_R + {}^{u}_{k} {}_k P_R u^c \tilde{u}_L + {}^{e}_{ki} {}_k P_R e^c \tilde{e}_{Li} + {}_k \bar{u} P_R e^c \tilde{d}^c_L \right) + H.c.: \end{aligned} \tag{173}$$

The subscripts $k;i = 1;2;3$ denote generations, while $n = 1;2;3;4$ enumerates the neutralino mass eigenstates. The first term is generated by the rotation to the neutral/charged fermion mass basis from the SM W {e{ and the MSSM W { { interaction terms while the rest originates from the MSSM neutralino (chargino)-fermion-sfermion interactions {q{e{q, {q{e{q (for the MSSM Lagrangian see, for instance, [2]). Note that the trilinear fermion-sfermion couplings in L_{mix} are not present among the superpotential trilinear , ^{0} terms in (58){(59). The coefficients in (173) depend on the mixing matrix elements introduced in eqs. (23) and (50). In the leading order in the small expansion parameters $_i=M_Z$, $h_ei=M_Z$ we obtain

$$\begin{aligned} {}_n &= \sum_{m=1}^{4} {}_{1m} N_{nm} \left(\sqrt{2} {}^{L}_{11} N_{n2} - {}^{L}_{12} N_{n3} \right); \qquad = \frac{1}{\sqrt{2}} {}^{L}_{11}; \\ {}^{e}_{ki} &= \frac{1}{\sqrt{2}} {}^{L}_{11} V^{(*)}_{ik} - \sum_{j=1}^{3} \frac{1}{2} V^{(*)}_{jk} \left(\tan {}_W {}_{j1} + {}_{j2} {}_{i1} \right); \\ {}^{u}_{k} &= \frac{1}{6} \sum_{j=1}^{3} V^{(*)}_{jk} \left(\tan {}_W {}_{j1} + 3 {}_{j2} \right); \qquad {}^{d}_{k} = \frac{1}{3} \tan {}_W \sum_{j=1}^{3} V^{(*)}_{jk} {}_{j1}: \end{aligned} \tag{174}$$

The notations used in these formulas are explained in sect. 2.3.1 and 2.3.2. Here we just recall that the parameters depend on the sneutrino VEVs h_ei and on the lepton-Higgs mixing parameters $_i$ from the superpotential (4).

Integrating out the heavy fields from the diagrams in Fig. 13 one can derive the effective Lagrangian which reproduces their contributions to $0\nu\beta\beta$ decay in the first or in the second order of perturbation theory. Let us show only those terms which yield most stringent constraints on the R_p parameters (for the complete expressions we refer reader to the original papers [53, 100, 101], [106]{[108].

$$L_e \ (L = 1;2) = L(\text{Fig. 13(a)}) + L(\text{Fig. 13(b,c)}) + L(\text{Fig. 13(d)}); \tag{175}$$

where the contributions of the different diagrams in Fig. 13 are separated into different terms. They can be written explicitly as

$$L(\text{Fig. 13(a)}) = G_F \sqrt{2} (e \ P_L \ _k) V^{(*)}_{1k} J \ + \ J \ J \ (e P_R e^c); \tag{176}$$

$$L(\text{Fig. 13(b,c)}) = G_F \sqrt{2} [({}^{(k)} + 4 {}^{(k)}_{R}) ({}_k P_R e^c) J + ({}^{(k)}_{;q} + 4 {}^{(k)}_{LR}) \bar{}_k \ P_R e^c \ J \ ]; \tag{177}$$

$$L(\text{Fig. 13(d)}) = \frac{4 G_F^2}{m_p} e P_R e^c [({}_{e} + {}_{e}) J J \ - \frac{1}{4} {}_{e} J \ J \ ]: \tag{178}$$

Here we introduced the color singlet quark currents

$$J = u \ P_R d \ ; \quad J \ = u \ \ P_R d \ ; \quad J \ = u \ \ P_L d \ ; \tag{179}$$

The effective parameters accumulating the dependence on the initial R_p SUSY parameters are defined as

$$^{(k)} = \frac{g_2 \ ^{0}_{i11}}{2 G_F} \left(2 \frac{ {}^{e}_{ki} }{ m^2_{\tilde{e}_{Li}} } \ \frac{ {}^{d}_{k} }{ m^2_{\tilde{d}_R} } \ {}_{i1} \ \frac{ {}^{u}_{k} }{ m^2_{\tilde{e}_L} } \ {}_{i1} + \frac{1}{ m^2_{\tilde{d}_L} } \ {}_{ik} \right); \tag{180}$$

$$\overset{(k)}{{}_{;q}} = \frac{g^{0}_{i11}}{8G_F}\left[\frac{u_k}{m^2_{\tilde{e}_L}}\right]_{i1}\left[\frac{d_k}{m^2_{\tilde{e}_R}}\right]_{i1} + \frac{c}{m^2_{\tilde{e}_L}}\Big]_{ik}; \tag{181}$$

$$= \sum_{i=1}^{4}\frac{m_p}{m_i}\left[\frac{m_p}{hm\,i}\right]^2; \tag{182}$$

$$\overset{(k)}{{}_{LR}} = \frac{{}^{0}_{11}{}^{0}_{i}{}_{ni1}V^{(\,)}_{nk}}{2^{\overline{P}=}2G_F}\sin 2\,{}^{d}_{(k)}\left(\frac{1}{m^2_{\tilde{e}_{1(k)}}} - \frac{1}{m^2_{\tilde{e}_{2(k)}}}\right)A; \tag{183}$$

$$\tilde{e}_q = \frac{2\,{}^{0^2}_{111}}{9G_F^2 m^4_{\tilde{e}_q}}\left[2\,{}_s\frac{m_p}{m_{\tilde{g}}} + \frac{3}{4}\,{}_2\frac{m_p}{m}\,(\,{}^2_{Rd} + \,{}^2_{Lu})A\right]; \tag{184}$$

$$\tilde{e}_e = \frac{2\,{}^{0^2}_{111}}{9G_F^2 m^4_{\tilde{e}_q}}\left[2\,{}_s\frac{m_p}{m_{\tilde{g}}} + \frac{3}{2}\,{}_2\frac{m_p}{m}\,\frac{m_{\tilde{e}_q}}{m_{\tilde{e}}}\right]^2 C^A: \tag{185}$$

Here

$$C = 6\,{}^2_{Le}\left[\frac{m_{\tilde{e}_q}}{m_{\tilde{e}}}\right]^2\,{}_{Rd\,Le}\,{}_{Lu\,Rd}\left[\frac{m_{\tilde{e}}}{m_{\tilde{e}_q}}A\right]\,{}_{Lu\,Le}: \tag{186}$$

In the above formulas we used the standard notations $_2 = g_2^2=(4\ )$ and $_s = g_3^2=(4\ )$ for the $SU(2)_L$ and $SU(3)_c$ gauge coupling constants. We also denoted the gluino $\tilde{g}$ and the lightest neutralino masses as $m_{\tilde{g}}$ and m respectively. Neutralino couplings are defined as [2]

$$_{Li}(\ ) = \quad T_3(\ )N_{i2} + \tan\ _W\ (T_3(\ )\quad Q(\ ))N_{i1}; \tag{187}$$

$$_{Ri}(\ ) = \ Q(\ )\tan\ _W N_{i1}: \tag{188}$$

Here Q and T_3 are the electric charge and the weak isospin of the fields $= u;d;e$. The neutralino mixing matrix matrix N_{ij} was introduced in (35).

The mixing between scalar superpartners $\tilde{f}_{L;R}$ of the left and right-handed fermions $f_{L;R}$ is essential for the diagram Fig. 13(b). The contribution vanishing in the absence of this effect is represented by the terms proportional to $_{LR}$ in (183) which contains the mixing angle $\sin 2\ ^{d}$. The mixing occurs due to non-diagonality of the mass matrix which can be written as

$$M^{\,2}_{\tilde{f}} = \begin{pmatrix} m^2_{\tilde{f}_L} + m^2_f & 0{:}42D_Z\quad m_f(A_f + \quad\tan\ ) \\ m_f(A_f + \quad\tan\ ) & m^2_{\tilde{f}_R} + m^2_f\quad 0{:}08D_Z \end{pmatrix}: \tag{189}$$

Here, $f = d;s;b$ and $\tilde{f}$ are their superpartners. $D_Z = M_Z^2\cos 2\ $ with $\tan\ = hH_2^0i=hH_1^0i$. $m_{\tilde{f}_{L;R}}$ are soft sfermion masses, A_f are soft SUSY breaking parameters describing the strength of trilinear scalar interactions in eq. (6), and $$ is the supersymmetric Higgs(ino) mass parameter. Once sfermion mixing is included, the current eigenstates $\tilde{f}_L$, $\tilde{f}_R$ become superpositions of the mass eigenstates $\tilde{f}_i$ with the masses $m_{\tilde{f}_i}$ and the corresponding mixing angle ^{f}

$$\sin 2\ ^{f} = \frac{2m^2_{(f)LR}}{m^2_{\tilde{f}_1}\quad m^2_{\tilde{f}_2}};$$

$$m^2_{\tilde{f}_{1;2}} = \frac{1}{2}\left[m^2_{LL} + m^2_{RR}\quad\sqrt{(m^2_{LL}\quad m^2_{RR})^2 + 4m^4_{LR}}\right] \tag{190}$$

where m^2_{LR}, m^2_{LL}, m^2_{RR} denote the (1,2), (1,1), (2,2) entries of the mass matrix (189).

The next step deals with reformulation of the quark-lepton interactions in (176){(178) in terms of the effective hadron-lepton interactions. This is necessary for the subsequent nuclear structure calculations.

These questions are lie far beyond the scope of the present paper. The detailed study of the hadronic and nuclear structure side of the 0 decay can be found in [101, 111].

Here only the following notes are in order. Hadronic and nuclear structure cause speci c enhancements of the R$_p$ SUSY contributions to the 0 decay described by the diagrams in Fig. 13(b,c,d) [106, 107]. The diagram in Fig. 13(d) is enhanced by the pion-exchange currents in nuclei. This fact can be understood by taking into account that the corresponding contribution shown in (178) contains product of the pseudoscalar quark currents $^2 = u\ _5 d\ \ u\ _5 d$. One can incorporate quark elds from this operator into the two virtual pions [107]. Now nn ! pp+ 2e transition is mediated by the charged pion-exchange between the decaying nucleons (N-mode). Since the interaction region extends to the distances 1=m this mode is not suppressed by the nucleon repulsion. An additional enhancement of the N-mode comes from the hadronization of the R$_p$ SUSY e ective vertex operator ^{2} replaced by its hadronic image ^{2}. The enhancement occurs due to the fact that the local pseudoscalar quark bilinear u $_5$d can be directly associated with the e ective $^+$-meson eld.

The diagrams in Fig. 13(b,c) are enhanced because of the chiral structure of the leptonic current in (177). The bottom parts of these diagrams are the SM charged current interactions of the form (u P$_L$d)(e P$_L$ $_n V_{en}^{(\ )}$), while the top parts contain the leptonic currents $\bar{}_k P_R e^c$ or $\bar{}_k$ P$_R$e^c. The resulting leptonic tensor after combining the two neutrino elds into a propagator takes the form

$$L\ _{L=2}\quad e\ P_L h0jT(\ _k\ \bar{}_n)j0iP_R\ e^c\quad \overset{(\ )}{V}_{ek} V_{en}^{(\ )}\quad e\quad P_R\ e^c\quad q\!\!\!/\, q^2\quad \frac{1}{p_F}; \tag{191}$$

where q is the neutrino momentum and = 1, . An important observation [51] used in the above formula is that the average neutrino momentum in a nucleus can be estimated as hqi p$_F$ 100 MeV, where p$_F$ is the nucleon Fermi momentum. This should be compared with the contribution of the diagram in Fig. 13(a) with the neutrino internal line. The leptonic tensor in this case is

$$L\ _{L=0}\quad e\ P_L h0jT(\ _k\ \bar{}_n)j0iP_L\ \ e^c V_{ek}^{(\ )} V_{en}^{(\ )} e\ _i\ P_R e^c\quad hmi=q^2; \tag{192}$$

where hm i = m $_n V_{en}^{(\ )} V_{en}^{(\ )}$. Comparing eqs. (191) and (192) one can see that the SUSY contribution corresponding to the L = 2 operators receives a huge enhancement compared to the contribution of the L = 0 operators. In fact

$$L\ _{L=2}=L\ _{L=0}\quad p_F=hm\ i\quad 10^8\quad (1\ eV=hmi): \tag{193}$$

Due to these enhancement factors the diagrams in Fig. 13(b,c) become phenomenologically valuable. However, these arguments do not exclude the diagram in Fig. 13(a) mediated by the Majorana neutrino exchange from the list of dominant diagrams. It was found [53] that this contribution is important even without enhancement factors which were important for the diagrams in Fig. 13(b,c).

Starting from the Lagrangian (175) the corresponding half-life formula for 0 decay was obtained in [53, 101, 100], [106]{[108]. It includes various nuclear matrix elements which were calculated within the renormalized Quasiparticle Random Phase Approximation (pn-RQRPA) [112]. This nuclear structure method has been developed from the proton-neutron QRPA approach, which has been frequently used in the 0 -decay calculations. The pn-RQRPA is an extension of the pn-QRPA by incorporating the Pauli exclusion principle for the fermion pairs.

The nal half-life formula is rather complex and can be found in the cited original paper. Comparing this formula with the most stringent experimental lower limit on the 0 -decay half-life has been obtained for ^{76}Ge [54]

$$T^{0}_{1=2}\quad {}^{exp}(0^+ \ !\ 0^+)\qquad 1:1\quad 10^{25}\ \text{years}\qquad (90\%\ C.L.) \tag{194}$$

the following upper limits on the R$_p$ parameters were obtained [53, 101, 100], [106]{[108]:

$$^{0}_{111}\quad 1:3\quad 10^{4}\ \frac{m_{\tilde{e}_L}}{100\ GeV}^{2}\ \frac{m_{\tilde{e}_R}}{100\ GeV}^{1=2};\qquad ^{0}_{111}\quad 9:3\quad 10^{4}\ \frac{m_{\tilde{e}_R}}{100\ GeV}^{2}\ \frac{m_{\tilde{}}}{100\ GeV}^{1=2} \tag{195}$$

$$^{0}_{112}\,^{0}_{121} \quad 1{:}8 \quad 10^{-6}\left(\frac{m_{SUSY}}{100\ GeV}\right)^{3}; \qquad ^{0}_{113}\,^{0}_{131} \quad 6{:}2 \quad 10^{-8}\left(\frac{m_{SUSY}}{100\ GeV}\right)^{3}: \tag{196}$$

$$|\ _{1}| \quad 470\ KeV; \quad |\tilde{e}_{1i}| \quad 840\ KeV; \quad |\ _{1}\ ^{0}_{111}| \quad 100\ eV; \quad |\tilde{e}_{1i}\ ^{0}_{111}| \quad 55\ eV: \tag{197}$$

The limits (195) are the most stringent ones among the known constraints on the $\not{R}_p$ parameters. As shown in [53], [106]–[108]. so small couplings are out of reach of the present and the near future accelerator experiments. On the other hand limits on the sneutrino VEVs $\langle\tilde{e}_i\rangle$ and on the lepton–Higgs mixing parameter $_i$ in (197) are significantly weaker than the corresponding limits derived in sect. 3.2 from the Super-Kamiokande atmospheric neutrino data.

5.2 Muon–electron conversion in nuclei

The –e conversion in the R-parity conserving SUSY models has been studied by several groups [113]–[115]. In this case the SUSY contribution appears only at the loop-level. A typical conclusion made in [113]–[115] is that the other lepton flavour violating processes such as ! e are about an order of magnitude more sensitive to the R-parity conserving SUSY than –e conversion. As was recently shown in [64, 65, 109] the situation in the $\not{R}_p$ SUSY is opposite. The sensitivity of the –e conversion to the certain $\not{R}_p$ interactions is significantly better compared to the ! e and many other lepton flavor violating processes. This is mainly caused by the fact that in the $\not{R}_p$ MSSM there exist the tree-level contributions to the –e conversion. Also important is that some of the 1-loop $\not{R}_p$ contributions receive a significant enhancement due to the presence of large logarithms.

5.2.1 Tree-level mechanisms

In this subsection we follow the paper [109] where all the tree level $\not{R}_p$ MSSM contributions to the –e conversion amplitude were analyzed. The leading diagrams are presented in Fig 14.

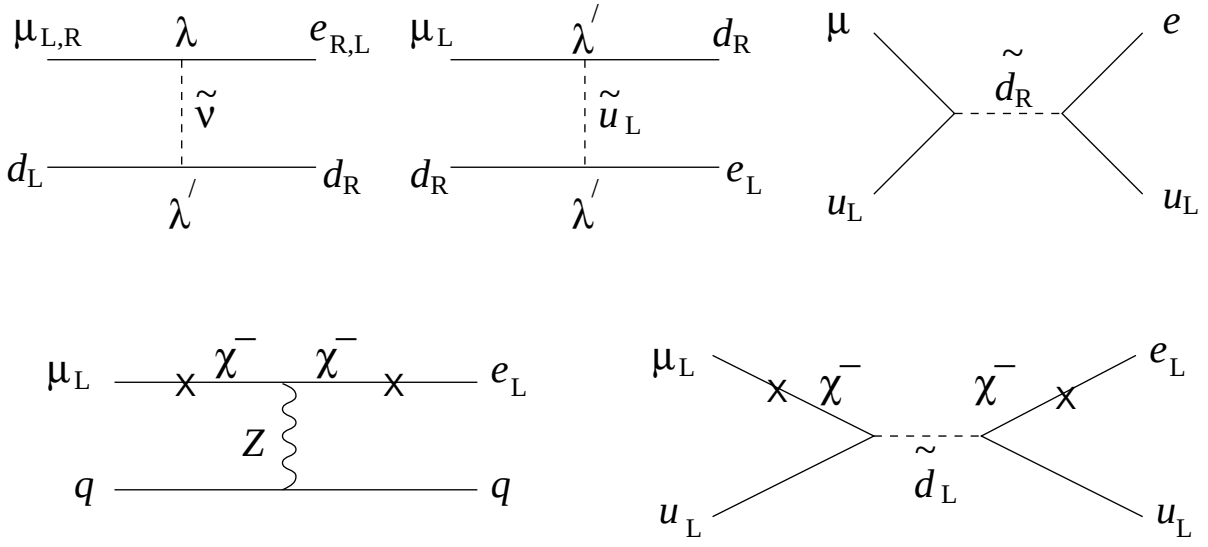

Fig. 14. Leading $\not{R}_p$ MSSM diagrams contributing to –e conversion. The crossed fermion lines denote the contributions induced by lepton–gaugino–Higgsino mixing (1).

Let us specify those vertex operators which are encountered in these diagrams. They include

$$\begin{aligned} L_{\ e} \;=\; & 2\ _{i21}\, e_{Li}\bar{e}P_L \;+\; ^{0}_{ijj}\, e_{Li}\bar{d}_j P_L d_j \;\; ^{0}_{ijk}V_{nj}\, u_{Ln}\bar{e}_i P_R d_k + \tilde{d}_{Rk}\bar{u}_n P_R e_i^c \\ & +\; g_2\ _i V_{jk}\ \bar{}_j P_R e_i^c \tilde{d}_{Lk} + a_Z Z\ \bar{e}\ P_L \;\; \frac{g_2}{\cos\ _W} Z\ \bar{q}\ (\ _L P_L + \ _R P_R) q: \end{aligned} \tag{198}$$

The first three terms in (198) originate from the superpotential trilinear $\not{R}_p$ terms. In component fields the first -term can be found among the terms of (58) while the next two ^{0}-terms are given in the

quark mass basis according to the definition of (64). Rotation to the mass basis of the charged fermions of the R_p MSSM according to (50) generate the new lepton flavor violating interactions represented in (198) by the 4th and the 5th terms. They are generated from the R_p-conserving interactions $Z\{\ \ \{$ and $\ \ \{q\{q$ respectively. The last term in (198) is the ordinary SM Z-boson interaction with the quark neutral currents with $\ = T_3\ \ Q\sin\ _W$. The coefficients a_Z and $\ _i$ in (198) depend on the mixing matrix elements introduced in (50). Again as in the case of the $0\ \ \ $ decay, we use for these coefficients the leading order expressions in small expansion parameters $\ _i=M_Z$, $he i=M_Z$. This yields

$$a_Z = \frac{1}{2\cos\ _W}\ ^L_{11}\ ^L_{21}; \qquad \ _i = \ ^L_{i1}: \tag{199}$$

The notations used in these formulas are explained in sect. 2.3.2.

Integrating out the heavy fields from the diagrams in Fig. 14 and carrying out Fierz reshuffling one obtains the effective Lagrangian which allows one to reproduce the low-energy contribution of these diagrams in the first order of perturbation theory. It takes the form

$$L_e^q = \frac{G_F}{\sqrt{2}}\Big[\ ^{ui}_L J_{uL(i)} + \ ^{ui}_R J_{uR(i)} + \ ^{di}_L J_{dL(i)} + \ ^{di}_R J_{dR(i)}\Big] + \frac{G_F}{\sqrt{2}}\Big[\bar{\ }^{di}_R J_{dR(i)} j_L + \bar{\ }^{di}_L J_{dL(i)} j_R\Big]: \tag{200}$$

The index i denotes generation so that $u_i = u;c;t$ and $d_i = d;s;b$. The coefficients accumulate dependence on the R_p SUSY parameters in the form

$$\begin{aligned}
^{ui}_L &= \frac{1}{\sqrt{2}}\sum_n \frac{^{0\ \ 0}_{2ln\ \ 1mn}}{G_F m^2_{\tilde{e}R(n)}} V_{il}V_{im} + \frac{2}{3}(3\ \ 4\sin^2\ _W)\ ^L_{11}\ ^L_{21} + \frac{g_2^2}{\sqrt{2}}\sum_n \frac{^{L\ \ L}_{11\ \ 21}}{G_F m^2_{\tilde{e}L(n)}} V_{in}j^2;\\
^{di}_R &= \frac{1}{\sqrt{2}}\sum_n \frac{^{0\ \ 0}_{2mi\ \ 1li}}{G_F m^2_{\tilde{e}L(n)}} V_{nm}V_{nl} + \frac{4}{3}\sin^2\ _W\ ^L_{11}\ ^L_{21}; \qquad (201)\\
^{di}_L &= \frac{2}{3}(3\ \ 2\sin^2\ _W)\ ^L_{11}\ ^L_{21}; \qquad ^{ui}_R = \frac{8}{3}\sin^2\ _W\ ^L_{11}\ ^L_{12};\\
\bar{\ }^{di}_L &= \frac{p}{2}\sum_n \frac{^0_{nii\ \ n12}}{G_F m^2_{\tilde{e}(n)}}; \qquad \bar{\ }^{di}_R = \frac{p}{2}\sum_n \frac{^0_{nii\ \ n21}}{G_F m^2_{\tilde{e}(n)}}:
\end{aligned}$$

Here $m_{\tilde{q}(n)}$ and $m_{\tilde{e}(n)}$ are the squark and sneutrino masses. In (200) we introduced the color singlet currents

$$J_{q_{L;R}(i)} = \bar{q}_i\ \ P_{L;R}\,q_i; \qquad J_{d_{L;R}(i)} = \bar{d}_i P_{L;R}\,d_i; \qquad j = e\ \ P_L\ ; \qquad j_{L;R} = eP_{L;R}\ ; \tag{202}$$

We denoted $q_i = (u_i; d_i)$ with the subscript i being the generation index.

The $\{e$ conversion involves the structure of the participating nucleus (A,Z) and the constituent nucleons. These structure effects have to be taken into account in calculating the $\{e$-conversion rate $(\ \ \ e)$. The detailed study of these questions were recently made in [109]. Note that this study takes into account previously overlooked contribution of the strange component of nucleon. As will be seen below this contribution allows one to establish new stringent constraints on the R_p parameters. For coherent conversion rate the following formula was found [109]

$$(\ \ \ !\ e) = \frac{G_F^2 p_e E_e}{2}\Big[\ _pM^{\ 2}_p(p_e) + \ _nM^{\ 2}_n(p_e) + \ _{pn}M_{\ p}(p_e)M_{\ n}(p_e)\Big]; \tag{203}$$

with $p_e\ \ \ m\ = 105$ MeV, neglecting the electron mass and the small nuclear recoil. The coefficients in (203) are defined as

$$\begin{aligned}
_N &= a_{0N}^2 + \frac{1}{2}a_{+N}^2 + \frac{1}{2}a^2_{\ N} + a_{0N}(a_{+N} + a_{\ N}); &(204)\\
_{pn} &= 2a_{0p}a_{0n} + 2a_{+p}a_{+n} + 2a_{\ p}a_{\ n} + a_{0p}(a_{+n} + a_{\ n}) + a_{0n}(a_{+p} + a_{\ p}); &(205)
\end{aligned}$$

where we used the definitions

$$a_{0N} = \frac{1}{2}\left({}^{(0)}_{V} + {}_{N}\,{}^{(3)}_{V}\right); \qquad a_{N} = \frac{1}{2}\left({}^{(0)}_{S} + {}_{N}\,{}^{(3)}_{S}\right); \tag{206}$$

with $N = p,n$, ${}_{p} = +1$; ${}_{n} = -1$ and

$${}^{(0)}_{V} = \frac{1}{8}(G_V^{(u)} + G_V^{(d)})({}^{u}_{R} + {}^{u}_{L} + {}^{d}_{R} + {}^{d}_{L}); \qquad {}^{(3)}_{V} = \frac{1}{8}(G_V^{(u)} - G_V^{(d)})({}^{u}_{R} + {}^{u}_{L} - {}^{d}_{R} - {}^{d}_{L});$$

$${}^{(3)}_{S} = \frac{1}{16}(G_S^{(u)} - G_S^{(d)})({}_{L} - {}_{R}); \qquad {}^{(0)}_{S} = \frac{1}{16}(G_S^{(u)} + G_S^{(d)})({}_{L} - {}_{R}) + \frac{1}{8}G_S^{(s)}({}^{s}_{L} - {}^{s}_{R});$$

$${}^{(0)}_{P} = \frac{1}{16}(G_P^{(u)} + G_P^{(d)})({}_{L} - {}_{R}) - \frac{1}{8}G_P^{(s)}({}^{s}_{L} - {}^{s}_{R}); \qquad {}^{(3)}_{P} = \frac{1}{16}(G_P^{(u)} - G_P^{(d)})({}_{L} - {}_{R}):$$

The nucleon form factors are defined as

$$hp;nj\bar{u}\,{}_{S;V}u|p;ni = G_{S;V}^{(u;d)}\,\bar{}_{p;n}\,{}_{S;V}\,{}_{p;n}; \qquad hp;nj\bar{d}\,{}_{S;V}d|p;ni = G_{S;V}^{(d;u)}\,\bar{}_{p;n}\,{}_{S;V}\,{}_{p;n}; \tag{207}$$

$$hp;nj\bar{s}\,{}_{S;V}s|p;ni = G_{S;V}^{(s)}\,\bar{}_{p;n}\,{}_{S;V}\,{}_{p;n}; \tag{208}$$

where ${}_{S} = 1$, ${}_{V} =$ with the numerical values at zero momentum transfer

$$G_V^{(u)} = 2; \qquad G_V^{(d)} = 1; \qquad G_S^{(u)} = 5:1; \qquad G_S^{(d)} = 4:3; \qquad G_S^{(s)} = 2:5: \tag{209}$$

Let us point out that the strange quarks significantly contribute to the {e -conversion rate via the strange nucleon sea (208).

The nuclear matrix elements $M_{p,n}(p_e)$ were calculated in [109] for the two experimentally most interesting nuclei

$$^{48}Ti: \qquad M_{p}(p_e) = 0:104 \text{ fm}^{3=2}; \qquad M_{n}(p_e) = 0:127 \text{ fm}^{3=2}; \tag{210}$$

$$^{208}Pb: \qquad M_{p}(p_e) = 0:434 \text{ fm}^{3=2}; \qquad M_{n}(p_e) = 0:566 \text{ fm}^{3=2}: \tag{211}$$

Now having all the definitions at hand one can extract the constraints on the R-p parameters involved in the above formulas. To this end one can compare formula in eq. (203) with the best experimental limit on the branching ratio

$$R_e^{Ti} = \frac{(\quad ! \quad e)}{(\quad ! \quad \text{capture})} < 7:0 \quad 10^{13} \tag{212}$$

measured by the SINDRUM II experiment [116] with the ^{48}Ti target nucleus. The measured value of the muon capture in ^{48}Ti is $(\quad ! \quad \text{capture}) = 2:590 \quad 0:012 \quad 10^{6}\text{ sec}^{1}$. Assuming as usual that only one product of the R-p parameters is a dominant one at a time one can extract from (212) rather stringent upper limits for these parameters listed in the second column of the Table 13. (See comments at the end of the next subsection on the rescaling of these limits for the expected in the future new experimental constrains on R_e^{Ti}.)

5.2.2 1-loop mechanism

The 1-loop mechanism of the {e conversion mediated by the one-photon exchange between lepton {e current and nucleus was studied in [64]. The diagrams of this mechanism formally coincide with those for the ! e shown in Fig. 4. In these diagrams it is implied that the photon is attached to each charged line. In case of the {e conversion the photon is virtual and connects the lepton current with nucleus. As shown in [64] the R-p interactions in the 1-loop mechanism contribute to the {e conversion with a large logarithm. The R-p contribution is located in the leptonic current which can be parameterized as

$$j_{(\text{photon})} = e\,(f_{E0} + {}_{5}f_{M0}) \quad g\left[\frac{q\,q}{q^2} + (f_{M1} + {}_{5}f_{E1})\,i\right]\frac{q}{m}; \tag{213}$$

where the form factors f_{E0}, f_{E1}, f_{M0} and f_{M1} to be computed from an underlying theory. The contribution of the diagrams in Fig. 4 has been calculated in [64]. Here we show only the final result. Starting from the Lagrangian (58) and using dimensional regularisation the following expressions were derived

$$f_{E0}^{f=\ell} = f_{M0}^{f=\ell} = \frac{2(\quad)}{3(4\quad)^2}\frac{q^2}{m_f^2}\left(\ln\frac{q^2}{m_f^2} + F_f(r)\right); \tag{214}$$

$$f_{E0}^{f=u} = f_{M0}^{f=u} = \frac{(\quad')N_c}{9(4\quad)^2}\frac{q^2}{m_f^2}\left(\ln\frac{q^2}{m_f^2} + F_f(r) \quad \frac{1}{12}\right); \tag{215}$$

$$f_{E0}^{f=d} = f_{M0}^{f=d} = \frac{(\quad')N_c}{18(4\quad)^2}\frac{q^2}{m_f^2}\left(\ln\frac{q^2}{m_f^2} + F_f(r) \quad \frac{1}{3}\right); \tag{216}$$

$$f_{M1}^{f=\ell} = f_{E1}^{f=\ell} = \frac{(\quad)}{3(4\quad)^2}\frac{m^2}{m_f^2}; \tag{217}$$

$$f_{M1}^{f=u} = f_{E1}^{f=u} = \frac{(\quad')N_c}{24(4\quad)^2}\frac{m^2}{m_f^2}; \tag{218}$$

$$f_{M1}^{f=d} = f_{E1}^{f=d} = 0: \tag{219}$$

Here the superscripts $f = \ell$; $f = u$ and $f = d$ denote contributions from the diagrams with leptons, u- and d-quarks in the loop respectively, $r = m_f^2/(\quad q^2)$; where f stands for the virtual fermion in the loop, $N_c = 3$ is the number of colours and

$$F_f(r) = \frac{1}{3} + 4r + \ln r + (1 \quad 2r)\sqrt{1+4r}\ln\frac{\sqrt{1+4r}+1}{\sqrt{1+4r} \quad 1}: \tag{220}$$

There are three important limiting cases. If $r \to 0$ then $F_f = \quad 1=3$; if $r \quad 1$ then $F_f \quad 1:52$ and if $r \quad 1$ then $F_f = \ln r + 4=3$:

The form factors (214), (215), (216) contain large logarithms while the form factors (217), (218), (219) do not. The presence of these large logarithms allows one to derive stringent limits on the products of the $\not{R}_p$ couplings standing in front of the form factors (214){(216). The dependence of the form factors on particular combination of R-parity violating couplings as well as on the signs in the form factors coming from the leptonic loops should be fixed when calculating the constraints on the products of couplings.

The coherent {e-conversion branching ratio for the present case of the photonic mechanism reads [117]

$$R_e^{\text{photon}} = C\,\frac{8\ ^5 m^5 Z_e^4\ |\overline{F_p}(p_e)|^2 Z}{\text{caption}}\quad\frac{^2_0}{q^4}; \tag{221}$$

where

$$^2_0 = |f_{E0} + f_{M1}|^2 + |f_{E1} + f_{M0}|^2: \tag{222}$$

The numerical values of the coefficients for the ^{48}Ti were calculated in [117,118] $C = 1:0$; $Z_e = 17:61$, and the proton nuclear form factor is $\overline{F_p}^{Ti}(p_e) = 0:55$.

Now it is straightforward to derive from the experimental constraint (212) the constraints on the products and ^{0} ^{0}. Towards this end one again has to assume that the only one product is dominant at a time. The results are presented in the third column of Table 13.

Very likely all the constraints in Table 13, both for the tree-level and for 1-loop mechanisms, will be significantly, (for an order of magnitude) improved in the near future. This expectation relies on the planed enhancement in sensitivity by three or even four orders of magnitude in the ongoing experiments at the PSI (using ^{48}Ti target) [116] and the designed MECO experiment at the Brookhaven (using ^{27}Al target) [119]. Having this in mind let us note that for a future experimental limit R_e^{future} on the {e-conversion branching ratio one can easily obtain the corresponding constraints on the $\not{R}_p$ parameters

Table 13. Upper limits on the products of the R_p parameters from μ–e conversion in ^{48}Ti. The loop constraints are given for the scalar masses 100 GeV and 1 TeV. The tree-level bounds scale quadratically with the sfermion mass and given only for $m_{\tilde{e}}$ 100 GeV. The scaling factor B is defined in the text and currently B = 1.

	μ–e at tree-level/B	μ–e at loop level/B	
	$m_{\tilde{e}}$ = 100 GeV	$m_{\tilde{e}}$ = 100 GeV	$m_{\tilde{e}}$ = 1 TeV
$\lambda'_{211}\lambda'^{*}_{111}$	$6.2 \cdot 10^{8}$	$4.4 \cdot 10^{6}$	$3.3 \cdot 10^{4}$
$\lambda'_{212}\lambda'^{*}_{112}, \lambda'_{213}\lambda'^{*}_{113}$	$1.7 \cdot 10^{8}$	$4.4 \cdot 10^{6}$	$3.3 \cdot 10^{4}$
$\lambda'_{221}\lambda'^{*}_{111}$	$7.6 \cdot 10^{8}$	$1.5 \cdot 10^{5}$	$1.0 \cdot 10^{3}$
$\lambda'_{222}\lambda'^{*}_{112}, \lambda'_{223}\lambda'^{*}_{113}$	$7.6 \cdot 10^{8}$	$1.5 \cdot 10^{5}$	$1.0 \cdot 10^{3}$
$\lambda'_{231}\lambda'^{*}_{111}$	$8.3 \cdot 10^{6}$	$4.8 \cdot 10^{4}$	$3.3 \cdot 10^{2}$
$\lambda'_{232}\lambda'^{*}_{112}, \lambda'_{233}\lambda'^{*}_{113}$	$8.3 \cdot 10^{6}$	$4.8 \cdot 10^{4}$	$3.3 \cdot 10^{2}$
$\lambda'_{211}\lambda'^{*}_{121}$	$7.6 \cdot 10^{8}$	$3.0 \cdot 10^{5}$	$1.0 \cdot 10^{3}$
$\lambda'_{212}\lambda'^{*}_{122}, \lambda'_{213}\lambda'^{*}_{123}$	$7.6 \cdot 10^{8}$	$3.0 \cdot 10^{5}$	$1.0 \cdot 10^{3}$
$\lambda'_{221}\lambda'^{*}_{121}$	$1.4 \cdot 10^{8}$	$8.0 \cdot 10^{6}$	$4.8 \cdot 10^{4}$
$\lambda'_{222}\lambda'^{*}_{122}, \lambda'_{223}\lambda'^{*}_{123}$	$3.3 \cdot 10^{7}$	$8.0 \cdot 10^{6}$	$4.8 \cdot 10^{4}$
$\lambda'_{231}\lambda'^{*}_{121}$	$3.7 \cdot 10^{5}$	$1.6 \cdot 10^{4}$	$8.8 \cdot 10^{3}$
$\lambda'_{232}\lambda'^{*}_{122}, \lambda'_{233}\lambda'^{*}_{123}$	$3.7 \cdot 10^{5}$	$1.6 \cdot 10^{4}$	$8.8 \cdot 10^{3}$
$\lambda'_{211}\lambda'^{*}_{131}$	$8.3 \cdot 10^{6}$	$4.8 \cdot 10^{4}$	$3.3 \cdot 10^{2}$
$\lambda'_{212}\lambda'^{*}_{132}, \lambda'_{213}\lambda'^{*}_{133}$	$8.3 \cdot 10^{6}$	$4.8 \cdot 10^{4}$	$3.3 \cdot 10^{2}$
$\lambda'_{221}\lambda'^{*}_{131}$	$3.7 \cdot 10^{5}$	$1.6 \cdot 10^{4}$	$8.8 \cdot 10^{3}$
$\lambda'_{222}\lambda'^{*}_{132}, \lambda'_{223}\lambda'^{*}_{133}$	$3.7 \cdot 10^{5}$	$1.6 \cdot 10^{4}$	$8.8 \cdot 10^{3}$
$\lambda'_{231}\lambda'^{*}_{131}$	$1.3 \cdot 10^{8}$	$3.5 \cdot 10^{5}$	$1.3 \cdot 10^{3}$
$\lambda'_{232}\lambda'^{*}_{132}, \lambda'_{233}\lambda'^{*}_{133}$	$4.0 \cdot 10^{3}$	$3.5 \cdot 10^{5}$	$1.3 \cdot 10^{3}$
$\lambda'_{212}\lambda'^{*}_{211}\lambda'_{312}\lambda'^{*}_{311}\lambda'_{121}\lambda'^{*}_{111}\lambda'_{312}\lambda'^{*}_{311}$	$4.1 \cdot 10^{9}$	{	{
$\lambda'_{212}\lambda'^{*}_{222}\lambda'_{312}\lambda'^{*}_{311}\lambda'_{121}\lambda'^{*}_{122}\lambda'_{321}\lambda'^{*}_{322}$	$7.7 \cdot 10^{9}$	{	{
$\lambda'_{121}\lambda'^{*}_{122}$	{	$1.7 \cdot 10^{6}$	$1.3 \cdot 10^{4}$
$\lambda'_{131}\lambda'^{*}_{132}, \lambda'_{231}\lambda'^{*}_{232}$	{	$2.1 \cdot 10^{6}$	$1.6 \cdot 10^{4}$
$\lambda'_{231}\lambda'^{*}_{131}, \lambda'_{232}\lambda'^{*}_{132}$	{	$3.4 \cdot 10^{6}$	$2.7 \cdot 10^{4}$
$\lambda'_{233}\lambda'^{*}_{133}$	{	$6.8 \cdot 10^{6}$	$4.0 \cdot 10^{4}$
$\lambda'_{e_1}\lambda'_{e_2}$ GeV^{-2}, $\lambda'_{1\ 2}$ GeV^{-2}	$4.4 \cdot 10^{4}$	{	{
$\lambda'_{e_1}\lambda'_{1\ 2}$ GeV^{-2}, $\lambda'_{e_2}\lambda'_{1\ 1}$ GeV^{-2}	$6.4 \cdot 10^{4}$	{	{

from the Table 13 simply multiplying the given numbers by the scale factor:

$$B = \sqrt{\frac{7.0 \cdot 10^{-13}}{R_e^{future}}} \tag{223}$$

The experimental prospects for searches of muon number violation have been recently reviewed in [120]. For a discussion of the lepton flavor violating limits in conjunction with other theoretical predictions the reader is referred to the recent survey of [121].

6 Atomic parity violation

Parity violation in the standard model (SM) results from exchanges of weak gauge bosons. In electron-hadron neutral current (NC) processes parity violation is due to vector axial-vector (VA) and axial-vector vector (AV) interaction terms in the Lagrangian. These interactions are tested at low momentum

transfers ($Q^2 \quad 0$) by the latest atomic parity violation (APV) measurements [122] and at high momentum transfers ($Q^2 > 2500\ GeV^2$) by deep inelastic NC scattering at HERA. The new interactions beyond the SM, in particular $R\!\!\!/_p$ interactions, may contribute to the parity violation and, therefore, can be constrained by the APV measurements.

6.1 APV and $R\!\!\!/_p$ interactions

The parity violating part of the NC Lagrangian is commonly parameterized by constants C_{1q} and C_{2q} as

$$L_{ehadron} = \frac{G_F}{\sqrt{2}} \sum_q C_{1q}\ e \quad {}^5e \quad q \quad q + C_{2q}(e \quad e)\ q \quad {}^5q \quad : \tag{224}$$

APV experiments [123] are mostly sensitive to C_{1q}, for which the radiatively corrected SM values are:

$$C_{1q}^{SM} = {}^0_{eq} \quad \left[T_{3q} + 2Q_q \left({}^0_{eq} \sin^2 {}_W \right) \right] ; \quad \sin^2 {}_W = 0.2236; \quad {}^0_{eq} = 0.9884; \quad {}^0_{eq} = 1.036: \tag{225}$$

There are several methods used for measurements of atomic parity violation [124]. The most recent and precise experiment measures a parity-odd atomic transition in Cesium atoms [122]. The advantage of using the heavy Cs atom, with only a single valence electron, is the smallness of the theoretical uncertainty due to atomic wave-function effects.

APV experiments probe the weak charge Q_W which scales the parity violating Hamiltonian [125]

$$H_{APV} = \frac{G_F}{2\sqrt{2}} Q_W \quad {}_{nucleus}(r) \quad {}_5; \qquad Q_W = \quad 2C_{1u}(2Z + N) + C_{1d}(Z + 2N) ; \tag{226}$$

where Z and N are the number of protons and neutrons in the nucleus of the atom, respectively and ${}_{nucleus}(r)$ is the nuclear density. For ${}^{133}_{55}Cs$, the relation of Q_W to the C_{1q} is

$$Q_W = \quad 376C_{1u} \quad 422C_{1d} : \tag{227}$$

With the radiatively corrected C_{1q} of (225), the SM value of Q_W for Cs is [126]

$$Q_W^{SM} = \quad 73.11 \quad 0.05 : \tag{228}$$

The recent precise measurement on Cesium atoms finds

$$Q_W^{exp} = \quad 72.11 \quad 0.27\ (stat.) \quad 0.89\ (theor.) ; \tag{229}$$

This result shows better agreement with the SM than previously. The Q_W measurement places strong constraints on possible new physics contributions [127, 128], C_{1u} and C_{1d}, defined as

$$Q_W \quad Q_W \quad Q_W^{SM} = \quad 2\ C_{1u}(2Z + N) + \ C_{1d}(Z + 2N) \quad ! \quad Q_W = 1.00 \quad 0.93: \tag{230}$$

The effective Lagrangian describing the $R\!\!\!/_p$MSSM contributions to the APV consist of the two terms corresponding to the t-channel $\tilde{d}_R$ and s-channel $\tilde{u}_L$ squark exchange diagrams:

$$L_{APV} = \frac{{}^{0\,2}_{ijk}}{m^2_{\tilde{e}_{Lj}}} (\bar{e}_{iL} d_{kR})\ \bar{d}_{kR} e_{iL} \ + \frac{{}^{0\,2}_{ijk}}{m^2_{\tilde{d}_{Rk}}} \ \overline{(e_{iL})^c} u_{jL} \quad \bar{u}_{jL} (e_{iL})^c \quad : \tag{231}$$

Fierz rearrangement casts these terms into a product of leptonic and hadronic vector- or axial-vector currents, as in (224). The resulting squark contributions to C_{1q} are given by

$$C_{1d} = \frac{\sqrt{2}}{G_F} \left(\frac{{}^{0\,2}_{1j1}}{8m^2_{\tilde{e}_{Lj}}} \right) ; \qquad C_{1u} = \quad \frac{\sqrt{2}}{G_F} \left(\frac{{}^{0\,2}_{11k}}{8m^2_{\tilde{d}_{Rk}}} \right) : \tag{232}$$

which cause a shift in Q_W of

$$Q_W = (2.4\ \mathrm{TeV})^2 \left[\frac{{}^{0}_{11k}{}^2}{m^2_{\tilde{e}_{Rk}}} - 1.12 \frac{{}^{0}_{1j1}{}^2}{m^2_{\tilde{e}_{Lj}}} \right] . \qquad (233)$$

Using the value of the weak charge given in (230) one has for $m = 100$ GeV the upper limit [23, 129]

$${}^{0}_{1j1} \quad 0.035 . \qquad (234)$$

This constraints may have far reaching phenomenological consequences, in particular, for $e^+ q \to e^+ q$ scattering since it casts limits on the s-channel squark resonance contribution due to the $\not{R}_p$ interactions. A detailed survey of the situation [130] with the well known HERA high Q^2-anomaly concludes that an interpretation of this anomaly as the s-channel squark resonance is only marginally consistent with the APV limit in (234). In this and the similar cases it might be important to remember that the weak charge Q_W measured in atomic parity violation experiments can receive compensating contributions from more than one new physics source. It was shown in [124] explicitly that the Q_W contribution from the exchange of an extra Z-boson can cancel that from the s-channel scalar top or scalar charm exchange in R-parity violating SUSY model.

6.2 Factors relaxing APV constraints

A low energy $\not{R}_p$ SUSY and an extra Z boson with mass of order 1 TeV are both natural consequences of string theory [131]. The Lagrangian describing the SM Z boson (Z_1^0) and an extra Z boson (Z_2^0) can be written as [132]

$$L_{Z_1^0 Z_2^0} = g_1 Z_1^0 \sum_i {}_i \left(g_L^{i(1)} P_L + g_R^{i(1)} P_R \right) {}_i + g_2 Z_2^0 \sum_i {}_i \left(g_L^{i(2)} P_L + g_R^{i(2)} P_R \right) {}_i ; \qquad (235)$$

where $g_1 = e/(\sin {}_W \cos {}_W)$, $g_L^{i(1)} = T_{3i} \quad \sin^2 {}_W Q_i$ and $g_R^{i(1)} = \quad \sin^2 {}_W Q_i$, $g_2/g_1 = \sqrt{\frac{}{5 \sin^2 {}_W}}/3$ and $\ ' 1$. In general, the SM Z boson and the extra Z boson will mix to form the physical mass eigenstates Z_1 and Z_2,

$$\begin{pmatrix} Z_1 \\ Z_2 \end{pmatrix} = \begin{pmatrix} \cos & \sin \\ \sin & \cos \end{pmatrix} \begin{pmatrix} Z_1^0 \\ Z_2^0 \end{pmatrix} \qquad (236)$$

with $M_{Z_1} = 91.1863$ GeV is the mass of the lightest experimentally observed Z boson. One can neglect the mixing since it is constrained to be small by the LEP and SLC data at the Z pole. For $= 0$ the Lagrangian (235) describes the interactions of physical Z_1 and Z_2 bosons. The contributions from the extra Z boson to the coefficients C_{1q} and C_{2q} are

$$C_{1q} = 2 \left(\frac{M_{Z_1}}{M_{Z_2}} \right)^2 \left(\frac{g_2}{g_1} \right)^2 g_a^{e(2)} g_v^{q(2)} ; \qquad C_{2q} = 2 \left(\frac{M_{Z_1}}{M_{Z_2}} \right)^2 \left(\frac{g_2}{g_1} \right)^2 g_v^{e(2)} g_a^{q(2)} ; \qquad (237)$$

where $g_v = g_L + g_R$ and $g_a = g_L \quad g_R$. Weakly-coupled extended gauge models, like E_6, give the coupling constant g_2 on the order of the weak coupling constant $g_1 = e/\sin {}_W$. One can take $= 1$ for which $g_2/g_1 \ ' 0.62$.

In the considered $\not{R}_p$ SUSY model with the extra Z boson eq. (233) for the weak charge is modified by Z_2-contribution and takes the form:

$$Q_W = (2.4\ \mathrm{TeV})^2 \left[\frac{{}^{0}_{11k}{}^2}{m^2_{\tilde{e}_{Rk}}} - 1.12 \frac{{}^{0}_{1j1}{}^2}{m^2_{\tilde{e}_{Lj}}} - 0.42 \frac{g_a^{e(2)}}{M^2_{Z_2}} \left(g_v^{u(2)} + 1.12 g_v^{d(2)} \right) \right] . \qquad (238)$$

One can see that the Z_2 contribution can make the overall Q_W positive. For example, for mass of the Z_2 boson about 1 TeV with $g_a^{e(2)} = \quad 1 = \quad g_v^{u(2)}$ and $g_v^{d(2)} = 0$, the Z_2 contribution to Q_W is $+2.4$.

The authors of [124] conclude that: (i) The deviation Q_W of the cesium APV measurement from the SM is positive, but the deviation is only 1 . (ii) The Q_W contribution of the scalar top or scalar charm via R-parity violating $\tilde{e}_L e^+ d$ or $\tilde{e}_L e^+ d$ couplings are negative. (iii) The Q_W contributions of the scalar bottom or scalar strange are positive, but they are likely too small to cancel the contribution from the scalar top or scalar charm because of the tight constraints on their couplings and masses. (iv) Extra Z boson contributions to Q_W can naturally be positive and sufficiently large to compensate negative contributions of scalar top or scalar charm and make the overall Q_W positive. (v) In particular, a scalar top interpretation of the HERA anomaly with the MSSM branching fraction of $B(\tilde{e}_L \to e^+ d) \quad 0{:}1$ is not excluded, since positive extra Z contributions to Q_W may compensate the negative contributions from the scalar top.

7 Cosmological implications

There are very strict bounds on all $R\!\!\!/_p$ interactions if one assumes that the presently observed matter–antimatter asymmetry was created above the electroweak scale. Valuable information can also be extracted from consideration of the conditions for the LSP to be the cold dark matter particle candidate and constraints on its lifetime from the accelerator searches.

7.1 Bounds from Baryogenesis

The scenarios of baryogenesis leading to the ratio of baryon number to entropy densities of the Universe today at the extremely small value of

$$B = n_B/s \quad 10^{10}$$

raise to three basic problems [133]:
(i) Generation of a baryon asymmetry at some temperature, T_{BA}. The question of the relevant mechanism and the scale of T_{BA} is not yet commonly settled. For the latter a variety of possibilities are envisaged: in the high-energy GUTs $T_{BA} \quad m_X/10$; in the low-energy SM $T_{BA} \quad T_C = m_W/_W$; or intermediate non-perturbative approach as in the Dine–Affleck squarks condensate mechanism.
(ii) Erasure of the preexisting baryon asymmetry. It may happen via B and/or L violating interactions inducing reactions among quarks and leptons or gauge and Higgs bosons, which might be in thermal equilibrium at some temperature, $T < T_{BA}$ during the cosmic expansion. This is formulated in terms of the reaction rate $_D$ and the Universe expansion rate,

$$H \quad 20\frac{T^2}{M_{Pl}}; \tag{239}$$

by the out-of-equilibrium condition, $_D/H < 1$. The erasure takes place for all linear combinations, $B + aL$, except for the (non-thermalizing modes) which remain conserved by the interactions.
(iii) The non-perturbative contributions associated to the electroweak sphalerons, which induce vacuum transition processes,

$$(\text{vacuum}) \to \prod_i (u_{iL} u_{iL} d_{iL} l_{iL}); \qquad (\text{vacuum}) \to \prod_i (u_{iL} d_{iL} d_{iL} \ _{iL}); \tag{240}$$

violating B and L via the anomalous combination, $(B + L) = 2N_{gen}$, while conserving $B_i \quad L_i$ with $i = 1;2;3$. Accounting for the flavour changing interactions of quarks, the effectively conserved combinations are in fact, $(B/3 \quad L_i)$. Since the sphaleron induced rates, over the wide period, $m_X < T < T_C$, are very much faster than the expansion rate,

$$\frac{_{sphal}}{H} \quad \frac{T}{H} \ e^{\ 2m_W/(2 \ _W T)} \quad 10^{7}; \tag{241}$$

this will damp the $(B + L)$ component of the asymmetry, while leaving the components $(B/3 \quad L_i)$ constant. A necessary condition for baryon asymmetry erasure in the presence of sphalerons is then

that this must have been produced via $(B-L)$ or $(B-L_i)$ (for some fixed i) violating interactions [134, 135].

The out-of-equilibrium conditions, taking into account the set of $2\to 2$ processes, $u+d\to \tilde{d}+\tilde{\chi}^0$, $u+e\to \tilde{d}+\tilde{\chi}^0$, $\gamma+e\to \tilde{\gamma}\to \gamma+\tilde{\chi}^0$, and $2\to 1$ processes, $d+\gamma\to \tilde{d}$, $u+e\to \tilde{d}$, $\gamma+e\to \tilde{\gamma}$, give on all $R\!\!\!/_p$ coupling constants the strong bounds,

$$\lambda,\lambda',\lambda''<5\times 10^{-7}\left(\frac{m_{\tilde{f}}}{1\ \mathrm{TeV}}\right)^{1/2}. \tag{242}$$

corresponding to an updated version [136] of previous analysis [134, 137].

A more refined analysis [136], accounting for all the relevant symmetries of the SM, through the equations on the particles chemical potentials expressing chemical equilibrium constraints, turns out to lead to milder constraints. Thus, it is found that the bounds on the B-violating λ'' interactions are removed in the absence of sphalerons, but remain in force when these are included. For the L-violating interactions, only a subset of the coupling constants, λ, λ', remains bounded. The reason is that one need impose the out-of-equilibrium conditions only for one lepton family, say J, corresponding to one conserved combination, $(B/3-L_J)$. The above bounds would then hold only for the subsets, λ_{Jjk}, λ'_{Jjk}. An indicative analysis of the fields basis dependence of these bounds is made in [27].

For the dimension $D>5$ non-renormalizable operators, the out-of-equilibrium conditions, as formulated by the inequalities:

$$\Gamma_D\sim T\left(\frac{T}{M_{Pl}}\right)^{2(D-4)}<H\sim 20\frac{T^2}{M_{Pl}}; \tag{243}$$

lead to the bounds [134]:

$$>\left[\frac{T^{2(D-4)-1}M_P}{20}\right]^{1/2(D-4)}. \tag{244}$$

The strongest bound, associated with $T=T_{GUT}\sim 10^{14}$ GeV, is:

$$>10^{14+2/(D-4)}\ \mathrm{GeV}. \tag{245}$$

The above discussed bounds on all the couplings are extremely stringent. If it is valid then $R\!\!\!/_p$ is irrelevant for collider physics and can only have cosmological effects. It is important, however, to note that these baryogenesis erasure constraints are really sufficient conditions and do not constitute strict bounds. They could be evaded if baryogenesis occurred at the electroweak scale or in non-perturbative models in case of an insufficient reheat temperature.

There are two important loop-holes in this argument. The first and most obvious one is that the matter genesis occurred at the electroweak scale or below [138]. The second loop-hole has to do with the inclusion of all the symmetries and conserved quantum numbers [136, 139, 140]. The electroweak sphaleron interactions do not just conserve $B-L$. They conserve the three quantum numbers $B/3-L_i$, one for each lepton flavour. These can also be written as $B-L$ and two independent combinations of L_i-L_j. First, again consider an additional UDD operator. If the matter genesis at the GUT scale is asymmetric in the lepton flavours, $(L_i-L_j)|_{M_{GUT}}\neq 0$, then this lepton-asymmetry is untouched by the sphalerons and by the $B\neq 0$ operators UDD operators. The baryon asymmetry is however erased. Below the electroweak scale, the lepton-asymmetry is partially converted into a baryon-asymmetry via (SM) leptonic and supersymmetric mass effects [136]. If now instead, one adds a lepton-number violating operator, one will retain a matter asymmetry as long as one lepton flavour remains conserved. In order for L for example to be conserved, all L violating operators must remain out of thermal equilibrium above the elctroweak scale, i.e. satisfy the bound (242). From the low-energy point of view this is completely consistent with the assumption of only one large dominant coupling at a time. Thus in these simple scenarios the bounds (242) are evaded.

7.2 Long-lived LSP

One can consider three distinct ranges for the lifetime of the LSP

$$\text{(i)}\ \ _{LSP} < 10^{\ 8}\ \text{s}; \qquad \text{(ii)}\ 10^{\ 8}\ \text{s} < \ _{LSP} < 10^{7}\ _{U}; \qquad \text{(iii)}\ \ _{LSP} > 10^{7}\ _{U}; \tag{246}$$

where $_{U}$ 10^{10} years is the present age of the Universe. The first case relevant to "standard" R-parity violating LSP collider phenomenology. The third case is indistinguishable from the R_p-MSSM with the LSP being a good dark matter candidate. In the second case, the LSP can provide a long-lived relic whose decays can potentially lead to observable effects in the Universe. There are bounds excluding any such relic with lifetimes [141]

$$1\ \text{s} < \ _{LSP} < 10^{17}\ \text{years}:$$

The lower end of the excluded region is due to the effects of hadron showers from LSP decays on the primordial abundances of light nuclei [142]. The upper bound is from searches for upward going muons in underground detectors which can result from $\ $'s in LSP decays [143]. Note that even if $_{LSP} > \ _{U}$ the relic abundance is so large that the decay of only a small fraction can lead to observable effects.

The above restrictions on decay lifetimes can be immediately applied to the case of $R\!\!\!/_p$ MSSM. Including LSP decays in collider experiments one gets a gap of eight orders of magnitude in lifetimes $10^{\ 8}\text{s} < \ _{LSP} < 1\text{s}$ where no observational tests are presently known. It is very important to find physical effects which could help to close this gap. Since the lifetime depends on the square of the $R\!\!\!/_p$ Yukawa coupling this corresponds to a gap of four orders of magnitude in the coupling. For a photino LSP one can translate the above bounds into bounds on the $R\!\!\!/_p$ Yukawa couplings [144]:

$$10^{\ 22} < (\ ;\ ^{0};\ ^{00})\ \ \frac{200\ \text{GeV}}{m_{\tilde{}}}\ ^{2}\ \ \frac{M_{\ e}}{100\ \text{GeV}}\ ^{!\ 5=2} < 10^{\ 10}:$$

Note that the lower range of these bounds extends well beyond the already strict bound from proton decay. For a generic neutralino LSP the lifetime depends strongly on the MSSM parameters [145, 146] and the bounds can only be transferred with caution.

The simplest possible decay mode of the lightest neutralino is $\tilde{}_1^0 \ ! \ eud$ with the rate given by Dawson's formula [147]:

$$_{e_0}^{\ 1} = \frac{3}{128\ ^{2}}\,j\ ^{0}_{121}j^{2}\frac{M_{e_1^0}^{\ 5}}{m_{\tilde{e}}^{\ 4}}: \tag{247}$$

The requirement of the LSP decaying within a detector can be quantified as $c\ _{L\ \tilde{}_0} < 1\ \text{m}$ and leads to the constraint

$$j\ ^{0}_{121}j > 1{:}4\ \ \ 10^{\ 6}\sqrt{\ _{L}}\ \ \frac{m_{\tilde{e}}}{200\ \text{GeV}}\ ^{2}\left(\frac{100\ \text{GeV}}{M_{\ e}}\right)^{5=2}; \tag{248}$$

where $_{L}$ is the Lorentz boost factor. On the other hand, from the experimental absence of a long-lived relic LSP whose decay would lead to detectable upward going muons, one can infer [148] that $1\ \text{s} < \ _{e} < 10^{17}$ years leads to the forbidden interval $10^{\ 10} \lesssim j\ ^{0};\ ^{00}j \lesssim 10^{\ 22}$. Note that $_{e} > 10^{17}$ years would make $R\!\!\!/_p$MSSM indistinguishable from MSSM. Furthermore, the interval $10^{\ 8}\ \text{s} < \ _{e_1} < 1\ \text{s}$ is practically out of observational reach.

8 Accelerator search for R-parity violation

Supersymmetric particles can be produced in pairs via the MSSM gauge couplings or singly via the $R\!\!\!/_p$ Yukawa couplings. The former benefits from large couplings while being kinematically restricted to masses lower then $\sqrt{s}/2$. The latter case has double the kinematic reach but has a suppression

factor due to smallness of the R_p couplings. The single SUSY particles are produced by resonant and non-resonant mechanisms. The resonant production mechanisms are

$$e^+ + e^- \to \tilde{e}_{Lj} \quad [L_1 L_j E_1^c]; \qquad e^- + u_j \to \tilde{d}_{Rk} \quad [L_1 Q_j D_k^c]; \qquad e^- + d_k \to \tilde{u}_{Lj} \quad [L_1 Q_j D_k^c];$$

$$u_j + d_k \to \tilde{e}_{Li} \quad [L_i Q_j D_k^c]; \qquad d_j + d_k \to \tilde{e}_{Li} \quad [L_1 Q_j D_k^c];$$

$$u_i + d_j \to \tilde{d}_{Rk} \quad [U_i^c D_j^c D_k^c]; \qquad d_j + d_k \to \tilde{u}_{Ri} \quad [U_i^c D_j^c D_k^c]:$$

These processes can be realized at e^+e^--colliders, at HERA, and at hadron colliders, respectively. There are many further t-channel single sparticle production processes. For example at an e^+e^--collider, there might be $e^+ + e^- \to \tilde{\chi}_1^0 + \gamma$ via t-channel selectron exchange. The t-channel exchange of squarks (sleptons) can also contribute to $q\bar{q}$ ($\ell^+\ell^-$) pair production, leading to indirect bounds [149].

Another feature of the R_p MSSM accelerator phenomenology related to the fact that the LSP is unstable (sect. 7.2). If for example the neutralino is the LSP and the dominant R_p operator is $L_1 Q_2 D_1^c$ it can decay as shown in Fig. 2(c). For LSP = $\tilde{\gamma}$ the decay rate is given by eq. (247) [147, 150]. The decay occurs in the detector if $c\gamma_L\,\tau(\tilde{\gamma}) < 1$ m, where γ_L is the Lorentz boost factor. This gives constraint (248), which is well below the existing bounds on the R_p couplings. These numerical results for a photino is given for simplicity and clarity. The full analysis with a neutralino LSP has been performed in [145, 146]. It involves several subtleties due to the R_p-MSSM parameter space which can have significant effects on the lifetime. Due to the LSP decay, supersymmetry with broken R_p has no natural dark matter candidate.

8.1 Squark Pair Production at the Tevatron

Squark pair production at the Tevatron proceeds via the known gauge couplings of the R_p MSSM

$$q\bar{q},\ gg \to \tilde{q}_i + \bar{\tilde{q}}_i:$$

The squarks produced in the R_p interactions decay to an R_p-even final state. Let us consider a dominant $L_i L_j E_k^c$ operator. The couplings λ_{ijk} are bounded to be smaller than gauge couplings. Thus one may expect the squarks to cascade decay to LSPs as in the MSSM. The LSPs in turn will then decay via the operator $L_i L_j E_k^c$ to two charged leptons and a neutrino (see Fig. 2(c)). If each squark decays directly to the LSP (assuming it is the second lightest superparticle)

$$q\bar{q},\ gg \to \tilde{q}_i + \bar{\tilde{q}}_i \to qq + \tilde{e}_1^0\tilde{e}_1^0 \to qq + l^+ l^- l^+ l^- \quad : \tag{249}$$

One therefore has a multi-lepton signal which is detectable [151]. To date it has not been searched for with R_p in mind. However, before the top quark discovery there was a bound from CDF on a di-lepton production cross section. Making corresponding cuts and with some simple assumptions this can be translated into a bound on the rate of the process (249) and thus a lower bound on the squark mass [151]. The assumptions are: (i) $B(\tilde{q}_i \to q\tilde{\gamma}) = 100\%$, ($m_{\tilde{q}_i} < m_{\tilde{g}}$), (ii) LSP = $\tilde{\gamma}$ with $M_{\tilde{\gamma}} = 30$ GeV, (iii) $\tilde{\gamma}$, $\tilde{\chi}^0$ satisfy the bound (248). For various dominant operators the bounds are given in Table 14.

Table 14. Squark mass bounds from the Tevatron for various dominant R_p-operators.

	$L_{1,2}Q_{1,2}D_k^c$	$L_{1,2}L_3E_3^c$	$L_1L_2E_3^c$	$L_{1,2}L_3E_{1,2}^c$	$L_1L_2E_{1,2}^c$
$m_{\tilde{q}_i}$	100 GeV	100 GeV	140 GeV	160 GeV	175 GeV

No attempt was made to consider final state τ's due to lack of data. These bounds are comparable to the R_p-MSSM squark mass bounds. Since, the theoretical analysis has been improved to allow for neutralino LSPs, more involved cascade decays and the operator $U^cD^cD^c$ [152, 153]. However, to date no experimental analysis has been performed.

8.2 Resonant Squark Production at HERA

HERA offers the possibility to test the operators $L_1Q_jD_k^c$ via resonant squark production [154]

$$e^+ + d_k \;\to\; \tilde{u}_j \;\to\; (e^+ + d_k;\; e_1^0 + u_j;\; e_1^+ + d_j);$$
$$e^+ + \bar{u}_j \;\to\; \tilde{\bar{d}}_k \;\to\; (e^+ + \bar{u}_j;\; \bar{\nu}_e + \bar{d}_j;\; e_1^0 + \bar{d}_k):$$

These decay modes are expected to be dominant. Note that HERA has accumulated most of its data as a positron proton collider. The neutralino and chargino would decay as in Fig. 2(c)

$$e_1^0 \;\to\; (e\;\nu\;) + 2\,\text{jets};\quad e_1^+ \;\to\; (e^+;\;\nu\;) + 2\,\text{jets}: \tag{250}$$

The neutralino can decay to the electron or positron since it is a Majorana fermion. Thus one lefts with several distinct decay topologies.

(i) If the squark is the LSP it will decay to $e^+ + q$ or $\bar{\nu}_e + q$ ($\tilde{\bar{d}}_k$). The first looks just like neutral current DIS, except that for $x_{Bj} \ll m^2(\tilde{q})/s$ it results in a flat distribution in y_e whereas NC-DIS gives a $1/y_e^2$ distribution. The latter looks just like CC-DIS.

(ii) If the gauginos are lighter than the squark the gaugino decay will dominate. The clearest signal is a high p_T electron which is essentially background free. The high p_T positron or the missing p_T of the neutrino can also be searched for.

All five signals have been searched for by the H1 collaboration [155] in the 1994 e^+ data ($\mathcal{L} = 2.83\,\text{pb}^{-1}$). The observations were in excellent agreement with the SM. The resulting bounds on the couplings are summarized in Table 15.

Table 15. Exclusion upper limits at 95% C.L. on λ'_{1jk} for $m(\tilde{q}) = 150$ GeV and $m(e_1^0) = 40$ GeV for two different dominant admixtures of the neutralino.

	λ'_{111}	λ'_{112}	λ'_{113}	λ'_{121}	λ'_{122}	λ'_{123}	λ'_{131}	λ'_{132}	λ'_{133}
e-like	0.056	0.14	0.18	0.058	0.19	0.30	0.06	0.22	0.55
$\tilde{Z}^0$-like	0.048	0.12	0.15	0.048	0.16	0.26	0.05	0.19	0.48

After rescaling the bounds of Table 14 one sees that the direct search is an improvement for λ'_{121}; λ'_{131}; and λ'_{132}. In the more recent data, an excess has been observed in high Q^2 NC-DIS [17]. If this persists it can possibly be interpreted as the resonant production of a squark via an $L_1Q_jD_k^c$ operator [156, 157].

8.3 Neutrino-lepton and neutrino-quark scattering

The neutral current scattering processes are able to efficiently constraint the new physics interactions such as the $\not{R}_p$ ones. The elastic ν scattering processes, $\nu + e_i \to \nu + e_j$, $\nu + q_i \to \nu + q_j$, at energies well below m_Z, are described at tree level by Z-boson exchange contributions in terms of the effective Lagrangian,

$$\mathcal{L} \;=\; -\frac{4G_F}{\sqrt{2}}(\bar{\nu}_L\;\gamma^\mu\;\nu_L)(g_L^f\bar{f}_L\;\gamma_\mu\;f_L + g_R^f\bar{f}_R\;\gamma_\mu\;f_R): \tag{251}$$

The related $\bar{\nu}_e$ scattering processes include an additional t-channel contribution. The $\not{R}_p$ corrections read [23]

$$\begin{aligned}
g_L^e &= (\,\frac{1}{2} + \sin^2\theta_W)(1 - r(\tilde{e}_R)) - r(\tilde{e}_R);\\
g_R^e &= \sin^2\theta_W\,(1 - r(\tilde{e}_R)) + r_{211}(\tilde{e}_{L1}) + r_{231}(\tilde{e}_{L3});\\
g_L^d &= (\,\frac{1}{2} + \frac{1}{3}\sin^2\theta_W)(1 - r(\tilde{e}_R)) - r'(\tilde{d}_R);\\
g_R^d &= -\frac{\sin^2\theta_W}{3}(1 - r(\tilde{e}_R)) + r'(\tilde{d}_L):
\end{aligned}$$

Here the following notations are used:

$$r_{ijk}(\tilde{e}_{Rk}) = \frac{M_W^2}{g_2^2 m^2_{\tilde{e}_{Rk}}} \lambda_{ijk}^2; \qquad r_{ikj}(\tilde{e}_{Lk}) = \frac{M_W^2}{g_2^2 m^2_{\tilde{e}_{Lk}}} \lambda_{ikj}^2; \tag{252}$$

$$r'_{ijk}(\tilde{d}_{Rk}) = \frac{M_W^2}{g_2^2 m^2_{\tilde{d}_{Rk}}} \lambda'^2_{ijk}; \qquad r'_{ijk}(\tilde{d}_{Lj}) = \frac{M_W^2}{g_2^2 m^2_{\tilde{d}_{Lj}}} \lambda'^2_{ijk};$$

$$r(\tilde{e}_R) = \sum_{k=1}^{3} r_{12k}(\tilde{e}_{Rk}); \qquad r'(\tilde{d}_R) = \sum_{k=1}^{3} r'_{21k}(\tilde{d}_{Rk}); \qquad r'(\tilde{d}_L) = \sum_{k=1}^{3} r'_{2k1}(\tilde{d}_{Lk}):$$

From the experimental data on the neutrino scattering processes $\nu + e_i \to \nu + e_j$, $\nu + q_i \to \nu + q_j$ one derives the constraints for the common SUSY mass 100 GeV [23]:

$$\lambda_{121} \quad 0.29; \qquad \lambda_{122} \quad 0.34; \qquad \lambda_{123} \quad 0.34; \qquad \lambda_{233} \quad 0.26; \qquad \lambda'_{222} \quad 0.22; \qquad \lambda'_{231} \quad 0.22:$$

8.4 Fermion-antifermion pair production

The forward-backward angular asymmetries (FB) in the differential cross sections for the reactions, $e^+ + e \to f + f$, with $f = l, q$ can be parameterized in terms of the axial vector coupling in the effective Lagrangian density,

$$L = \frac{4G_F}{\sqrt{2}} A^e A^f (e \quad _5 e)(f \quad _5 f); \tag{253}$$

where $A^f = T_{3L}^f$ is the SM value. The off Z-boson pole asymmetry is defined as,

$$A_{FB} = \frac{3\sqrt{2} G_F s m_Z^2}{16 \pi (m_Z^2 \quad s)};$$

and the Z-boson pole asymmetry as,

$$A_{FB} = \frac{3}{4} A^e A^{l,q}.$$

The formulas for the R_p corrections to the Z-pole asymmetries in terms of the products of parameters $A^e A^f$ with notations (252) read [23]

$$A^e A \quad = \quad \frac{1}{4} \quad \frac{1}{2} r_{ijk}(e_{kL}); \qquad \text{where} \quad (ijk) = (122); (132); (121); (321);$$

$$A^e A \quad = \quad \frac{1}{4} \quad \frac{1}{2} r_{ijk}(e_{kL}); \qquad \text{where} \quad (ijk) = (213); (313); (131); (231);$$

$$A^e A^{u_j} \quad = \quad \frac{1}{4} \quad \frac{1}{2} r'_{1jk}(\tilde{d}_{kL}); \qquad A^e A^{d_k} = \frac{1}{4} \quad \frac{1}{2} r'_{1jk}(\tilde{u}_{jL}):$$

Using the experimental data on the asymmetries [21] the following limits were obtained for $m_{\tilde{f}} = 100$ GeV

$$|\lambda_{ijk}| < 0.10, \quad ijk = 121; 122; 132; 231; \qquad |\lambda_{ijk}| < 0.24, \quad ijk = 123; 133; 131; 232;$$

$$|\lambda'_{12k}| < 0.45; \qquad |\lambda'_{1j3}| < 0.26:$$

The product $|\lambda_{131}\lambda_{232}|$ can also be constrained by high energy experiments at e^+e and $\mu^+\mu$ colliders [158]–[160]. The s-channel exchanges of $\tilde{e}_L$ and $\tilde{e}_L$ (depending on the coupling, there could also be t-channel diagrams), contribute to the process $e^+e \to \mu^+\mu$. The inclusion of scalar tau-sneutrino exchanges will affect both the cross section and the forward-backward asymmetry in muon-pair production. The change in cross section due to s-channel resonance production is given by

$$= \frac{|\lambda_{131}\lambda_{232}|^2}{32} \frac{s}{(s \quad m^2_{\tilde{e}_L})^2 + \quad ^2_{\tilde{e}_L} m^2_{\tilde{e}_L}}:$$

If the product of s is of an appreciable size and the mass of the scalar tau-sneutrino is below the energy of the machine, the LEP2 and the future NLC experiments should be able to see a prominent peak by scanning over the center-of-mass energy (LEP2 has effectively done that due to the initial state radiation); otherwise, the null result should be able to constrain the product of s. If the mass of the scalar tau-sneutrino is above the center-of-mass energy of the machine, only the effect from the tail of the scalar tau-sneutrino can be seen and, therefore, the limit on s is much weaker.

The L3 collaboration has recently published the 90% C.L. upper limit on

$$j_{131}j = j_{232}j < 0:04$$

for $m_{e_L} = 110\{170$ GeV by measuring the cross section and the forward-backward asymmetry in muon-pair production. The future experiment at the NLC can probe heavier scalar tau-sneutrino with $j_{131\ 232}j$ down to 10^{-4} level, assuming $_{e_L}=m_{e_L}$ 1% and an integrated luminosity of 50 fb^{-1}.

8.5 LEP precision measurements of Z widths

Heavy virtual chiral fermions induce sizable loop corrections to (Z ! f f) (f is a light fermion) via fermion-sfermion mediated triangle graphs [161, 162]. Since vertices involving $^{0}_{i3k}$ or $^{00}_{3jk}$ could allow top quark in internal lines of a triangle diagram, [161, 162] the bounds on them are most interesting. For $m_{\tilde{}} = 100$ GeV and at 1 , the following bounds emerge ($R_l = _{had}=_l$; $R_l^{SM} = 20:756$ with Higgs boson mass m_H treated as a free parameter):

$$\begin{array}{lllll} ^{0}_{13k} & 0:34 & \text{from} & R_e^{exp} = 20:757 & 0:056; \\ ^{0}_{23k} & 0:36 & \text{from} & R^{exp} = 20:783 & 0:037; \\ ^{0}_{33k} & 0:48 & \text{from} & R^{exp} = 20:823 & 0:050; \\ ^{00}_{3jk} & 0:50 & \text{from} & R_l^{exp} = 20:775 & 0:027: \end{array} \qquad (254)$$

9 Summary and outlook

The R$_p$ SUSY models offer an essentially richer low-energy phenomenology than the SUSY models, which conserve the R-parity. We specified the main differences between these two options of the low energy SUSY at the end of sect. 2. In this paper we mainly concentrated on the lepton/quark flavor and number violating interactions allowed in the R$_p$ SUSY. We reviewed many processes in which these interaction can be probed. It could be noticed that the main direction of the present activity in this field is aimed to derivation of the constraints on the R$_p$ parameters. The R$_p$ MSSM contains only in the superpotential 48 parameters more than the R-parity conserving MSSM. Unless no underlying theory is implied to connect different parameters the predictive power of the R$_p$ SUSY remains rather weak. Fortunately many processes depend on the the same R$_p$ couplings or on their products. Thus in certain cases it becomes possible having the relevant R$_p$ parameters constrained from one process to predict the upper bound for the branching of the other processes or to help in the interpretation of certain experimental signatures. A typical example is given by the well known HERA anomaly. There were attempts to explain this anomaly as the s-channel squarks resonance. Since from the 0 decay $^{0}_{111}$ coupling had been stringently constrained it became possible to exclude from consideration the up squark. This was a step forward in understanding for an origin of the HERA anomaly. There are other examples of this type. Knowing constraints on the R$_p$ parameters allows one to estimate prospects of a certain experiment in searching for the R$_p$ SUSY and, thus, to significantly help in planning new experiments of this type. Many experiments intending to search for the R$_p$ SUSY signal are now in progress or on the stage of preparation. Having these issues in mind we present in Tables 16 and 17 the most stringent constraints for the R$_p$ parameters and for their products.

In Table 17 we listed constraints only for those products which are, as we think, the most phenomenologically important. Let us note that these products are more stringently constrained from the

Table 16. Upper bounds on $\not{R}_p$ couplings for $m_{\tilde{q}} = 100$ GeV. The numbers with (?) correspond to 2 limits and those with (y) are basis-dependent limits.

Coupling	Bound	Source	Coupling	Bound	Source
λ_{121}	0.05?	CC universality	λ''_{112}	10^{-6}	$NN \to K$'s
λ_{122}	0.05?	CC universality	λ''_{113}	10^{-3}	$n\bar{n}$ oscillation
λ_{123}	0.05?	CC universality	λ''_{123}	1.25	Pert. unitarity
λ_{131}	0.06	$(\to e\ )/(\to\ )$	λ''_{212}	1.25	Pert. unitarity
λ_{132}	0.06	$(\to e\ )/(\to\ )$	λ''_{213}	125	Pert. unitarity
λ_{133}	0.003	$_e$ mass	λ''_{223}	1.25	Pert. unitarity
λ_{231}	0.06	$(\to e\ )/(\to\ )$	λ''_{312}	0.50	$\tilde{\ }/\tilde{\ }_h$ (LEP 1)
λ_{232}	0.06	$(\to e\ )/(\to\ )$	λ''_{313}	0.50	$\tilde{\ }/\tilde{\ }_h$ (LEP 1)
λ_{233}	0.06	$(\to e\ )/(\to\ )$	λ''_{323}	0.50	$\tilde{\ }/\tilde{\ }_h$ (LEP 1)

Coupling	Bound	Source	Coupling	Bound	Source	Coupling	Bound	Source
λ'_{111}	0.00013	$(\ )_0$	λ'_{211}	0.09	R	λ'_{311}	0.10	$\to$
λ'_{112}	0.02?	CC univ.	λ'_{212}	0.09	R	λ'_{312}	0.10	$\to$
λ'_{113}	0.02?	CC univ.	λ'_{213}	0.09	R	λ'_{313}	0.10	$\to$
λ'_{121}	0.035?	APV	λ'_{221}	0.18	D decay	λ'_{321}	0.20y	$D^0\bar{D}^0$ mixing
λ'_{122}	0.02	$_e$ mass	λ'_{222}	0.18	D decay	λ'_{322}	0.20y	$D^0\bar{D}^0$ mixing
λ'_{123}	0.20y	$D^0\bar{D}^0$ mixing	λ'_{223}	0.18	D decay	λ'_{323}	0.20y	$D^0\bar{D}^0$ mixing
λ'_{131}	0.035?	APV	λ'_{231}	0.22?		λ'_{331}	0.48	R (LEP)
λ'_{132}	0.16	$b \to e\ X_c$	λ'_{232}	0.36	R	λ'_{332}	0.48	R (LEP)
λ'_{133}	0.0007	$_e$-mass	λ'_{233}	0.36	R	λ'_{333}	0.48	R (LEP)

Table 17. Upper bounds on some important product couplings for $m_{\tilde{q}} = 100$ GeV.

Combination	Bound	Source	Combination	Bound	Source
$\lambda'_{11k}\lambda''_{11k}$	10^{-27}	Proton decay	$\lambda'_{ijk}\lambda''_{lmn}$	10^{-10}	Proton decay
$\lambda'_{11k}\lambda''_{11k}$	10^{-22}	Proton decay			
$\lambda_{1j1}\lambda_{1j2}$	$7 \cdot 10^{-7}$	$\to 3e$	$\lambda_{231}\lambda_{131}$	$7 \cdot 10^{-7}$	$\to 3e$
$\lambda'_{i12}\lambda'^{*}_{i21}$	$8 \cdot 10^{-12}$	m_K	$\lambda'_{i12}\lambda'_{i21}$	$1 \cdot 10^{-9}$	m_K
$\lambda'_{i13}\lambda'_{i31}$	$8 \cdot 10^{-8}$	m_B	$\lambda'_{1k1}\lambda'_{2k2}$	$8 \cdot 10^{-7}$	$K_L \to e$
$\lambda'_{k11}\lambda'_{k12}$	$4.8 \cdot 10^{-9}$	$Ti \to eTi$	$\lambda'_{11j}\lambda'_{21j}$	$7.6 \cdot 10^{-8}$	$Ti \to eTi$
$\lambda''_{i32}\lambda''_{i21}$	0.008	$(B^{ch} \to K^{neut}K^{ch})$	$\lambda''_{i31}\lambda''_{i21}$	0.006	$(B^{ch} \to K^{neut}\ ^{ch})$

sources displayed in the Table than it could be derived by multiplication of the corresponding individual constraints from Table 16. We would also like to remind that most of the constraints on were derived under the assumption that only one parameter or a product of the $\not{R}_p$ parameters dominates at a time. This assumption is invoked by the fact that the amplitude of a process used to constrain the $\not{R}_p$ parameters typically depends on many SUSY parameters.

Thus most of the constraints are not inevitable conditions for the phenomenological studies and model-building but only indicative ones. With this precautions we conclude our review in which we of course could not cover all $\not{R}_p$ SUSY phenomenology. Questions not discussed here can perhaps be found in other recently appeared original and review papers [13, 14, 16].

References

[1] P. Nath et al., Applied N = 1 Supergravity (World Scientific, Singapore, 1984); H.-P. Nilles, Phys. Rep., 110 (1984) 1; Testing the Standard Model, eds. M. Cvetic and P. Langacker (World Scientific, Singapore, 1991) p. 633; G.G. Ross, Grand Unified Theories (Benjamin, New York, 1984); R.N. Mohapatra, Unification and Supersymmetry (Springer, New York, 1986, 1992); The Building Blocks of Creation, eds. S. Raby and T. Walker (World Scientific, Singapore, 1994) p. 291.

[2] H.E. Haber and G.L. Kane, Phys. Rep., 117 (1985) 75; J.F. Gunion, H.E. Haber and G.L. Kane, Nucl. Phys., B 272 (1986) 1.

[3] G. Farrar, P. Fayet, Phys. Lett., B 76 (1978) 575.

[4] L.J. Hall, M. Suzuki, Nucl. Phys., B 231 (1984) 419.

[5] T. Banks, Y. Grossman, E. Nardi, Y. Nir, Phys. Rev., D 52 (1995) 5319; hep-ph/9505248.

[6] H.-P. Nilles, N. Polonsky, Nucl. Phys., B 484 (1997) 33; hep-ph/9606388.

[7] E. Nardi, Phys. Rev., D 55 (1997) 5772; hep-ph/9610540.

[8] F. de Campos, M.A. Garcia-Jareno, A.S. Joshipura, J. Rosiek and J.W.F. Valle, Nucl. Phys. B 451 (1995) 3.

[9] F.M. Borzumati, Y. Grossman, E. Nardi and Y. Nir, Phys. Lett., B 384 (1996) 123.

[10] C. Aulakh and R. Mohapatra, Phys. Lett., B 119 (1983) 136.

[11] G.G. Ross and J.W.F. Valle, Phys. Lett., B 151 (1985) 375; J. Ellis, G. Gelmini, C. Jarlskog, G.G. Ross and J.W.F. Valle, Phys. Lett., B 150 (1985) 142; A. Santamaria and J.W.F. Valle, Phys. Lett., B 195 (1987) 423; Phys. Rev., D 39 (1989) 1780; Phys. Rev. Lett., 60 (1988) 397; A. Masiero and J.W.F. Valle, Phys. Lett., B 251 (1990) 273; J.W.F. Valle, "Physics from Planck scale to electroweak scale", Proc. US-Polish Workshop, (21-24 Sept. 1994, Warsaw); C.A. Santos and J.W.F. Valle, Phys. Lett., B 288 (1992) 311; M.C. Gonzalez-Garcia, J.C. Romao and J.W.F. Valle, Nucl. Phys., B 391 (1993) 100; R. Barbieri, D.E. Brahm, L.J. Hall and S.D.H. Hsu, Phys. Lett., B 238 (1990) 86.

[12] For a review see "Physics Beyond the Desert" by J.W.F. Valle, In. Proc. Workshop on Physics beyond the Standard Model, Castle Ringberg, Tegernsee, Germany, 8-14 June, 1997; hep-ph/9712277.

[13] Herbi Dreiner, hep-ph/9707435.

[14] Gautam Bhattacharyya, Nucl. Phys. Proc. Suppl. 52A (1997) 83; hep-ph/9709395.

[15] Probir Roy, hep-ph/9712520.

[16] R. Barbier et al. Report of the group on the R-parity violation, hep-ph/9810232.

[17] C. Adlo et al., Z. Phys., C 74 (1997) 191, hep-ex/9702012; J. Breitweg et al., Z. Phys., C 74 (1997) 207, hep-ex/9702015.

[18] H.P. Nilles, Phys. Lett., B 115 (1982) 193.

[19] S. Weinberg, Phys. Rev., D 26 (1982) 287; S. Dimopoulos, S. Raby, and F. Wilczek, Phys. Lett., B 112 (1982) 133; N. Sakai and T. Yanagida, Nucl. Phys., B 197 (1982) 83.

[20] M. Nowakowski and A. Pilaftsis, Nucl. Phys., B 461 (1996) 19; A. Joshipura and M. Nowakowski, Phys. Rev., D 51 (1995) 2421.

[21] Review of Particle Properties, Eur. Phys. J. C 3 (1998) 1.

[22] S. Dimopoulos and L. Hall, Phys. Lett., B 207 (1987) 210.

[23] V. Barger, G.F. Giudice and T. Han, Phys. Rev., D 40 (1989) 2987.

[24] K. Agashe and M. Graesser, Phys. Rev., D 54 (1996) 4445; hep-ph/9510439.

[25] D. Choudhury, F. Eberlein, A. Konig, J. Louis and S. Pokorski, Phys. Lett., B 342 (1995) 180; hep-ph/9408275.

[26] B. de Carlos, J.A. Casas and J.M. Moreno, hep-ph/9512360.

[27] S. Davidson and J. Ellis, Phys. Rev., D 56 (1997) 4182.

[28] J. Ellis, S. Lola and G.G. Ross, CERN-TH/97-205; hep-ph/9803308.

[29] J. Ellis et al., Phys. Lett., B 150 (1985) 142; S. Dawson, Nucl. Phys., B 261 (1985) 297.

[30] V. Barger et al., Phys. Rev., D 53 (1995) 6407.

[31] B. de Carlos, P.L. White, Phys. Rev., D 54 (1996) 3427; hep-ph/9602381.

[32] A.Yu. Smirnov and F. Vissani, Phys. Lett., B 380 (1996) 317; hep-ph/9601387.

[33] D. Brahm, L. Hall, Phys. Rev., D 40 (1989) 2449; K. Tamvakis, Phys. Lett., B 382 (1996) 251; hep-ph/9604343.

[34] G.F. Giudice, R. Rattazzi, CERN-TH-97-076, hep-ph/9704339.

[35] R. Barbieri, A. Strumia and Z. Berezhiani, Phys. Lett., B 407 (1997) 250, hep-ph/9704275.

[36] K. Tamvakis, Phys. Lett., B 383 (1996) 307; hep-ph/9602389.

[37] R. Hemping, Nucl. Phys., B 478 (1996) 3; hep-ph/9511288.

[38] A.Yu. Smirnov, F. Vissani, Nucl. Phys., B 460 (1996) 37; hep-ph/9506416.

[39] M.C. Bento, L. Hall, G.G. Ross, Nucl. Phys., B 292 (1987) 400; N. Ganoulis, G. Lazarides, Q. Shafi, Nucl. Phys., B 323 (1989) 374.

[40] L.M. Krauss, F. Wilczek, Phys. Rev. Lett., 62 (1989) 1221; T. Banks, Nucl. Phys., B 323 (1989) 90.

[41] L.E. Ibanez, G.G. Ross, Phys. Lett., B 260 (1991) 291; Nucl. Phys., B 368 (1992) 3.

[42] T. Banks, M. Dine, Phys. Rev., D 45 (1992) 1424.

[43] A.H. Chamseddine, H. Dreiner, Nucl. Phys., B 458 (1996) 65; hep-ph/9504337.

[44] M. Bisset, O.C.W. Kong, C. Macesanu and H. Lynne, hep-ph/9811498.

[45] Z. Maki, M. Nakagawa, S. Sakata, Progr. Theor. Phys., 28 (1962) 870; B. Pontecorvo, Sov. Phys.-JETP, 26 (1968) 984.

[46] Y. Fukuda et al., Phys. Rev. Lett., 81 (1998) 1562.

[47] V. Barger, K. Whisnant, D. Cline and R.J.N. Phillips, Phys. Lett., B 93 (1980) 194.

[48] CHOOZ coll., Phys. Lett., B 420 (1998) 397.

[49] V. Barger, T.J. Weiler and K. Whisnant, Phys. Lett., B 440 (1998) 1.

[50] V. Bednyakov, A. Faessler and S. Kovalenko, Phys. Lett., B 442 (1998) 203; hep-ph/9808224.

[51] M. Doi, T. Kotani and E. Takasugi, Progr. Theor. Phys., Suppl., 83, 1 (1985).

[52] G. Pantis, F. Simkovic, J.D. Vergados and A. Faessler, Phys. Rev., C 53, 695 (1996).

[53] Amand Faessler, Sergey Kovalenko and Fedor Simkovic, Phys. Rev., D 57 (1998) 055004; hep-ph/9712535.

[54] M. Gunther et al., Phys. Rev., D 55, 54 (1997); L. Baudis et al., Phys. Lett., B 407, 219 (1997).

[55] J. Helmig, H.V. Klapdor-Kleingrothaus, Z. Phys., A 359 (1997) 361; H.V. Klapdor-Kleingrothaus, M. Hirsch, Z. Phys., A 359 (1997) 382.

[56] J.F. Donoghue, Phys. Rev., D 18 (1978) 1632.

[57] E.P. Shabalin, Sov. J. Nucl. Phys., 28 (1978) 75.

[58] M. Dugan, B. Grinstein, L.J. Hall Nucl. Phys., B 255, (1985) 416.

[59] M. Frank and H. Hamidian, hep-ph/9706510.

[60] W. Bernreuther, M. Suzuki, Rev. Mod. Phys., 63 (1991) 313.

[61] Kingman Cheung and Ren-Jie Zhang, hep-ph/9712321. K. Hagiwara and S. Matsumoto, hep-ph/9712260.

[62] W. Fetscher, H.-J. Gerber and K.F. Johnson, Phys. Lett., B 173 (1986) 102.

[63] M. Chaichian and K. Huitu, hep-ph/9603412.

[64] K. Huitu, J. Maalampi, M. Raidal, and A. Santamaria, Phys. Lett., B 430 (1998) 355; hep-ph/9712249.

[65] Jihn E. Kim, Pyungwon Ko and Dae-Gyu Lee Phys. Rev., D 56 (1997) 100; hep-ph/9701381.

[66] W.S. Hou, hep-ph/9605204, and references therein.

[67] D. Choudhury and P. Roy, Phys. Lett., B 378 (1996) 153; hep-ph/9603363.

[68] G. Bhattacharyya and D. Choudhury, Mod. Phys. Lett., A 10 (1995) 1699.

[69] B. Mukhopadhay and S. Roy, Phys. Rev., D 55 (1997) 7020.

[70] C.E. Carlson, P. Roy and M. Sher, Phys. Lett., B 357 (1995) 99.

[71] J.L. Goity, M. Sher, Phys. Lett., B 346 (1995) 69, erratum -ibid. B 385 (1996) 500.

[72] I. Hinchliffe and T. Kaeding, Phys. Rev., D 47 (1993) 279.

[73] G. Bhattacharyya and P.B. Pal, hep-ph/9809493.

[74] G. Bhattacharyya and P.B. Pal, hep-ph/9806214, to appear in Phys. Lett. B.

[75] A. Masiero, Int. School for Advanced studies, Grand unification with and without supersymmetry and cosmological implications (World Scientific, Singapore, 1984).

[76] D. Guetta and E. Nardi, hep-ph/9707371.

[77] Y. Grossman, Z. Ligeti and E. Nardi, Phys. Rev., D 55 (1997) 2768; hep-ph/9607473.

[78] R. Ammar et al., Phys. Rev., D 49 (1994) 5701; CDF Collaboration, Fermilab Conf. 95/201-E (1995).

[79] G. Bhattacharyya and A. Raychaudhuri, hep-ph/9712245.

[80] J-H. Jang, J.K. Kim and J.S. Lee, Phys. Rev., D 55 (1997) 7296, hep-ph/9701283.

[81] J-H. Jang, J.K. Kim and J.S. Lee, Phys. Lett., B 408 (1997) 367; hep-ph/9704213.

[82] J.-H. Jang, Y.G. Kim and J.S. Lee, Phys. Rev., D 58 (1998) 035006; hep-ph/9711504.

[83] A. Ali, hep-ph/9606324.

[84] P. Ko, Phys. Rev., D 45 (1992) 174 and references therein.

[85] S. Adler et al., Phys. Rev. Lett., 79 (1997) 2204; hep-ex/9708031.

[86] G. Buchalla, A. Buras and M. Lautenbacher, Rev. Mod. Phys., 68 (1996) 1125, hep-ph/9512380.

[87] G. Bhattacharyya, hep-ph/9608415.

[88] B. de Carlos and P. White, Phys. Rev., D 55 (1997) 4222; hep-ph/9609443.

[89] D.E. Kaplan, hep-ph/9703347.

[90] S.A. Abel, Phys. Lett., B 410 (1997) 173; hep-ph/9612272.

[91] J. Erler, J.L. Feng and N. Polonsky, Phys. Rev. Lett., 78 (1997) 3063; hep-ph/9612397.

[92] Y. Grossman and Z. Ligeti, Phys. Lett., B 332 (1994) 373; hep-ph/9403376.

[93] J. Kalinowski, Phys. Lett., B 245 (1990) 201.

[94] A.F. Falk, Z. Ligeti, M. Neubert and Y. Nir, Phys. Lett., B 326 (1994) 145; hep-ph/9401226.

[95] M. Acciarri et al, Z. Phys., C 71 (1996) 379.

[96] A. Ali, G. Hiller, L.T. Handoko and T. Morozumi, Phys. Rev., D 55 (1997) 4105; hep-ph/9609449.

[97] C.E. Carlson and J. Milana, Phys. Rev., D 49 (1994) 5908; Phys. Lett., B 301 (1993) 237.

[98] S. Brodsky and P. Lepage, Phys. Rev., D 22 (1980) 2157.

[99] C.-D. Lu and D.-X. Zhang, Phys. Lett., B 392 (1997) 193; hep-ph/9611351.

[100] K.S. Babu and R.N. Mohapatra, Phys. Rev. Lett., 75 (1995) 2276; hep-ph/9506354.

[101] M. Hirsch, H.V. Klapdor-Kleingrothaus and S.G. Kovalenko, Phys. Rev. Lett., 75 (1995) 17; Phys. Rev., D 53 (1996) 1329; hep-ph/9502385.

[102] B. Brahmachari and Roy P. Phys. Rev., D 50 (1994) 39, ibid. D 51 (1995) 3974 (E).

[103] V. Barger, M. S. Berger, W.-Y. Keung, R. J. N. Phillips and T. Wohrmann, Nuc. Phys. (Proc. Suppl.), B 52B (1997) 69; V. Barger, M. S. Berger, R. J. N. Phillips and T. Wohrmann, Phys. Rev., D 53 (1996) 6407.

[104] R.N. Mohapatra, Phys. Rev., D 34 (1986) 3457.

[105] J.D. Vergados, Phys. Rep., 133 (1986) 1.

[106] M. Hirsch, H.V. Klapdor-Kleingrothaus and S.G. Kovalenko, Phys. Lett., B 372 (1996) 181; H. Paes, M. Hirsch, H.V. Klapdor-Kleingrothaus, hep-ph/9810382.

[107] A. Faessler, S. Kovalenko, F. Simkovic, J. Schwieger, Phys. Rev. Lett., 78 (1997) 183; hep-ph/9612357.

[108] M. Hirsch, J.W.F. Valle, hep-ph/9812463.

[109] Amand Faessler, T.S. Kosmas, S.G. Kovalenko, J.D. Vergados, hep-ph/9904335.

[110] J.D. Vergados, Phys. Lett., B 184, 55 (1987).

[111] A. Faessler, S. Kovalenko and F. Simkovic, Phys. Rev., D 58 (1998) 115004; hep-ph/9803253.

[112] J. Toivanen, J. Suhonen, Phys. Rev. Lett., 75 (1995) 410; J. Schwieger, F. Simkovic, A. Faessler, Nucl. Phys., A 600 (1996) 179.

[113] R. Barbieri and L. Hall, Phys. Lett., B 338 (1994) 212; hep-ph/9408406.

[114] R. Barbieri, L. Hall and A. Strumia, Nucl. Phys., B 445 (1995) 219, hep-ph/9501334.

[115] T.S. Kosmas and J.D. Vergados, Phys. Rep., 264 (1996) 251, and references therein.

[116] C. Dohmen et al., Phys. Lett., B 317 (1993) 631; H.K. Walter, Phys. Atom. Nucl., 61 (1998) 1253.

[117] H.C. Chiang et al., Nucl. Phys., A 559 (1993) 526.

[118] H.C. Chiang, E. Oset and P. Fernandez de Cordoba, Nucl. Phys., A 510 (1990) 591.

[119] W. Molzon, "The MECO Experiment: A search for N ! e N with sensitivity below 10^{16}", Int. Conf. on "Symmetries in Physics at Intermediate and High Energies and Applications", Ioannina-Greece, Sept. 30 – Oct. 5, 1998.

[120] A. Czarnecki, hep-ph/9710425.

[121] T.S. Kosmas, J.D. Vergados, and A. Faessler, Phys. Atom. Nucl., 61 (1998) 1161.

[122] C.S. Wood et al., Science, 275 (1997) 1759.

[123] P. Langacker, M. Luo, and A. Mann, Rev. Mod. Phys., 64 (1992) 87.

[124] V. Barger, Kingman Cheung, D.P. Roy, and D. Zeppenfeld, Phys. Rev., D 57 (1998) 3833; hep-ph/9710353.

[125] S. Blundell, J. Sapirstein, and W. Johnson, Phys. Rev., D 45 (1992) 1602.

[126] G.-C. Cho, K. Hagiwara and S. Matsumoto, hep-ph/9707334.

[127] V. Barger, K. Cheung, K. Hagiwara, and D. Zeppenfeld, hep-ph/9707412.

[128] A. Deandrea, hep-ph/9705435.

[129] S. Davidson, D. Bailey and B. Campbell, Z. Phys., C 61 (1994) 613; hep-ph/9309310.

[130] G. Altarelli, Nucl. Phys. (Proc. Suppl.), 62 (1998) 3; hep-ph/9708437.

[131] M. Cvetic and P. Langacker, Phys. Rev., D 54 (1996) 3570; hep-ph/9511378.

[132] V. Barger, K. Cheung, and P. Langacker, Phys. Lett., B 381 (1996) 226; hep-ph/9604298.

[133] E.W. Kolb and M.S. Turner, The Early Universe, (Addison-Wesley Publishing Company, 1990).

[134] B.A. Campbell, S. Davidson, J. Ellis, K.A. Olive, Phys. Lett., B 256 (1991) 457.

[135] W. Fischler, G.F. Giudice, R.G. Leigh, S. Paban, Phys. Lett., B 258 (1991) 45.

[136] H. Dreiner, hep-ph/9311286. H. Dreiner, G.G. Ross, Nucl. Phys., B 410 (1993) 183; hep-ph/9207221.

[137] A. Bouquet and P. Salati, Nucl. Phys., B 284 (1987) 557.

[138] For a recent review of baryogenesis at the electroweak scale within supersymmetry see: M. Carena, C.E.M. Wagner, in "Perspectives on Higgs Physics II", ed. G.L. Kane, World Scientific, Singapore, hep-ph/9704347.

[139] For a related argument on majorana neutrino masses see: A.E. Nelson, S.M. Barr, Phys. Lett., B 246 (1990) 141.

[140] B.A. Campbell, S. Davidson, J. Ellis, K.A. Olive Phys. Lett., B 297 (1992) 118. hep-ph/9302221.

[141] J. Ellis, G.B. Gelmini, J.L. Lopez, D.V. Nanopoulos and S. Sarkar, Nucl. Phys., B 373 (1992) 399.

[142] M.H. Reno, D. Seckel, Phys. Rev., D 37 (1988) 3441.

[143] P. Gondolo, G.B. Gelmini, S. Sarkar, Nucl. Phys., B 392 (1993) 111.

[144] B.A. Campbell, S. Davidson, J. Ellis, K.A. Olive, Astropart. Phys., 1 (1992) 77.

[145] H. Dreiner, P. Morawitz, Nucl. Phys., B 428 (1994) 31, hep-ph/9405253.

[146] E. Perez, Y. Sirois, H. Dreiner, in "Workshop on Future Physics at HERA", DESY, May 1996, hep-ph/9703444.

[147] S. Dawson, Nucl. Phys., B 261 (1985) 297.

[148] E.A. Baltz, Paolo Gondolo, hep-ph/9704411 and hep-ph/9709445.

[149] S. Komamiya, CERN seminar, Feb. 25, 1997, OPAL, internal report PN280.

[150] The more general formula for a neutralino LSP can be found in [145].

[151] D.P. Roy, Phys. Lett., B 283 (1992) 270.

[152] H. Dreiner, G.G. Ross, Nucl. Phys., B 365 (1991) 597.

[153] S. Dimopoulos, R. Esmailzadeh, L. Hall, G. Starkman, Phys. Rev., D 41 (1990) 2099; V. Barger, M.S. Berger, P. Ohmann, Phys. Rev., D 50 (1994) 4299; H. Baer, C. Kao, X. Tata, Phys. Rev., D 51 (1995) 2180, hep-ph/9410283; M. Guchait and D.P. Roy, Phys. Rev., D 54 (1996) 3276, hep-ph/9603219.

[154] J. Hewett, In: Proc. of the 1990 Study on High Energy Physics, Snowmass 1009; J. Butterworth, H. Dreiner, In: Proc. of the 2nd HERA Workshop, DESY, March - Oct. 1991; J. Butterworth, H. Dreiner, Nucl. Phys., B 397 (1993) 3; T. Kon and T. Kobayashi, Phys. Lett., B 270 (1991) 81.

[155] S. Aid et al., Z. Phys., C 71 (1996) 211; hep-ex/9604006.

[156] G. Altarelli, J. Ellis, G.F. Giudice, S. Lola and M. L. Mangano, Nucl. Phys., B 506 (1997) 3; hep-ph/9703276.

[157] D. Choudhury and S. Raychaudhuri, Phys. Lett., B 401 (1997) 54, hep-ph/9702392; H. Dreiner and P. Morawitz, Nucl. Phys., B 503 (1997) 55, hep-ph/9703279; J. Kalinowski, R. Ruckl, H. Spiesberger and P.M. Zerwas, J. Phys., C 74 (1997) 595; hep-ph/9703288.

[158] J. Kalinowski, R. Ruckl, H. Spiesberger and P.M. Zerwas, Phys. Lett., B 406 (1997) 314.

[159] M. Acciarri et al. (L3 Collaboration), CERN-PPE/97-99 (July 1997).

[160] J.L. Feng, J.F. Gunion and T. Han, hep-ph/9711414.

[161] G. Bhattacharyya, J. Ellis and K. Sridhar Mod. Phys. Lett., A 10 (1995) 1583. J. Ellis, S. Lola, K. Sridhar, Phys. Lett., B 408 (1997) 252.

[162] G. Bhattacharyya, D. Choudhury and K. Sridhar, Phys. Lett., B 355 (1995) 193.